THE UNIVERSITY OF ADELAIDE

School of Electrical and Electronic Engineering

Performance Evaluation of Measurement Algorithms used in IEDs

Mohammad Nizam IBRAHIM

A thesis presented for the degree of Doctor of Philosophy

January 2012

Performance Evaluation of Measurement Algorithms used in IEDs

Mohammad Nizam IBRAHIM

Submitted for the degree of Doctor of Philosophy

January 2012

Abstract

Many Intelligent Electronic Devices (IEDs) are available for the protection of power systems. These IEDs use a series of mathematical algorithms for fault detection and execute various protection functions. The first and essential mathematical algorithm of any IED is the measurement algorithm. The aim of the measurement algorithm is to estimate the fundamental frequency component (phasor) of input current and voltage signals. Most protection algorithms use the estimated phasor for their executions. The most important factors for the successful use of the protection algorithms in IEDs are accuracy and speed of the phasor estimation by the measurement algorithms.

A fault in a power system produces step changes in the current and voltage phasors recorded by IEDs as well as a variety of nuisance signals. The nuisance signals introduce significant input distortions to measurement algorithms. Measurement algorithms that estimate the fundamental frequency phasor component from the distorted input signals produce some errors. Different measurement algorithms produce different amounts of

error. This is because their design is based on different approaches with different assumptions that result in different performance in the presence of nuisance signals.

It is important to evaluate the performance of measurement algorithms in the presence of nuisance signals. The evaluation is to ensure that measurement algorithms estimate the fundamental frequency component at the required design accuracy and speed. The result of the performance evaluation can be used to select appropriate measurement algorithms for specific protection applications. However, the parameters of nuisance signals are uncertain due to their dependence on unpredictable factors such as fault location and fault impedance. Thus, a methodology for the evaluation of measurement algorithm performance should take into account the uncertainty of the parameters of nuisance signals.

The traditional method of evaluating the performance of measurement algorithms is based on the local sensitivity method using a linear function approximation at a nominal point. The local sensitivity method varies only a single nuisance parameter (factor) while other factors are fixed at their nominal values. The studied factor is varied to observe errors in the output of the measurement algorithm. Such an approach, however, does not provide the overall performance of measurement algorithms. Besides, varying the single factor does not represent realistic scenarios.

This thesis proposes a new methodology to evaluate the performance of measurement algorithms implemented in IEDs. The proposed methodology uses the global uncertainty and sensitivity analysis method. In this method, all factors representing nuisance components are varied simultaneously. Uncertainty analysis measures the uncertainty in output of the measurement algorithm due to the uncertainty of input factors. Sensitivity analysis measures the contribution of all factors and their interactions to output uncertainty.

In general, the global uncertainty and sensitivity method that is based on the Monte Carlo approach requires extensive evaluations. Its implementation can be prohibitive, particularly in practical testing, because the number of factors is large. Thus, a two-stage methodology with a significantly smaller number of evaluations is used. The first-stage is the use of the Morris method as a preliminary (screening of factors) sensitivity analysis and

the second-stage is the implementation of the Extended Fourier Amplitude Sensitivity Test (EFAST) technique for comprehensive global uncertainty and sensitivity analysis. A single evaluation involves one run of the IED injection test which can take a few minutes. Thus, it is justifiable to search for the methodology that is uses the smaller number of evaluations.

The proposed methodology contributes to an automated testing method integrating ATP/EMTP, MATLAB and SIMLAB programs as well as the injection test facility. The ATP/EMTP program is used to generate fault test scenarios. The MATLAB program is used to model elements of the IED to calculate performance indices on the output of measurement algorithms and automatically control the process of extensive evaluations (simulations). The main role of the SIMLAB is to analyze the uncertainty and sensitivity of the measurement algorithms outputs.

The proposed methodology has been demonstrated by evaluating the performance of a known measurement algorithm in simulation and an unknown measurement algorithm of a commercial IED (SEL-421). The methodology has been successfully performed in the simulation as well as in practical testing. The results of the analysis indicate that the performance is typically most sensitive to a few parameters out of many possible factors. These important parameters should then be the focus of research for the optimization of measurement algorithms.

Declaration and Publications

This work contains no material which has been accepted for the award of any other degree or diploma in any university or other tertiary institution and, to the best of my knowledge and belief, contains no material previously published or written by another person, except where due reference has been made in the text.

I give consent to this copy of my thesis when deposited in the University Library, being made available for loan and photocopying, subject to the provisions of the Copyright Act 1968.

The author acknowledges that copyright of published works contained within this thesis (as listed in the following) resides with the copyright holder(s) of those works.

List of Publications

(P1)   Ibrahim, M.N.; Zivanovic, R.; "An advanced method for evaluation of measurement algorithms used in digital protective relaying," *Power Engineering Conference, 2009 (AUPEC 2009). Australasian Universities on*, vol., no., pp.1-6, Adelaide, Australia, 27-30 Sept. 2009.

(P2)   Ibrahim, M.N.; Rohadi, N.; Zivanovic, R.; "Methodology for automated testing of transmission line fault locator algorithms," *Power Engineering Conference, 2009 (AUPEC 2009). Australasian Universities on*, vol., no., pp.1-4, Adelaide, Australia, 27-30 Sept. 2009.

(P3)   Ibrahim, M.N.; Zivanovic, R.; "Impact of CVT transient on measurement algorithms implemented in digital protective relays," *Electrical Energy and Industrial Electronic Systems (EEIES 2009), International Conference on*, vol., no., pp.1-6, Penang, Malaysia, 7-8 December 2009.

(P4)   Ibrahim, M.N.; Zivanovic, R.; "Impact of CT saturation on phasor measurement algorithms: Uncertainty and sensitivity study," *Probabilistic Methods Applied to Power Systems (PMAPS 2010), 2010 IEEE 11th International Conference on* , vol., no., pp.728-733, Singapore, 14-17 June 2010.

(P5)   Ibrahim, M.N.; Zivanovic, R.; "Factor-Space Dimension Reduction for Sensitivity Analysis of Intelligent Electronic Devices," *TENCON 2011, 2011 IEEE Region 10 Conference on*, Bali, Indonesia, 21-24 November 2011.

(P6)   Ibrahim, M.N.; Zivanovic, R.; "A novel global sensitivity analysis approach in testing measurement algorithms used by protective relays," *Journal of European Transactions on Electrical Power*, February 2012. Doi: 10.1002/etep.673.

In Press Publications

(P7)   Ibrahim, M.N.; Zivanovic, R.; "Global Uncertainty and Sensitivity Analysis for Evaluation of Measurement Algorithm Performance as Affected by CVT Transients," *Journal of Electric Power Systems Research*. Submitted for review.

Signed: …………………………….   Date: …………………………….

Acknowledgements

Table of Contents

List of Figures

List of Tables

Symbols

ΔV	Voltage amplitude change
C	Equivalent capacitance
$EE_i(X)$	Elementary effect of changing the ith input factor
f_c	Cut-off frequency
$\acute{f}_c$	Frequency response of measurement algorithm
f_{max}	Maximum frequency
f_{min}	Minimum frequency
FRI	Ideal/benchmark frequency response
F_L	Fault location
h_3	Amplitude of third harmonic
h_5	Amplitude of fifth harmonic
G_1, G_2	Equivalent generator 1 and 2
H	The highest harmonic order
j	Integer frequency
L	Equivalent inductance

L_C	Compensation inductance
L_G	Number of grid level
L_M	Magnetizing inductance
L_P	Primary leakage inductance
L_S	Secondary leakage inductance
N	Number of sample per cycle
N_S	Number of simulation
$N1:N2$	Turn ratio
O_S	Overshoot
$p(X)$	Probability distribution of X
PI_{DC}	Performance index for DC amplitude attenuation
PI_{FA}	Performance index for fundamental aggregate criterion
PI_{H3}	Performance index for third harmonic amplitude attenuation
PI_{H5}	Performance index for fifth harmonic amplitude attenuation
R	Equivalent resistance
R_F	Fault resistance
R_M	Magnetizing resistance
R_P	Primary winding resistance
R_S	Secondary winding resistance
U_S	Undershoot
s	Scalar variable
$s(k)$	Sample of signals, $k = 1,2,3 \dots . \infty$
S_j	Imaginary part of the fundamental frequency
S_r	Real part of the fundamental frequency
S_{se}	Steady state error
SI_i	Sensitivity index for $i^{th.}$ factor
$SI_{i,j}$	Sensitivity index for interaction of $i^{th.}$ and $j^{th.}$ factor
$SI_{i,total}$	Total sensitivity index for $i^{th.}$ factor
T_S	Settling time
x_n	$n^{th.}$ nuisance factor
V_i	Variance contributed by $i^{th.}$ factor

$V_{i,j}$	Variance contributed by interaction of i and j factor
$V_{\sim i}$	Variance contributed by other than $i^{th.}$ factor
V_{group}	Variance contributed by a group of factors
V_{total}	Total variance
ω	Angular frequency
$\bar{y}$	Output mean value
ZB	Burden of CT
α	Amplitude of decaying DC offset
τ	Time constant of decaying DC offset
λ	Remanent flux
δf_1	Off-nominal fundamental frequency
β	Fault inception angle
y_{true}	True value of fundamental frequency amplitude
y_{max}	The maximum value of estimated fundamental frequency
y_{min}	The minimum value of estimated fundamental frequency
y_{∞}	Steady state value of fundamental frequency amplitude
μ	Mean of error value
σ	Standard deviation of error
min_{error}	Minimum of error
max_{error}	Maximum of error
Δ	Predetermined pertubation
A_j	Fourier cosine
B_j	Fourier sine
Λ_j	Variance spectrum

Abbreviations

A/D   Analogue to Digital Converter

ATP   Alternative Transient Program

ANOVA   Analysis of Variance

CB   Circuit Breaker

CT   Current Transformer

COMTRADE   Common Transient Data Exchange

CVT   Capacitive Voltage Transformer

DFT   Discrete Fourier Transform

EFAST   Extended Fourier Amplitude Sensitivity Test

EHV   Extra High Voltage

EMTP   Electromagnetic Transient Program

FAST   Fourier Amplitude Sensitivity Test

FIR   Finite Impulse Response

FSC   Ferro-resonant Suppression Circuit

GPS   Global Positioning System

LHS   Latin Hypercube Sampling

IED	Intelligent Electronic Device
IIR	Infinite Impulse Response
LPF	Low Pass Filter
MC	Monte Carlo
OAT	One Factor At A Time
PDF	Probability Distribution Function
PMU	Phasor Measurement Unit
PPE	Percentage peak error
PRMSE	Percentage root-mean-square error
p.u.	Per unit
QMC	Quasi-Monte Carlo
RL	Resistor-Inductor Element
RMS	Root-mean-square
RRTS	Remote Relay Test System
SA	Sensitivity Analysis
SIR	Source to Impedance Ratio
TSM	Taylor Series Method
TVE	Total Vector Error
U	Uniform distribution function
UA	Uncertainty Analysis
VT	Voltage Transformer

Chapter 1. Introduction

1.1. Background

In today's protection systems, the Intelligent Electronic Devices (IEDs) are the most widely used in electrical power systems. They are replacing the traditional type of relays, which are electromechanical and solid state, due to their many advantages. Some of the advantages of the IEDs over the traditional relays are that they are high performance, multi-function and small in size.

The primary function of the IEDs, as well as the traditional relays, is to detect any faults within their designated protection zone. However, unlike the traditional relays, the operation of the IEDs is based on digital values or samples. This means that they are highly sensitive to the implemented mathematical algorithms for processing samples of input signals.

Measurement algorithms are the first mathematical algorithms that process digital samples in the IEDs. The aim of the measurement algorithms is to estimate specific harmonic component (phasor) from their input signals [1]. Most commonly, they are

required to estimate the fundamental frequency component while attenuating non-fundamental components. The estimated fundamental frequency component is often used to calculate other quantities such as zero- and positive-sequence signals. Then a set of protection algorithms use those estimated and calculated quantities to detect faults. A variety of analysis algorithms such as a fault locator is also executed based on those quantities.

Thus, it is most important for measurement algorithms to produce high accuracy output in their fundamental frequency component estimation. The high accuracy output ensures the correct detection of faults as well as accurate identification of fault locations. Beside the accuracy, the speed of the fundamental frequency component estimation is also an important factor in some protection systems, such as an Extra High Voltage (EHV) transmission line. Accuracy and speed, therefore, are two basic criteria for the evaluation of measurement algorithms' performance [2].

The main input signals to measurement algorithms for fault detection and other protection functions are the current and voltage signals. These signals are the replication of primary signals in a power system network measured via instrument transformers. Ideally, these signals should contain only a fundamental frequency component. If this is the case, measurement algorithms produce not only high accuracy output, but also the speed of their estimation is fast. It should be mentioned that measurement algorithms are designed based on different lengths of the data window. High speed protection, as required in EHV systems, requires measurement algorithms with a short data window to increase the overall protection speed.

With the current technology focusing on the synchrophasor, the estimated fundamental frequency component is required to be time stamped. The time synchronization, commonly using the Global Positioning System (GPS) clock, improves monitoring and controlling of the power system during disturbances [3]. However, for each measurement point, high accuracy of the fundamental frequency component estimation can only be achieved if the input signals are purely the fundamental frequency component.

In practice, different processes in the power network, particularly fault conditions, distort the input signals. They initiate a variety of nuisance signals. The nuisance signals

are signals of non-fundamental frequencies such as decaying DC offset, harmonic components and noise [1, 4]. The initiated nuisance signals are mixed with the fundamental frequency component to produce distorted input signals to the measurement algorithms.

In this thesis, the nuisance signals/components are referred as the signals having non-fundamental frequency components initiated in fault conditions. In other words, any process in the system that causes the input signal to deviate from the sinusoidal with a fundamental frequency is considered important for testing.

The presence of nuisance signals not only distorts the primary fault signals but may also distort the secondary output signals of instrument transformers that are used to replicate those primary signals. For example, a high primary fault current, which is due to a high amplitude of decaying DC offset, tends to saturate the magnetic core of a current transformer (CT) [5]. If the CT is saturated, it produces a variety of harmonic components. As a result, the input signals to the measurement algorithm are distorted not only by the decaying DC offset but also by those harmonic components that are produced due to the CT saturation.

Furthermore, nuisance signals that are initiated on fault currents can be different on fault voltages. The decaying DC offset, for instance, is more pronounced on the fault current than the fault voltage [1, 6]. Regardless of nuisance signals on the fault current or voltage, their parameters are uncertain, because they depend on random factors such as fault inception angles. As an example, the amplitude of the decaying DC offset is uncertain in a way that it can vary from zero to as high as twice of the amplitude of the fundamental frequency component. This amplitude variation is determined by three factors: fault inception angle, fault resistance and fault location. All these factors are unpredictable in fault conditions.

The presence of nuisance signals in input fault signals, currents and voltages causes measurement algorithms to produce errors in their output fundamental frequency component estimation. As the measurement algorithms are the first mathematical algorithms that process samples of input signals, any produced errors would propagate through a subsequent set of protection algorithms and may result in the IEDs operating

incorrectly. It is important, therefore, to evaluate the performance of measurement algorithms of IEDs for their function, which is to estimate the fundamental frequency component while attenuating nuisance signals.

As the parameters of nuisance signals are uncertain, the produced errors in the output of measurement algorithms are uncertain as well. The uncertainty of the produced error is an indicator of the measurement algorithms' performance. In uncertainty analysis, two types of performance, accuracy and precision, can be calculated [7]. Accuracy indicates the closeness of the mean estimation value to its actual value whereas precision indicates the variance of the estimation value.

Besides calculating the uncertainty of errors on the output of measurement algorithms, it is also important to calculate the contribution of nuisance parameters, particularly a parameter that contributes the most to the calculated uncertainty of errors. The contribution of nuisance parameters can be calculated using a systematic analysis method, known as a global sensitivity analysis. Information about nuisance parameter contributions can be useful for the optimization of the measurement algorithms.

This thesis proposes a new methodology, and its implementation, to evaluate the performance of measurement algorithms in the transient response when its input signals are distorted by the uncertainty of nuisance signals. It is based on the global uncertainty and sensitivity analysis method. The proposed methodology is the only appropriate way for measuring output uncertainty and parameters' sensitivity when their inputs comprise uncertain parameters [8]. The proposed methodology can be used to measure the performance of measurement algorithms and the contribution of nuisance parameters from two types of measured signals, currents and voltages, during the occurrence of faults in power systems. Measurement algorithms are evaluated for their performance in estimating the fundamental frequency component from those types of measured signals that are distorted by a variety of nuisance components.

The uncertainty analysis measures the uncertainty of error on the output of the measurement algorithm due to the uncertainty of the input nuisance components. The sensitivity analysis, however, is a study as to how the variation in the output of a model

(numerical or otherwise) can be apportioned, qualitatively or quantitatively, to different sources of input variation [8].

Results from the proposed methodology can be useful in several ways. The result of the uncertainty analysis provides a level of confident for the output of measurement algorithms. If the output is uncertain within an acceptable boundary, the quality of measurement algorithms can be assured. Further, the result can be used to select appropriate measurement algorithms for specific protection applications.

The result of the sensitivity analysis identifies the contribution of factors to the output errors. This information can be useful for optimizing and prioritizing the area of research. Both results, therefore, can be used to better understand the output behavior of the measurement algorithms in transient responses during the presence of nuisance components.

In protective relay applications, performance evaluation is not only important in transient responses but also during the steady state [1]. Thus, the performance of measurement algorithms in the steady state is also evaluated. The performance of measurement algorithms in a steady state can be evaluated by analyzing their frequency responses [9]. In this state, frequency responses of measurement algorithms are analyzed for their capability to attenuate DC, third and fifth harmonic components, and to estimate fundamental frequency component while considering off-nominal frequency. Moreover, the off-nominal frequency is also considered since it is a common condition in power systems. The performance of measurement algorithms in the steady state is accessed using numerical indices.

1.2. Objectives

The primary objective of this study is to provide a new methodology for systematic performance evaluation of measurement algorithms used in IEDs. The proposed methodology applies global uncertainty and sensitivity analysis based on a statistical approach. The methodology shows how to measure the uncertainty in the output of measurement algorithms (i.e. performance) due to the uncertainties of its input nuisance

signals. Moreover, it also shows how to measure the contributions of the factors determining nuisance signals to the output uncertainty. The results of the global uncertainty and sensitivity analysis are useful for understanding the behavior of the measurement algorithm when its input signals are influenced by the uncertainty of nuisance signals.

Additionally, a methodology for the performance evaluation of measurement algorithms in the steady state is provided. As mentioned, the proposed method in the steady state evaluates the performance of measurement algorithms for attenuating DC, third and fifth harmonics components, and for estimating the fundamental frequency component that considers the off-nominal fundamental frequency.

The second objective is to develop evaluation platforms for the implementation of the proposed methodology in the transient response. Two platforms are developed and presented. The first platform is simulation-based. Models of fault system including CT, CVT, and IED are presented. The proposed method uses interfacing of three software tools; ATP/EMTP [10], MATLAB [11] and SIMLAB [8]. The ATP/EMTP provides fault current and voltage test scenarios; the MATLAB models elements of the IED, performs calculations of transient response characteristics and controls the process for extensive evaluation; and finally, the SIMLAB analyses the uncertainty and sensitivity output of the measurement algorithms.

The second platform is practical testing. The same methodology is implemented to evaluate the performance of the measurement algorithm used in a commercial IED (SEL-421). In any practical testing, more complex procedures than evaluating model simulation are required. Thus, two types of the evaluation platforms, simulation and practical, are separately presented in different sections.

The final objective is to demonstrate the implementation of the proposed methodology in transient responses using simulation and practical testing. In this study, the Cosine filter is selected as a measurement algorithm in the simulation and unknown measurement algorithm of a commercial IED in practical testing. It should be noted that most mathematical algorithms, including measurement algorithms of commercial IEDs, are the secret property of manufacturers. Thus, the detailed information of these algorithms

might be unknown to the public. The main reason is because the performance of IEDs of different manufacturers is highly differentiated by the implemented mathematical algorithms.

For the purpose of demonstrating the proposed methodology, the same input fault test scenarios, which are extensively simulated using the ATP/EMTP, are used and applied to both the IED model and the commercial device. The results of uncertainty analysis are produced and the most important (influential) parameters that contribute to the output uncertainty of the Cosine filter and unknown measurement algorithm in the SEL-421 are presented.

1.3. Contributions of the Thesis

The IEDs implement a variety of measurement algorithms. The measurement algorithms have a different performance since they are designed based on different assumptions. The implemented measurement algorithms only show high accuracy and produce fast speed of the fundamental frequency component estimation, as predicted by their design, if all the assumptions are satisfied.

If some of the assumptions are unsatisfied, which is a common case in fault conditions, the measurement algorithms can show poor performance. Different measurement algorithms perform differently. Thus, it is important to evaluate the performance of measurement algorithms in a way that enables their selection for specific protection applications. The main reason is because no single measurement algorithm is suitable for all types of protection applications. The selection, however, requires the understanding of the behavior of the measurement algorithms in fault conditions.

To understand the behavior of measurement algorithms in the presence of nuisance signals in fault conditions, the methodology for performance evaluation of measurement algorithms that is based on uncertainty and sensitivity analysis is proposed. The proposed methodology provides the following contributions:

1. A methodology for identifying the most important factors

Results drawn from the proposed sensitivity analysis identifies the most important parameters from a large number of possible factors. The most important parameters are the parameters that show the highest contribution to the uncertainty output of measurement algorithms (i.e. measurement error). This information will help measurement algorithm developers and researchers to prioritize the area of research. Thus, more studies are focused on the important parameters rather than unimportant parameters.

In contrast, the unimportant parameters that are identified through the sensitivity analysis can be used to simplify the model of evaluation. The simplified model can be important for a complex model, or a model that requires significant time to complete its execution. Thus, using the simplified model for performance evaluation, time and cost is saved.

2. A methodology for evaluating measurement algorithm performance

Results drawn through the global uncertainty analysis provide a performance indicator or a confidence level about the output of the measurement algorithm. The global uncertainty analysis measures the uncertainty in the output of the measurement algorithms due to the uncertainty parameters of input nuisance signals. A small output uncertainty indicates a good performance (high robustness) of the measurement algorithm. In contrast, a wider output uncertainty indicates a low performance.

3. A systematic method for verifying existing, newly developed measurement and protection algorithms

The presented advanced methodology in simulation and practical testing platforms can be adopted to assess the performance of a newly developed measurement algorithm or existing measurement algorithms implemented in IEDs. Many researchers have been proposing and implementing new measurement algorithms. Their performance, however, is commonly demonstrated using a limited number of fault test scenarios. Such test scenarios, however, do not represent all fault conditions. In contrast, the methodology that has been proposed can verify the performance of measurement algorithm in a global way, using systematic strategy in generating fault test scenarios. Moreover, the proposed methodology

can also be easily extended to measure the performance of analysis algorithms such as the fault locator algorithm.

4. Simulation and practical testing implementation

The proposed methodology provides feasible and inexpensive tools for implementation. In simulation, the proposed method interfaces with software tools of the ATP/EMTP, MATLAB and SIMLAB program for its implementation. In the development of any algorithms, the first stage is to evaluate the performance of the developed algorithms in simulation prior to their implementation and evaluation again in practice. The use of inexpensive tools in the simulation stage can be one important criterion for the selection of a method of evaluations. It should be noted that, except for the MATLAB program, the other two software tools, which are the ATP/EMTP and SIMLAB program, are royalty free.

It is important that the proposed methodology can be used to evaluate measurement algorithms' performance not only in simulation but also in practical testing. To achieve this practical testing, a combination of two sensitivity analysis methods is used. The first is the Morris method [12] and the second is the Extended Fourier Amplitude Sensitivity Test (EFAST) [13]. The aim of the combined methods is to increase the possibility for the implementation of the proposed methodology, particularly in practical testing.

Practical testing of measurement algorithms often requires a much longer time than its model simulation for each single scenario evaluation. Beside, the proposed global uncertainty and sensitivity analysis requires an extensive number of evaluations that depend on the number of studied parameters. For example, up to 10,000 evaluations are required for only three uncertain parameters [8]. Such a high number of evaluations may take months to complete the practical test of the measurement algorithm's performance, and therefore can be prohibitive.

One option to reduce the high number of evaluations is to eliminate some of the investigated parameters, particularly if the number of parameters is large. However, only unimportant parameters should be identified for the elimination. Thus, a strategy is to perform the two-stage method. The Morris method is used for screening important

(unimportant) parameters among all the studied parameters. Then, the EFAST is performed by using only those important nuisance parameters. In this way, the possibility for the performance of practical evaluation of measurement algorithms used in commercial IEDs is increased.

5. Evaluation of unknown measurement algorithms' performance

IED manufacturers may encrypt measurement algorithms or protection algorithms due to their secret property. However, the proposed methodology that is using the EFAST method is able to evaluate the performance of measurement algorithms implemented in any IEDs despite their mathematical algorithms being unknown (i.e. black box). The reason is that the EFAST method works based on a variance-based strategy and sampling. In the variance-based sensitivity analysis, the important thing is the knowledge of variations in the input factors and the computation of variance on the output of the measurement algorithms. Details of the evaluated measurement algorithm can be unknown. Thus, the EFAST method can be used to evaluate the performance of unknown measurement algorithms of any IED providing both the input and the output nodes of the unknown measurement algorithm can be accessed.

1.4. Outlines of the Thesis

This thesis is organized into seven chapters. Chapter I introduces the problem of the presence of nuisance signals in input signals of measurement algorithms implemented in the IEDs. The effect of the nuisance signals on the measurement algorithms output, resulting in poor performances:, low accuracy and slow speed of fundamental frequency component estimation, is described. The reason for the unpredictable parameters (factors) of nuisance signals in fault conditions is discussed. As the number of factors involved is high, and all factors are unpredictable, the existing methods, which vary one factor at a time while other factors are fixed at their nominal values, are not appropriate for evaluating measurement algorithms' performance during fault conditions. Thus, a methodology for the evaluation of the measurement algorithms' performance under the influence of the unpredictable parameters is described. The methodology uses the global uncertainty and

sensitivity analysis that can evaluate the performance of the measurement algorithms in transient response. Additionally, the evaluation of the measurement algorithms outputs in the steady state is also considered.

Chapter II presents the basic elements of IED and its principle operation for fault detection. Three mathematical algorithms, full-cycle DFT, half-cycle DFT and Cosine filter, which are the most popular measurement algorithms implemented in IEDs, are detailed. The literature review on the development of digital measurement algorithms and the popular measurement algorithms is presented. The literature review also includes the assessments of the performance of measurement algorithms from an uncertainty and sensitivity point of view. The deficiencies of the existing methods, which are based on a local sensitivity instead of a global uncertainty and sensitivity analysis, are discussed. Finally, the performance of those DFT measurement algorithms for input sinusoidal and non-sinusoidal signals are briefly illustrated.

Chapter III begins with the presentation of the general principle of the uncertainty and sensitivity analysis method. The Morris and the EFAST methods, which are the two global sensitivity analyses used in this thesis, are presented in more detail. Then, the nuisance components on fault current and voltage signals and their main sources are described. The uncertainty of nuisance signals and the factors describing them initiated from both the power network and the instrument transformers in fault conditions are discussed in detail.

Chapter IV describes the methodology for the evaluation of the measurement algorithms' performance in transient response and steady state. For the transient response, the methodology is based on the global uncertainty and sensitivity analysis method. Details of the model of fault network, CT, and CVT for creating fault transient test scenarios distorted by the uncertainty of nuisance components are described. The model of the IED is also described. Performance criteria in the output transient response of the measurement algorithms are defined. Then a general methodology, which is the principle for implementation of the proposed methodology for both the simulation and practical testing, is presented. Next, the methodology to evaluate the measurement algorithms performance in the steady state is presented. This is based on analyzing the frequency response of measurement algorithms. The performance criteria and indices are described.

Chapter V describes the implementation of the proposed methodology for the evaluation of measurement algorithm performance in the transient response and steady state. In the transient response, the methodologies implemented in computer simulation and practical testing are separately presented. The use of the ATP/EMTP program to model faults in power systems (i.e. fault network, CT and CVT models) for generating input fault currents and voltages to the measurement algorithm, is discussed. The model of the IED that was developed using the MATLAB program is described. The used of the SIMLAB program to calculate the uncertainty and sensitivity output of the measurement algorithms is also described. The ATP/EMTP, MATLAB and SIMLAB programs are the only software tools used for implementation of the proposed methodology in simulation. For practical testing, the required software and equipment tools are presented. In the steady state evaluation, the methodology that uses MATLAB script to automatically calculate the coefficients of measurement algorithms; plot their amplitude response and calculate the steady state performance indices, is presented.

Chapter VI presents the results of the implementation of the proposed methodology in the transient response and the steady state. In the transient response, the results of performance evaluation of the Cosine filter, which is in simulation, and the results of unknown measurement algorithms of a commercial IED, which is in practical testing; are presented. For each result, the uncertainty and sensitivity indices measured by the Morris as well as the EFAST method from two types of input fault signals, current and voltage, are presented. The results of the Morris method are graphically illustrated, whereas the results of the EFAST method are numerically tabulated. In the steady state, the results of the performance evaluation of the full-cycle DFT, half-cycle DFT and Cosine filter are presented. These algorithms are evaluated for their performance in attenuating the DC, third and fifth harmonic components, and estimating the fundamental frequency component considering the off-nominal power system frequency. The results in the steady state are numerically tabulated.

Chapter VII provides the summary and conclusions drawn during the completion of this study. An enhancement of the proposed method as well as the direction for further studies using the global uncertainty and sensitivity analysis method are also suggested.

1.5. Conclusion

The importance of the measurement algorithms to accurately and quickly estimating the fundamental frequency component for the correct operation of IEDs has been highlighted. The high accuracy and fast estimation of the fundamental frequency component by the measurement algorithms (i.e. good performance) can only be achieved in normal conditions. In fault conditions, however, significant measurement errors are produced by the measurement algorithms and these errors might propagate through subsequent protection algorithms to result in the incorrect operation of IEDs. The sources of the measurement errors are a variety of initiated nuisance components during fault conditions in which their parameters are uncertain.

The systematic and appropriate methodology that is able to evaluate the performance of the measurement algorithm when its inputs are uncertain nuisance components is briefly introduced. It involves the use of a systematic global uncertainty and sensitivity analysis method to measure the performance of measurement algorithms in a transient response. The proposed method measures the uncertainty of errors in the output of the measurement algorithms as well as the contribution of the nuisance factors to the uncertainty of the errors. The result of this methodology is useful for understanding the behavior of the measurement algorithms in fault conditions.

The importance of performance evaluation of the measurement algorithms in steady state is also highlighted. The objectives and organisation of this thesis, which presents a proposed methodology for evaluating the performance of measurement algorithms in transient response and steady state, have been outlined above.

Chapter 2. Measurement Algorithms of IEDs

2.1. Introduction

Intelligent Electronic Devices (IEDs) implement a number of different measurement algorithms. These algorithms are based on different technologies used by manufacturers. The most widely used measurement algorithms are based on some forms of the Discrete Fourier Transform (DFT) [14, 15]. The DFT measurement algorithms offer several advantages such as easy implementation and inexpensive computation [16, 17].

The aim of the measurement algorithms is to estimate the fundamental frequency component of input current and voltage signals. In normal conditions, measurement algorithms estimate the fundamental frequency component with high accuracy and fast speed, which means that they show high performance. However, in fault conditions, their high performance can be degraded to a poor performance. This is due to a variety of nuisance signals being presented in input signals.

The presence of nuisance signals produces input signals with distortion to the measurement algorithms. Consequently, the measurement algorithms that are sensitive to

the distorted input signals would show a low accuracy and slow speed in estimating the fundamental frequency component. Paper [18] shows that the DFT measurement algorithm produces a low accuracy output when the input fault current contains a decaying DC offset. It shows that the error in amplitude of the fundamental frequency component estimation can be up to 15%. Such significant errors not only degrade the performance of the DFT measurement algorithms but also the performance of the IED.

The successful operation of IEDs and their protection elements is highly sensitive to the output of the implemented measurement algorithms. However, the output of the measurement algorithms are influenced by a variety of nuisance signals. Different nuisance signals show different degrees of influence on the output of the measurement algorithm. Thus, it is important to investigate how each of these nuisance signals influences the output of the measurement algorithms.

Section 2.2 firstly describes the modern IED which is widely used in today's protection. A block diagram and basic elements in the IED and their operation for the detection of faults is presented. Section 2.3 reviews development of digital measurement algorithms. More emphasis is given to the three most popular and widely used DFT-based measurement algorithms: the full-, half-cycle DFT, and Cosine filter. Then the review of the existing techniques that evaluate the performance of measurement algorithms follows. Section 2.4 discusses the deficiencies in the literature of the performance evaluation, specifically on the methodology for the uncertainty and sensitivity analysis. Those studies have used the local sensitivity analysis to evaluate the performance of the measurement algorithms. Section 2.5 presents the mathematical algorithms of those popular DFT-based algorithms; and then illustrates a comparison of their output accuracy and speed for both fault and non-fault simulated signals. Finally, Section 2.6 provides the conclusion of this chapter.

2.2. Digital Protective Relay

The IEDs are widely used in today's protection system. They have been replacing conventional relays: electromechanical and solid state, because of their advantages in

performance, economics, multi-function and size. The operations of IEDs differ from the conventional relays mainly in a way of processing secondary signals from instrument transformers. Instrument transformers are the CT and CVT that are used to replicate and scale down the primary current and voltage signals, respectively.

The conventional relays use the secondary signals, which are the analogue signals. The IEDs, however, convert those analogue signals to a series of samples prior to processing them. The first and essential processing element in IEDs is the measurement algorithms. The measurement algorithms are a set of mathematical algorithms implemented in the microprocessor of the IEDs, in which their function is to estimate the fundamental frequency component of current and voltage signals. The estimated fundamental frequency component is used by a variety of protection functions as well as analysis algorithms. Thus, the performance of any IED is highly sensitive to the applied mathematical algorithms, specifially the measurement algorithms.

Figure 2.1 shows a typical transmission line system that has a connection to an IED. The transmission line system consists of two thevenin's equivalent generators: G_1 and G_2; and two buses: bus A and bus B. The protection zone is ideally between the two buses.
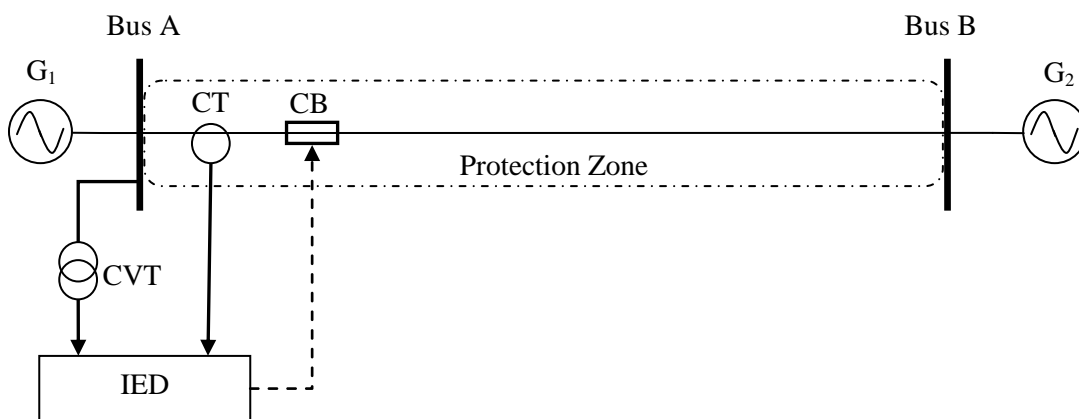
Figure 2.1 Typical power system protection

The CT and CVT are used to replicate the primary current and voltage signals respectively, and scale them down to a much lower amplitude that is suitable for operation of the IED. The IED uses these input signals to identify the system condition: normal or abnormal. The IED estimates current and voltage phasors and uses one or both of them for fault detection. Overcurrent digital relays only use the input current signals to detect the fault, whereas impedance digital relays use both the input current and voltage signals. Regardless of the types of digital relays, overcurrent or impedance, the IED implements measurement algorithms to estimate the fundamental frequency component (phasor) of the input signals.

The operation principle of the digital protective relay for performing a variety of protection functions is well documented [17, 19]. Figure 2.2 shows a basic block diagram of a digital protective relay. The function of each block for fault detection can be described as follows.

Input signals   Output signal

```
Anti-aliasing
LPF
A/D
Converter
```
Analog input
sub-system

Digital output
sub-system

```
Digital Output
Pre set
Protection
Functions
```

Measurement Algorithms

Processor sub-system
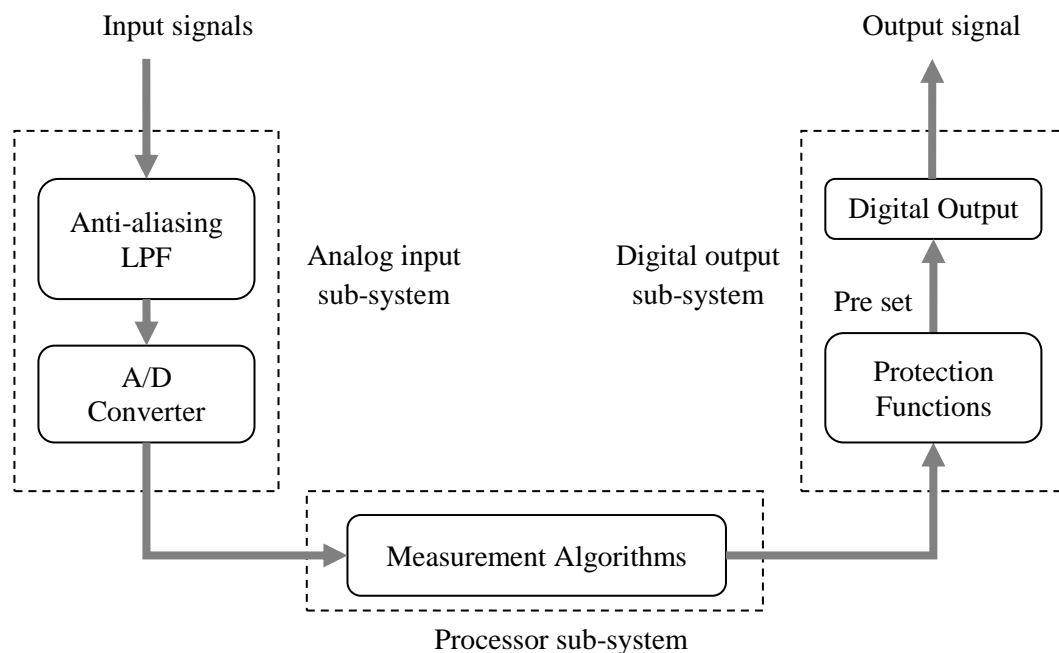
Figure 2.2 Basic block diagram of digital protective relay [19]

The basic digital protective relay is made up of three main sub-systems, which are the analog input, processor and digital output. The analog input sub-system receives two types of input analogue signals: currents and voltages supplied by the instrument transformers. The anti-aliasing low pass filter (LPF) in this sub-system is used to eliminate high frequency components. The LPF is also used to prevent the effect of signal aliasing on the analogue signals. The analogue signals with the eliminated high frequency components are then input to the analogue to digital converter (A/D).

The A/D is used to convert the analogue signals to digital samples by sampling those signals at discrete time intervals. The sampling frequency used is selected in a way that it satisfies the Nyquist criterion [20]. This criterion states that the sampling frequency used must be, at least, two times higher than the maximum frequency component in the analogue signals to avoid the aliasing effect. However, it is common for the IEDs to use a sampling frequency of 5 to 10 times higher than the maximum frequency for accurate representation of the analogue signals.

In the processor sub-system, measurement algorithms are the first mathematical algorithms that process digital samples. They are used to estimate the signal phasor. The phasor is the representation of the sinusoidal of current and voltage signals at the power system frequency. Most of the protection functions execute their algorithms based on the signal phasor (i.e. fundamental frequency component). The estimated amplitude and phase angle of the fundamental frequency component will be used directly or indirectly by a variety of subsequent protection functions. For example, overcurrent digital relays use directly the amplitude of current phasor estimation, whereas fault locator algorithms may use derived signals such as zero-, positive- and negative-sequence signals. However, the derived signals are also calculated from the estimated fundamental frequency component. Thus, the major factors for the successful use of the protection functions and hence the final tripping signal by any IEDs has greatly depended on the performance of their implemented measurement algorithms.

If a fault is detected, the digital output sub-system asserts the tripping signal to the circuit breaker (CB). To detect a fault, the protection functions of the IEDs compare voltages, currents or their combination between the pre-setting threshold and the estimated quantities. If the estimated quantities cross the threshold limit, the IEDs assert a tripping

signal to the CB. Overcurrent relays for example, assert a tripping signal if the estimated amplitude of the current exceeds the pre-setting current threshold. In contrast, impedance relays assert tripping signals if the estimated impedance is less than the pre-setting impedance threshold. For coordination among IEDs, the tripping signal may be delayed such as digital relays that are used for back-up protection.

2.3. Literature Review of Digital Measurement Algorithms

Developments in digital technology, particularly that of the microprocessor in 1980, have seen the implementation of relays that work based on digital samples (i.e. IEDs). These types of relay are also known as numerical or digital protective relays. They have been replacing the conventional relays: electromechanical and solid state due to their many advantages.

Many researchers have been involved in investigating and developing measurement algorithms so as to implement them in IEDs. The main aim of such research and development is to develop new measurement algorithms or to modify the existing measurement algorithms thus producing a better performance. Commonly, researchers develop measurement algorithms to meet several performance criteria in the transient response and the steady state. In the transient response, measurement algorithms should have the characteristics of fast response, low overshoot, high steady state accuracy and insensitive to nuisance signals. In the steady state, they should have the characteristics of unity amplitude gain at fundamental frequency component, and zero amplitude gain (i.e. complete attenuation) at non-fundamental frequency components [1].

2.3.1. Digital and DFT Algorithms

Measurement algorithms of IEDs for the protection system can be broadly classified into several methods: wavelet transform, artificial intelligence and algorithms based on transient signals [21, 22]. As mentioned, the DFT measurement algorithms are the most

widely used measurement algorithms in IEDs. This section focuses on a development in digital measurement algorithms, particularly in the DFT measurement algorithms.

Basically, measurement algorithms based on digital samples for digital protective relays have been proposed since 1970. Mann and Morrison proposed a Sample and First-derivative measurement algorithm in 1971 [23, 24]. This algorithm uses a sample and its first derivative values to estimate the peak amplitude of current and voltage signals. The proposed algorithm uses a moving data window that requires two consecutive sample values, which are used to calculate the sample and its first derivative. In this work, the authors assume that the input signals are a sinusoidal of the power system frequency in which the frequency does not vary with time.

Gilchrist, Rockerfeller and Udren proposed a First- and Second-derivative algorithm in 1971 [25, 26]. In this work, instead of using sample and derivative values, the algorithm uses two consecutive derivatives, which are the first- and the second-derivative values. The proposed algorithm uses a moving data window that requires three consecutive sample values.

In contrast to the derivative values, measurement algorithms that are based only on sample values have been proposed. Makino and Miki proposed a Two-sample method in 1975 [27]. This algorithm uses two consecutive sample values. Meanwhile, Gilbert and Shovlin proposed a Three-sample method in 1975 [28].

The previous literature on the early development of digital measurement algorithms is based on a short data window. A short data window, in this thesis, is defined as the window that is less than one cycle of the power system frequency. The advantages of using the measurement algorithms with a short data window are that their operation speed is fast and computationally inexpensive. However, their main disadvantage is that they are sensitive to the DC offset, fundamental frequency variation and harmonic components.

Figure 2.3 illustrates the impact of a simulated decaying DC offset on the three short data windows: the Two-sample method; Sample and First-derivative; and First- and Second-derivative measurement algorithms. It is clearly shown that all these measurement

algorithms are sensitive to the decaying DC offset. The Sample and First-derivative; and Two sample method; are the worst affected among these measurement algorithms.
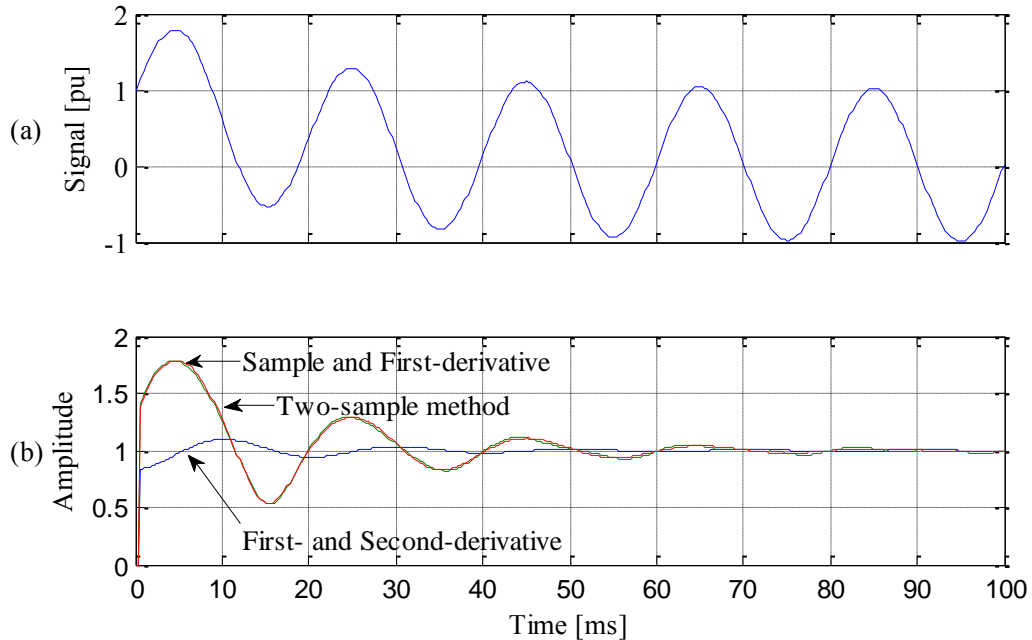
Figure 2.3 Transient response of short data window measurement algorithm to distorted signal. (a) Input signal with DC offset (b) Amplitude transient response

Next, Figure 2.4 illustrates the impact of the third harmonic amplitude on the same measurement algorithms. In this example, 1% of the third harmonic amplitude, which is based on the amplitude of the fundamental frequency component, is simulated. In this case, the First- and Second-derivative is the worst measurement algorithm. This measurement algorithm produces high oscillation within the true (1 per unit) amplitude of the fundamental frequency component.
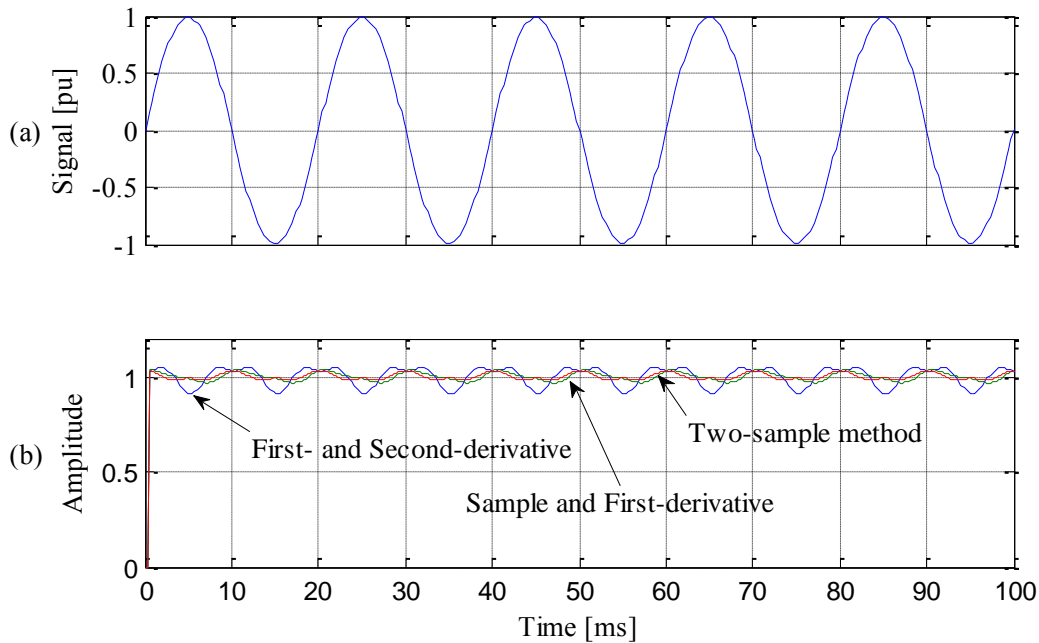
Figure 2.4 Transient response of short data window measurement algorithm to distorted signal. (a) Input signal with 1% third harmonic (b) Amplitude transient response

With the advantages of non-linear loads, particularly in relation to cost and performance, the usage of non-linear loads is expected to be increased. However, non-linear loads produce multiple harmonic components in both voltage and current signals. Beside, non-linear elements such as CT may also produce harmonic components if they are saturated. As previously illustrated, the impact of harmonic components as well as the DC offset on the measurement algorithms with the short data window is significant.

More recently, measurement algorithms that are based on the DFT theory have been introduced. The DFT measurement algorithms focus on the estimating fundamental frequency component while attenuating the DC offset and harmonic components. These algorithms can also be classified into short or long data window. The full-cycle DFT (long data window) is among the most popular DFT measurement algorithm implemented in IEDs [29]. The full-cycle DFT uses a one cycle moving data window. The advantage of the full-cycle DFT algorithm is its ability to attenuate the DC offset and all multiple harmonic components. Its main disadvantage is that its operation speed is one cycle delay.

To improve the response speed of the full-cycle DFT measurement algorithms, Phadke, Ibrahim and Hlibka proposed a DFT algorithm with a shorter data window, known as half-cycle DFT [30] in 1977. The half-cycle DFT, as its name indicates, uses only a half cycle moving data window during the estimation of the fundamental frequency component. This algorithm improves the estimation speed, by a factor of 2 in comparison with the full-cycle DFT. The improvement, however, is only true if input signals are purely sinusoidal of the fundamental frequency component, that is, during ideal normal conditions.

In contrast, if the input signals contain nuisance signals such as DC offset or even harmonics (2nd, 4th, 6th… so on), the estimation speed of the fundamental frequency component by the half-cycle DFT algorithms may take longer than the full-cycle DFT. The half-cycle DFT is able to attenuate only odd harmonic components (3rd, 5th, 7th… so on).

To improve the accuracy of the DFT measurement algorithms, Schweitzer III and Hou introduced a Cosine filter [1]. The Cosine filter algorithm uses 1.25 cycles moving data window. The Cosine filter is able to attenuate the DC offset and all higher order of harmonic components: even and odd. Their paper [1] also reveals that, although the data window of the Cosine filter is longer than both the full- and the half-cycle DFT, the Cosine filter performs faster and produces a more accurate steady state output of the fundamental frequency component when the DC offset is present in the fault current. For this reason, the Cosine filter is one of the most widely implemented measurement algorithms in practical IEDs [6].

2.3.2. Performance of Measurement Algorithms

A number of studies that investigate the performance of digital measurement algorithms can be found in the literature. Mostly, these studies focus on the performance of measurement algorithms when their inputs are signals distorted by the decaying DC offset and harmonic components. Besides, those studies commonly use a method that is based on a partial derivative, in which only a single parameter (i.e. factor) of signals distortion is investigated. The investigated parameter is varied using several discrete samples around nominal values. Although a few studies consider the effect of multiple factors, their effects

are also studied by only varying one factor at a time and using several discrete values, while the remaining factors are fixed at nominal values. This method is known as the local sensitivity analysis method, and has disadvantages in terms of evaluating performance of measurement algorithms in fault conditions. The disadvantages of the local sensitivity analysis method are described in the next section. In this section, the latest published papers on performance testing methods used to evaluate the measurement algorithms of IEDs are presented.

Kezunovic, Kreso, Cain and Perunicic presented a methodology for the sensitivity evaluation of digital protective relaying algorithms in 1988 [31]. The authors evaluated the variation (i.e. influential) of power system conditions such as the system frequency; and the variation of algorithm parameters such as the sampling rate; on the performance of relaying algorithms. The variation values are based on a limited number of discrete values such as the system frequency, which was varied at three values: (60, 63 and 57) Hz. This work uses a 138kV transmission line modeled in the EMTP program to generate a high number of fault test scenarios. This work reports the result of sensitivity in terms of the estimated resistance (R) and reactance (X) of transmission lines using a statistical mean and standard deviation.

Altuve, Diaz and Vazquez presented a comparison evaluation of Fourier and Walsh's digital algorithms used in distance protection in 1995 [32]. The authors evaluated the digital algorithms in steady and transient states. This work uses different power systems modeled in the EMTP to generate input signals distorted by harmonics, white noise, exponential DC offset and high frequency oscillations. The steady state evaluation shows the results of digital algorithms for the attenuation of the DC offset and harmonics in terms of 'goodness' qualitative performance. Furthermore, this work reports the results for tracking the resistance (R) and reactance (X) of transmission line impedance in a transient state. This work concludes that the Cosine filter and full-cycle DFTs are the best performance measurement algorithms.

Wang investigated the steady state magnitude responses of Mann-Morrison (sample and first-derivative), Prodar (first- and second-derivative), full- and half-cycle DFTs, the Cosine filter, and the Least square and Kalman filtering algorithms in 1999 [9]. The author evaluated the performance of these measurement algorithms in a frequency domain, using

a proposed normalized variation band of magnitude. The normalized magnitude is defined by the upper and lower boundaries of filtering algorithm magnitude responses. This work reports that all the studied filtering algorithms, except the Mann-Morrison and Prodar, produce an accurate magnitude estimation of the fundamental frequency component.

Pascual and Rapallini presented an analysis behavior of the Fourier, Cosine and Sine filtering algorithms for impedance calculation in 2001 [4]. The authors evaluated the behavior of the filtering algorithms in steady and transient response. In the steady state, this work investigated the impact of using a data window of different lengths, (0.5, 1, 1.5 and 2) cycles on the output of the filtering algorithms. Besides, this work also investigated the impact of two different anti-aliasing low pass filters (LPFs): Butterworth and Chebychev, with ranges of cut-off frequencies. In transient response, the authors evaluated the behavior of the filtering algorithms when input current signals are distorted by the CT saturation. A 400/5 CT power test set was used to generate the input's test current signals. This work reported that the second order Butterworth LPF with a cut-off frequency of 400Hz and one cycle data window is the appropriate LPF and filtering algorithms for distance protection.

Yu, Huang and Jiang proposed new full-cycle DFT and half-cycle DFT measurement algorithms that are immune to the decaying DC offset in 2010 [33]. The proposed measurement algorithms produce fast estimation of fundamental frequency component since they require a full or half cycle data window, without an additional extra sample. The proposed measurement algorithms are based on the original full- and half-cycle DFTs. The computation of the proposed method requires splitting the computations of the original DFTs into four groups in which the parameter of the decaying DC offset can be estimated. Then, the estimated parameter is used to eliminate the decaying DC offset. This work evaluated the proposed full-cycle DFT using input test signals containing decaying DC offset and harmonic components: even and odd. Furthermore, this work evaluated the proposed half-cycle DFT using input test signals containing the decaying DC offset and only odd harmonics. In both evaluations, the authors used four discrete values time constant, (1/40, 1/80, 1/120, 1/160) seconds, of the decaying DC offset. This work compared results of the proposed measurement algorithms with the original DFTs with mimic filter, and Gu's algorithms. The results indicated that the proposed measurement

algorithms produce less error than those original DFTs with mimic filters and Gu's algorithms, using the two calculated performance indices: percentage root-mean-square error (PRMSE) and percentage peak error (PPE).

Karimi-Ghartemani, Ooi and Bakhshai investigated the DFT measurement algorithms for Phasor Measurement Unit (PMU) application in 2010 [34]. The authors investigated the influence of four input signal characteristics: off-nominal fundamental frequency, harmonics, inter-harmonics and interfering signals on the DFT measurement algorithm in steady state conditions. This work reported that the DFT measurement algorithm produces accurate phasor estimation in the presence of harmonics, and off-nominal fundamental frequency if the DFT is applied on the three-phase balance system providing the off-nominal fundamental frequency is known. The information of the known off-nominal frequency is used to compensate for the error during the calculation of the positive-sequence signals using a three-phase set of signals. However, for a single phase system, the DFT still produces error if the input signal is off-nominal frequency. This work reported that the DFT produces significant errors in the presence of inter-harmonic and interfering signals. The inclusion of 10% for inter-harmonic and interfering signals, as stated by IEEE C37.118-2005 Synchrophasor Standard [35], results in the calculated Total Vector Error (TVE) exceeding the 1% acceptable standard.

2.4. Discussion

The previous section presented the literature review on the performance evaluation of measurement algorithms with or without the sensitivity study. The section of the literature that analyses the sensitivity of measurement algorithms, however, uses the local sensitivity analysis. The local sensitivity analysis is not an appropriate method for the evaluation of measurement algorithms performance in fault conditions. This method has two main disadvantages:

▪ The method only varies one input factor while other factors are fixed at their respective nominal values. Thus, the result of the local sensitivity analysis method does not account for the interactions between two or among factors.

▪ The method also only investigates the performance of measurement algorithms around the nominal factor. It does not explore the input factor variation in a full-range (complete) factor space. Commonly, this method uses a few discrete samples around the nominal factor to evaluate the performance of measurement algorithms. Thus, the result of the local sensitivity method does not represent the overall (global) performance of measurement algorithms.

However, in fault conditions, more than one factor may change while other factors may also be initiated. In the protection of transmission lines, for instance, the fault inception angle can be at any point within $(0 - 2\pi)$ radians while the fault location can be at any location within $(0 - 100)$ % of the protected transmission lines. Thus, varying only one factor, the inception angle or fault location, is not an appropriate way to measure the uncertainty and sensitivity of measurement algorithms output in a global way. Moreover, the local sensitivity analysis is only accurate for a linear model. In protection systems, IEDs implement a variety of protection functions, in which these algorithms can be non-linear. Further, the instrument transformers that are used to supply input signals to the IEDs are the non-linear elements. Thus, the local sensitivity analysis is not an appropriate method to measure uncertainty and the sensitivity output of non-linear measurement algorithms or measurement algorithms where their linearity or non-linearity is unknown. As previously mentioned, one aim of this study is to evaluate the performance of measurement algorithms of a commercial IED where their mathematical algorithms are unknown, which means, unknown their linearity or non-linearity.

No literature using the global uncertainty and sensitivity analysis method for performance evaluation of measurement algorithm has been found. Thus, the aim of this study is to propose and demonstrate a methodology for the performance evaluation of the measurement algorithm using the global uncertainty and sensitivity analysis method. The proposed method provides more realistic test scenarios than the existing local sensitivity analysis method. The systematic methodology for evaluating measurement algorithms' performance in fault conditions is presented in such a way that it can be adopted and extended to evaluate a newly developed measurement algorithm or protection algorithms of IEDs.

The literature on the performance evaluations of measurement algorithms discussed in Section 2.3, specifically in the context of the uncertainty and sensitivity studies, may have the following deficiencies:

▪ The previous literature places more focus on the performance of protection algorithms of IEDs than the measurement algorithms. Thus, those studies often present their results in terms of the estimated impedance, resistance and inductance of transmission lines. Limited literature presents the characteristics of the unit-step response of the measurement algorithm, such as overshoot and steady state error. It should be noted that the characteristics of the unit-step response are the main criteria for evaluating the output transient response of measurement algorithms because their aim is to tracking the amplitude and phase angle of fundamental frequency components of input fault signals. During fault conditions, the unit-step is the most appropriate response for representing the change of the fundamental component in fault signals.

▪ The published papers introduce a number of performance indices to measure errors on the output transient response of measurement algorithms such as the Percentage of Maximum Overshoot [18]. The introduced indices are useful indicators for measuring the performance of the measurement algorithms. However, none of the literature attempts to quantify the contribution of all input factors to the calculated errors using systematic analysis. All the published papers show only the calculation of errors on the output of measurement algorithms without knowing the fractional contribution of each input factor.

▪ The published papers perform a partial derivative, which is the local sensitivity analysis method. In this method, only one factor is varied while other factors remain unchanged. Moreover, the local sensitivity analysis method is unable to measure the influence of factor interactions on the output of measurement algorithms. As previously mentioned, fault conditions result in the variation of more than one factor. The interactions of factors can show a strong influence on the output of measurement algorithms. Thus, the global sensitivity analysis that can measure the influence of factor interactions on the output of measurement algorithms is the more appropriate way to analyze the performance of measurement algorithms, including their sensitivity, in fault conditions.

2.5. Discrete Fourier Transform Measurement Algorithms

The DFT measurement algorithms estimate the signal component of input signals based on the Fourier theory. The signal component should be a part of the input signals. The main process for the estimation of the signal component consists of the convolution of input signal samples with the DFT measurement algorithm coefficients, summation and multiplication to produce real and imaginary parts, and finally combining those parts [36]. The output of the estimated signal component (phasor) can be in the form of the peak or root-mean-square (RMS) value.

The DFT measurement algorithms can be classified according to two common categories: data window length; and recursive or non-recursive. Table 2.1 shows these categories with examples of the DFT measurement algorithms.

Table 2.1 Two common categories of DFT algorithms

Data window length	Recursive/Non-recursive
▪ Short data window Half-cycle DFT ▪ Long data window Full-cycle DFT, Cosine filter	▪ Recursive Half-cycle DFT, full-cycle DFT ▪ Non-recursive Half-cycle DFT, full-cycle DFT, Cosine filter

Based on the data window length, a short data window is defined as a measurement algorithm with a length of data window less than one-cycle of the fundamental frequency component. In contrast, a measurement algorithm with at least one cycle data window is considered as a long data window. The DFT measurement algorithms can also be configured to several multiple or half-multiple cycles of the data window such as one and

half-, two-, three-cycle, etc [4]. However, the most widely used is the half-cycle DFT for high-speed IEDs; and the full-cycle DFT and Cosine filter for non high-speed IEDs.

Measurement algorithms may also be categorized as recursive or non-recursive. Recursive algorithms, also known as the infinite impulse response (IIR), use a set of sample values and the previous estimation value for phasor estimation. In contrast, non-recursive algorithms or finite impulse responses (FIR) only use a set of sample values without the previous estimation value.

It is worth highlighting that the full- and half-cycle DFT can be configured as both recursive and non-recursive algorithms. However, the Cosine filter can only be configured as the non-recursive algorithm [37]. In the power system protection, the non-recursive algorithm is preferable to the recursive algorithm since it avoids the influence of pre-fault samples during fault detection [1]. In this thesis, the DFT measurement algorithms have been classified based on their data window length since the studied measurement algorithms: the full-, half-cycle DFT, and the Cosine filter, are all non-recursive algorithms.

Most of the protection algorithms use a fundamental frequency component for fault detection and executing protection functions. For this reason, most measurement algorithms, therefore, are required to estimate the fundamental frequency component. To describe how the fundamental frequency component is estimated by DFT measurement algorithms, consider an input signal to measurement algorithms as illustrated in Figure 2.5.
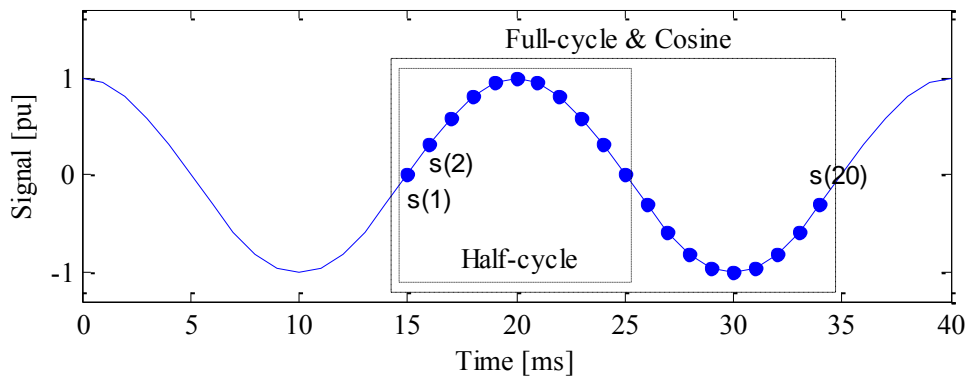
Figure 2.5 Data window of measurement algorithms

Figure 2.5 shows input signals (including sample points) and two types of data windows: the half-cycle DFT; and the full-cycle DFT or Cosine filter. The data window is used to obtain samples from the input signal and it always contains the same number of samples during the estimation process. As a new sample enters the data windows, the old sample will be discarded. In this Figure, for example, the data window of the full-cycle DFT will always contain the number of the sample point of ($N = 20$). The successful samples within the data windows will be processed to estimate the amplitude and phase angle of the fundamental frequency component. Details of the estimation process of three DFT measurement algorithms: the full- and half-cycle DFT and the Cosine filter are described next.

2.5.1. The Full-Cycle DFT

The full-cycle DFT estimates the fundamental frequency component based on a one-cycle moving data window. The samples within the data window, based on Figure 2.5, are $s(k)$ where $k = 1,2,...,20$. These samples are used to calculate the real and imaginary parts of the fundamental frequency component. The real and imaginary parts calculated by the full-cycle DFT are given by Equations (2.1) and (2.2) respectively.

$$S_{1r}(n) = \frac{2}{N} \sum_{k=1}^{N} s(n - N + k) . \cos \frac{2\pi k}{N} . \tag{2.1}$$

$$S_{1j}(n) = \frac{2}{N} \sum_{k=1}^{N} s(n - N + k) . \sin \frac{2\pi k}{N} . \tag{2.2}$$

Where N -   number of sample in one cycle of the fundamental frequency component

        subscript *1*   -   indicates full-cycle DFT

subscript r and j -   real and imaginary parts

Next, the full-cycle DFT estimates the peak amplitude and phase angle of the fundamental frequency phasor using Equations (2.3) and (2.4), respectively.

$$|S(n)| = \sqrt{S_{1r}^2(n) + S_{1j}^2(n)}. \qquad (2.3)$$

$$\theta(n) = \tan^{-1}\frac{S_{1j}(n)}{S_{1r}(n)}. \qquad (2.4)$$

2.5.2. The Half-Cycle DFT

The half-cycle DFT is the improved version of the full-cycle DFT in terms of its computation speed since it uses only half of one cycle data window. Ideally, the half-cycle DFT should produce faster speed in estimation of the fundamental frequency component than the full-cycle DFT by a factor of two. This is, however, only true if the input signals are purely the fundamental frequency component. If the input signal contains nuisance signals, particularly the decaying DC offset, the estimation speed of the fundamental frequency component can be longer than the full-cycle DFT.

The half-cycle DFT computes the fundamental frequency component in a similar way as the full-cycle DFT. However, as described, the half-cycle DFT uses a half-cycle data window. Equations (2.5) and (2.6) describe the calculation of the real and imaginary parts of the fundamental frequency component by the half-cycle DFT.

$$S_{2r}(n) = \frac{4}{N} \sum_{k=1}^{\frac{N}{2}} s(n - N + k) . cos\frac{2\pi k}{N}. \tag{2.5}$$

$$S_{2j}(n) = \frac{4}{N} \sum_{k=1}^{\frac{N}{2}} s(n - N + k) . sin\frac{2\pi k}{N}. \tag{2.6}$$

Where   subscript *2*   -   indicates half-cycle DFT

The half-cycle DFT estimates the amplitude and phase angle of the fundamental phasor in a similar way using Equations (2.3) and (2.4), respectively.

2.5.3. The Cosine Filter

The Cosine filter is a derivative of the full-cycle DFT measurement algorithm. The Cosine filter uses only the cosine term (i.e. Equation (2.1)) to calculate the real and imaginary parts of the fundamental frequency component. The real part calculated by the Cosine filter is exactly the same as the real part calculated by the full-cycle DFT. However, the imaginary part of the Cosine filter is a delay of its real part by a quarter of one cycle ($N/4$). Equations (2.7) and (2.8) describe the calculation of real and imaginary parts of the fundamental frequency component by the Cosine filter:

$$S_{3r}(n) = \frac{2}{N} \sum_{k=1}^{N} s(n - N + k) . cos\frac{2\pi k}{N}, \tag{2.7}$$

$$S_{3j}(n) = S_{3r}\left(n - \frac{N}{4}\right). \tag{2.8}$$

Where   subscript *3*   -   indicates the Cosine filter

The Cosine filter estimates the amplitude and phase angle of the fundamental phasor in a similar way using Equations (2.3) and (2.4) respectively.

In normal conditions, in which the input signals to measurement algorithms are purely the fundamental frequency components, all the DFT measurement algorithms: the full-, half-cycle DFT and Cosine filter, are able to estimate the fundamental frequency component with high accuracy in a steady state. The difference among them lies in their speed of estimation of the fundamental frequency component since they have different data window lengths.

To illustrate their difference in the estimation speed of the fundamental frequency component, Figure 2.6 shows the simulated purely fundamental frequency component and the amplitude estimation by the full-, half-cycle DFT and Cosine filter.
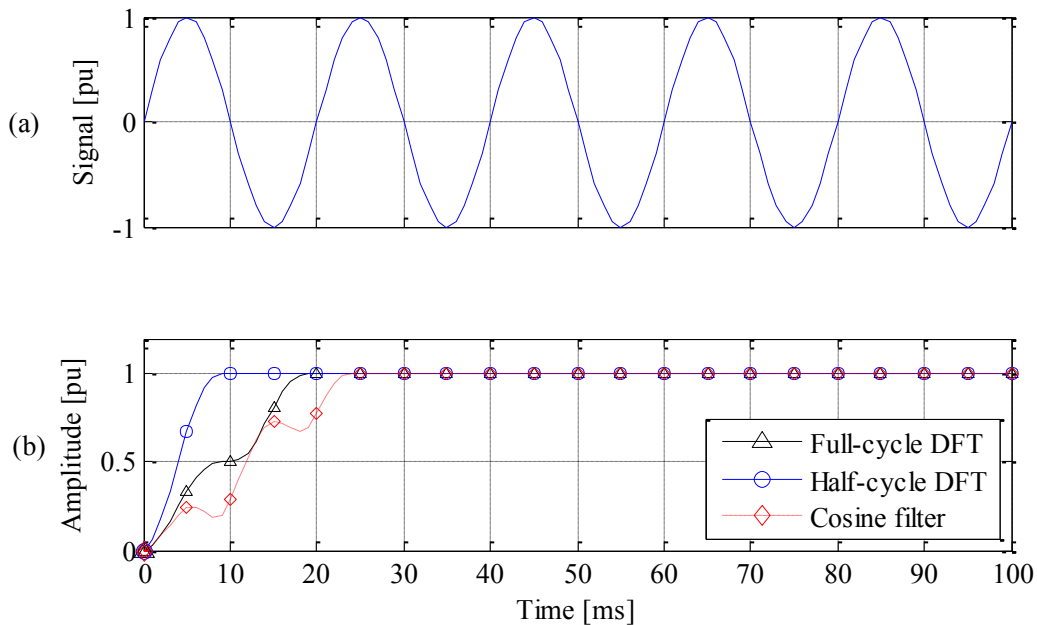
Figure 2.6 Transient responses of the DFT measurement algorithms to an input signal.
(a) A purely sinusoidal input signal (b) Amplitude transient responses

It shows that all measurement algorithms achieve a steady state value of 1 per unit (p.u.) after their respective data windows have elapsed. The data window of the half-, full-cycle DFT and Cosine filter are (10, 20 and 25) milliseconds respectively, that based on the 50Hz fundamental frequency component. The estimation speed by the half-cycle DFT is the fastest, which is 10ms. The second fastest is the full-cycle DFT (20ms), followed by the Cosine filter algorithm (25ms).

As previously mentioned, a variety of nuisance signals that distort input signals to measurement algorithms is produced in fault conditions. One of the most studied nuisance signals is the decaying DC offset. To briefly investigate how the decaying DC offset affects the full-, half-cycle DFT and Cosine filter, this signal is simulated in input to those measurement algorithms and we observe their outputs.

Figure 2.7 shows the simulated decaying DC offset on the input signal of the purely fundamental frequency component and the amplitude estimation by those three measurement algorithms. The half-cycle DFT is seen to be the worst measurement algorithm in terms of amplitude overshoot and settling time. The maximum amplitude overshoot of the half-cycle DFT, in this example, is almost 100%. Such high amplitude overshoot may result in the IEDs overreaching [38]. Moreover, the half-cycle DFT only achieves its steady state value nearly 80ms after the fault.
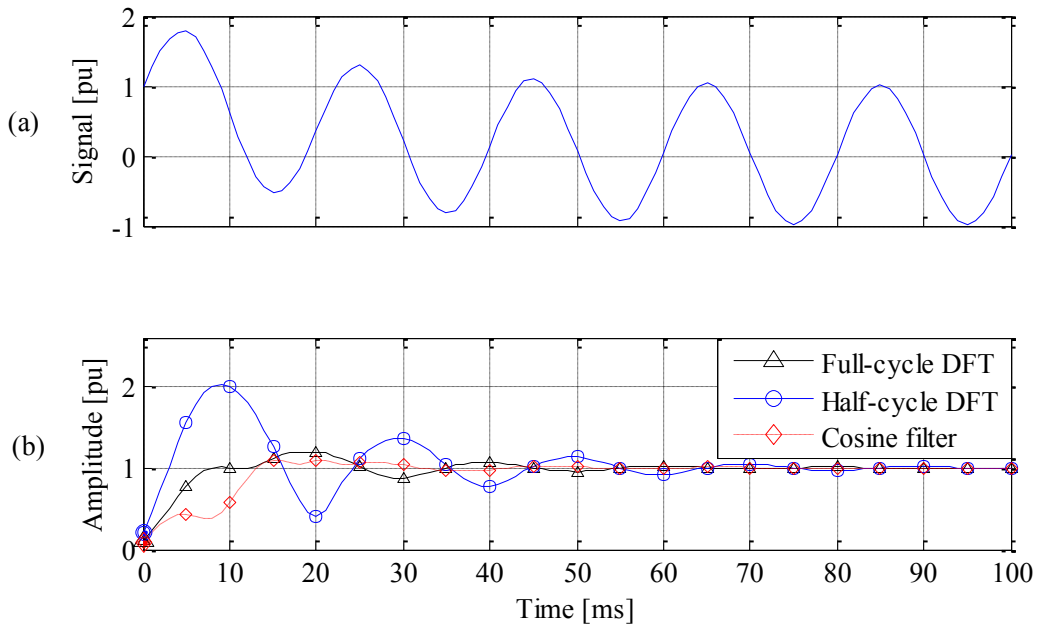
Figure 2.7 Transient responses of DFT measurement algorithms to an input signal. (a) An input signal with high DC offset (b) Amplitude transient responses

Figure 2.8 shows the enlarged version of Figure 2.7. Three labeled data tips, from left to right, show the maximum amplitude response of the half-, full-cycle DFT and Cosine filter respectively, after their respective data window has elapsed. The output of the full-cycle DFT shows that its maximum amplitude overshoot is 19.6%. The Cosine filter produces a maximum overshoot of only 7%.
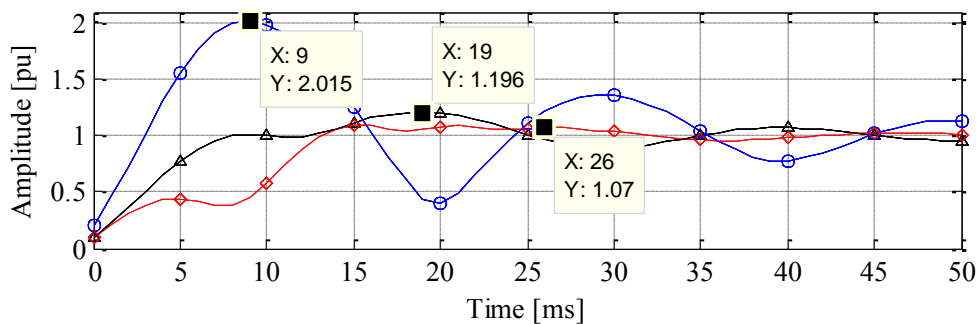
Figure 2.8 Enlarge version of amplitude transient responses of measurement algorithms to an input signal contains high DC offset

Due to the great performance of the Cosine filter when input fault signals containing the DC offset and other nuisance components, the Cosine filter algorithm has become one of the important measurement algorithms amongst the DFT based algorithms. Besides the performance, its practical implementation is easier than the full- and half-cycle DFT since the imaginary part of the Cosine algorithm avoids the multiplication and summation process as described by Equation (2.8). This advantage reduces the computational burden of the microprocessor used in IEDs. In this thesis, the proposed global uncertainty and sensitivity analysis is demonstrated by evaluating the performance of the Cosine filter in simulation-based.

The preceding brief investigation, however, demonstrates the effect of a single factor (i.e. decaying DC offset) without considering other factors such as multiple harmonic components that may also be present in the input signals. Further, the uncertainty of the decaying DC offset factors: amplitude and its time constant are not considered. Investigating the impact of all unpredictable factors within their ranges of uncertainties to the output performance of measurement algorithms, a global uncertainty and sensitivity analysis method is required. The concept of uncertainty analysis as well as sensitivity analysis and the main steps for their implementation will be described in the next chapter.

2.6. Conclusion

The basic elements of IEDs and their functions have been presented in this chapter. The importance of measurement algorithms to accurately and quickly estimate the fundamental frequency component for the successful use of a variety of protection algorithms and analysis algorithms is highlighted.

The literature on the early development of digital measurement algorithms that are based on the short data window for IEDs is presented. The literature on the three most popular DFT measurement algorithms: the full-, half-cycle DFT and Cosine filter implemented in the IEDs have also been presented.

The performance of measurement algorithms, particularly the DFT, and the method used for the performance evaluation studied by previous researchers have been reviewed.

The deficiencies of the method used, which is the local sensitivity analysis, are described. In contrast, the justification of using a new methodology, which is the global uncertainty and sensitivity analysis method, has been described.

The process for estimating the fundamental frequency component by the three popular DFT measurement algorithms is presented. The poor performances: low accuracy and slow speed in estimation of the fundamental frequency component by the DFT measurement algorithms when their inputs are the signal distortion, are briefly described. The comparison of the output transient responses among these three DFT measurement algorithms for tracking the fundamental frequency component, when the input signals are purely sinusoidal and non-sinusoidal, is illustrated.

Chapter 3. Uncertainty and Sensitivity Analysis Methods

3.1. Introduction

Currents and voltages are the main input signals to IEDs for the monitoring, controlling and protection of power systems. However, faults in power systems initiate a variety of nuisance signals that distort the input signals. As measurement algorithms of IEDs are sensitive to the input signals with distortion, they produce measurement errors that may result in incorrect operation of the IEDs.

The errors on the output of measurement algorithms are uncertain because the parameters of nuisance signals that contribute to those errors are unpredictable. The reason for unpredictable parameters is that they are dependent on random factors such as fault location. Due to the uncertainty of the produced errors, analyzing these errors cannot simply be done by calculating them using the nominal values of the nuisance parameters. Indeed, the calculation of errors that is based on nominal values does not represent the overall errors caused by uncertainty of nuisance signals. Thus, it is important to use an

appropriate method to calculate the uncertainty of errors on the output of measurement algorithms when their inputs are affected by the uncertainty of the nuisance components.

The appropriate method to analyze the errors influenced by the uncertainty of nuisance components is to perform a statistical error analysis, also known as the uncertainty analysis. The uncertainty analysis measures the uncertainties on the outputs (i.e. errors) of the measurement algorithm due to the uncertainties of nuisance signals in the input signals. This method is the most appropriate method for investigating the uncertainty of errors on the model outputs when the model inputs involve uncertain parameters.

Another analysis, which is closely related to the uncertainty analysis, is a sensitivity analysis. The sensitivity analysis measures the degree of contribution by a single input parameter and the interactions of parameters to the errors in the output of the measurement algorithms. Thus, the sensitivity analysis can be regarded as a complement to the uncertainty analysis. Both analyses may lead to better understanding of the behavior of measurement algorithm outputs during fault conditions.

In the uncertainty and sensitivity study, the terminology 'input factor' is commonly used to refer to the parameter of the input uncertain signals. Thus, the rest of this thesis uses the term 'factor' to to refer to the parameter of nuisance signals.

This chapter continues with Section 3.2, in which the concept of the uncertainty analysis is introduced. The uncertainty analysis is used to evaluate the performance of measurement algorithms. This section also describes the limitations of implementing the uncertainty analysis. Next, Section 3.3 presents the concept of the sensitivity analysis. Sections 3.4 and 3.5 present details of two global sensitivity analysis methods: the Morris and EFAST, respectively. These methods are the main techniques used in this thesis. Section 3.6 discusses the source of nuisance signals and the factors describing them. Section 3.7 shows the common factors studied and illustrates their influence on the output of the Cosine filter. Finally, Section 3.8 provides the conclusion of this chapter.

3.2. Uncertainty Analysis (UA)

In many fields of study, including engineering, inputs and parameters of mathematical models can be uncertain because of a variety of factors such as measurement errors or lack of information. These uncertainties result in the output of the mathematical model being uncertain as well. It is important to measure the degree of uncertainty in the model output since it provides a level of confidence, and thus, performance of the model.

Figure 3.1 shows a graphical illustration of how uncertainties in input factors propagate through the model to produce output uncertainty. Assume the n input uncertain factors so they are represented by $X = (x_1, x_2, \ldots, x_n)$. The uncertainty of each input factor depends on its possibility of occurrence, which is represented by a probability distribution $p(X)$. The uncertainties of these input factors propagate through the evaluated model $y = f(X)$ to produce the uncertainty output of the model.
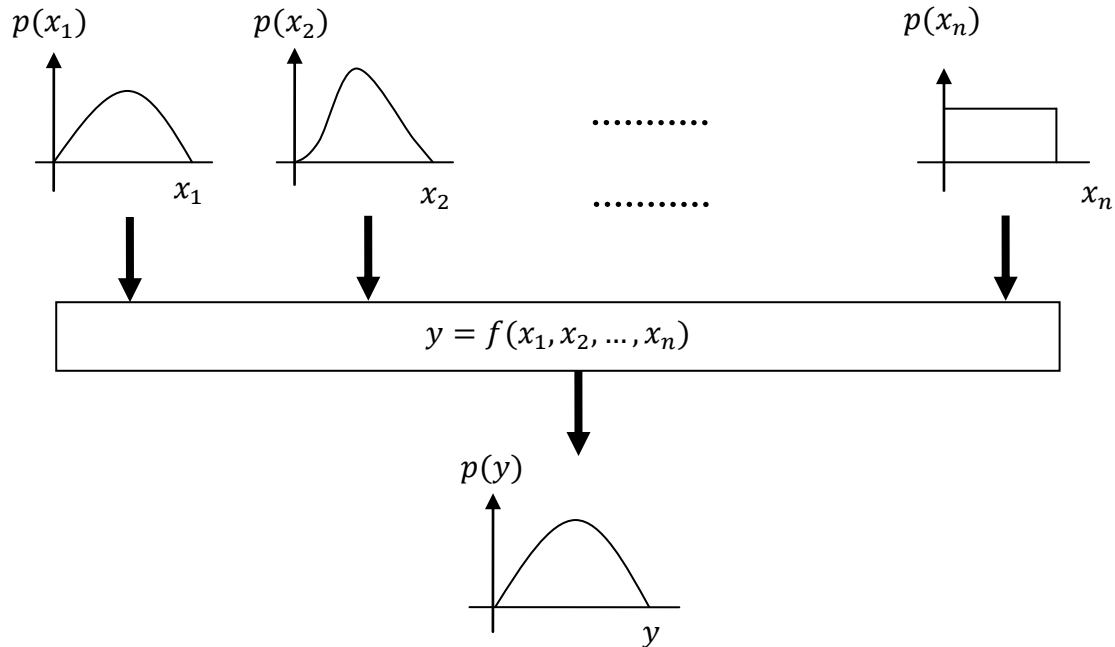
Figure 3.1 Graphical illustration of uncertainty analysis

Thus, the uncertainty analysis is a study of how the uncertainty in the input factor of a model produces the uncertainty in its outputs. As previously mentioned, the term 'input factors' used in the uncertainty and sensitivity study includes the parameter uncertainty of a model.

It should be emphasised, however, that uncertainty analysis differs from calculating an error. An error is a measurement of a difference between the true and measured value, which is represented by a fixed number. However, the uncertainty analysis consists of all possible measurement errors that are tabulated in terms of the probability distribution function (PDF).

There are two types of input uncertainties: aleatory and epistemic [39]. Aleatory uncertainty is due to the variability of a system in a natural way. It occurs naturally and, therefore, it is irreducible. Epistemic uncertainty, however, is due to lack of knowledge. It can be reduced if the knowledge of the uncertainty is improved. This thesis aims to evaluate measurement algorithms' performance by measuring their output uncertainty regardless of the types of input factor uncertainties.

The most common methods used in the uncertainty analysis study are the Taylor Series Method (TSM) and Monte Carlo (MC) method [40]. This thesis, however, uses the latter, which is a powerful method for uncertainty analysis [39]. The Monte Carlo method works based on input samples. Thus, this method requires the input factors to be sampled within their complete factor space uncertainties. Then, the method applies each sample point to the input of a model for execution. This process is repetitively executed using different sample points until all the input sample points are evaluated. The method tabulates the output deviation or errors that represent the uncertainty of the model output.

Ideally, the result of uncertainty analysis by the MC method is has a high degree of accuracy if a high number of sample points is used. The high number of sample points is required in such a way that it can represent the complete input factor distribution. However, the main limitation of using a high number of sample points is computational time. As the number of investigated input factors increases, the evaluation time by the MC method can be longer. This limitation might be uncritical in a computer simulation since a high-speed computer is available. However, the practical implementation of the uncertainty

analysis can be prohibitive since most often practical evaluations would require a much longer duration than its model simulations. It may take weeks or months to complete the evaluation process, depending on the execution time and the complexity of the model.

In this thesis, two consecutive global sensitivity analysis methods, known as the two-stage analysis, are performed in such a way that they can be easily performed in the simulation as well as implemented in practical testing. Details of the two methods, Morris and EFAST, will be described in Sections 3.5 and 3.6, respectively.

3.3. Sensitivity Analysis (SA)

Uncertainty analysis, described in the previous section, measures output uncertainty (i.e. performance) of a model due to the uncertainty of its input factors. This analysis does not provide information about the contribution of the input factors to the output uncertainty. In most studies, it is also important to measure the fractional contribution of input factors to the output uncertainty so that the information may be used to optimize the model output.

The sensitivity analysis is a method that can be used to measure the contribution of input factors to the uncertainty of model output. Thus, it is defined as a study on how the variation in the outputs of a model can be apportioned (qualitatively or quantitatively) to different sources of input variations [8].

A variation in the input factor to a model produces variation in the model output. The degree of the ouput variation is related to the sensitivity of the model output. A model output is considered to have a high sensitivity if a unit variation of the input factor produces a high variation in the model output. In contrast, the model output is considered to have a low sensitivity if the same unit of variation produces a low variation in the model output.

To overview and better understand the sensitivity analysis, consider a normal distribution of a single uncertain input factor (x_1) with two simple linear models: low sensitivity (y_1) and high sensitivity (y_2) curves, shown in Figure 3.2. The propagation of the uncertainty of the same input factor (x_1) through both models and the corresponding

output uncertainties is illustrated. Sensitivity analysis, therefore, tries to determine the relationship (sensitivity curve) between the input and the output uncertainties. In this simple example, the relationship can be obtained by mapping samples of the input factor to the samples of the output response of the model. This is known as the input to output mapping, which works well in simple models.
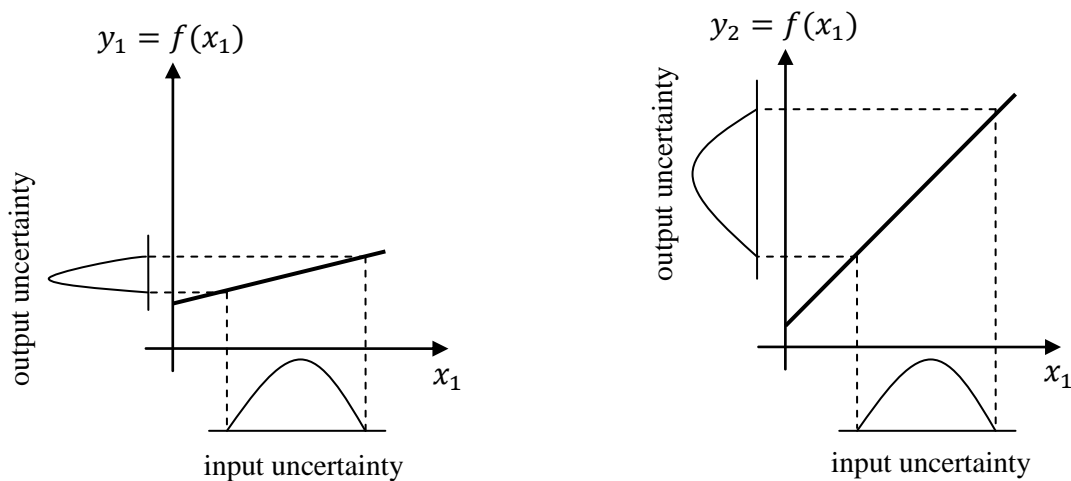
Figure 3.2 Sensitivity of two simple linear models

In general, the relationship between the input and output uncertainties can be linear or non-linear and monotonic or non-monotonic. Moreover, the number of uncertain factors to the model input can be high, in which each factor can be other than the normal distribution. Thus, a complex relationship between the input and output uncertainties may exist. Such a complex relationship, however, requires more robust and suitable methods than the method of mapping between the input and output samples. One option is a variance-based method, which is introduced in Section 3.6.1. A variance-based method is used as the main method for global uncertainty and sensitivity analysis.

There are many methods of the sensitivity analysis such as Morris, EFAST and Quasi-Monte Carlo (QMC) with Sobol sequence sampling [8, 12]. They can be classified in a variety of ways. Two common classes of sensitivity methods are based on the results

of sensitivity and the factor exploration. Table 3.1 shows the two classes of sensitivity analysis with their examples of the sensitivity method used.

Table 3.1 Two common classes of sensitivity analysis

Sensitivity results	Factor exploration
▪ Qualitative Morris	▪ Local Parameter perturbation, Differential analysis
▪ Quantitative FAST, EFAST, QMC with Sobol sampling sequence	▪ Global Morris, FAST, EFAST, QMC with Sobol sampling sequence

In this thesis, the sensitivity analysis has been divided into three classes: screening, local and global sensitivity analysis. They can be described as follows:

1. Screening

Screening is a sensitivity analysis method used to identify the important (also unimportant) input factors or clusters among the total investigated factors. The screening method ranks the important factors in a qualitative way. A qualitative result means that the fractional contribution of the input factor is unknown. Thus, the screening method is often used as a preliminary sensitivity analysis for a model that has many input factors. The screening method identifies the important factors in which these important factors will be used in the next comprehensive sensitivity analysis. As this method produces a qualitative, rather than quantitative sensitivity result, this method is computationally cheap.

2. Local Sensitivity Analysis

This method measures the sensitivity of the model output based on the variation of one input factor at a time (OAT) while other input factors are maintained at their nominal values. This method produces the first-order sensitivity index, also known as the first-order

effect. This index indicates the contribution of the main input factors on the model output. The computation requirement of this method is often moderate.

3. Global Sensitivity Analysis

The global sensitivity analysis measures the sensitivity of the model output based on the variation of all input factors simultaneously. Furthermore, this method varies all the input factors within their boundaries (globally) in multi-dimensions. Thus, this method explores uncertainty input factors in complete experimental spaces. This method produces the first- and higher-order sensitivity indices. The high-order sensitivity index shows the contribution of interactions of factors on the model output. This method requires more expensive computation in comparison with the local sensitivity analysis.

The aim of this study is to measure the performance of measurement algorithms implemented in IEDs using the global uncertainty and sensitivity analysis method. As discussed, the global uncertainty and sensitivity analysis method requires extensive evaluation, which means expensive computational time. To realize the implementation, specifically in practice, a two-stage global sensitivity analysis is performed. The first-stage is the Morris method [12] to screen unimportant nuisance factors among all factors being studied. The second-stage is the Extended Fourier Amplitude Sensitivity Test (EFAST) [13] method to provide results of the global uncertainty and sensitivity analysis. Sections 3.5 and 3.6 provide details of the Morris and EFAST method, respectively.

3.4. UA/SA Structures

The uncertainty and sensitivity analysis method requires four basic steps [8]. The same steps can be used to obtain uncertainty results as well as sensitivity results. Figure 3.3 shows these main steps for performing the global uncertainty and sensitivity analysis.

The first three steps for performing both uncertainty and sensitivity analyses require the same process. The final step, however, is to distinguish between the uncertainty and the sensitivity analyses. While the uncertainty analysis measures the uncertainty output of

measurement algorithms, the sensitivity analysis measures the contribution of the nuisance factor to the output uncertainty.
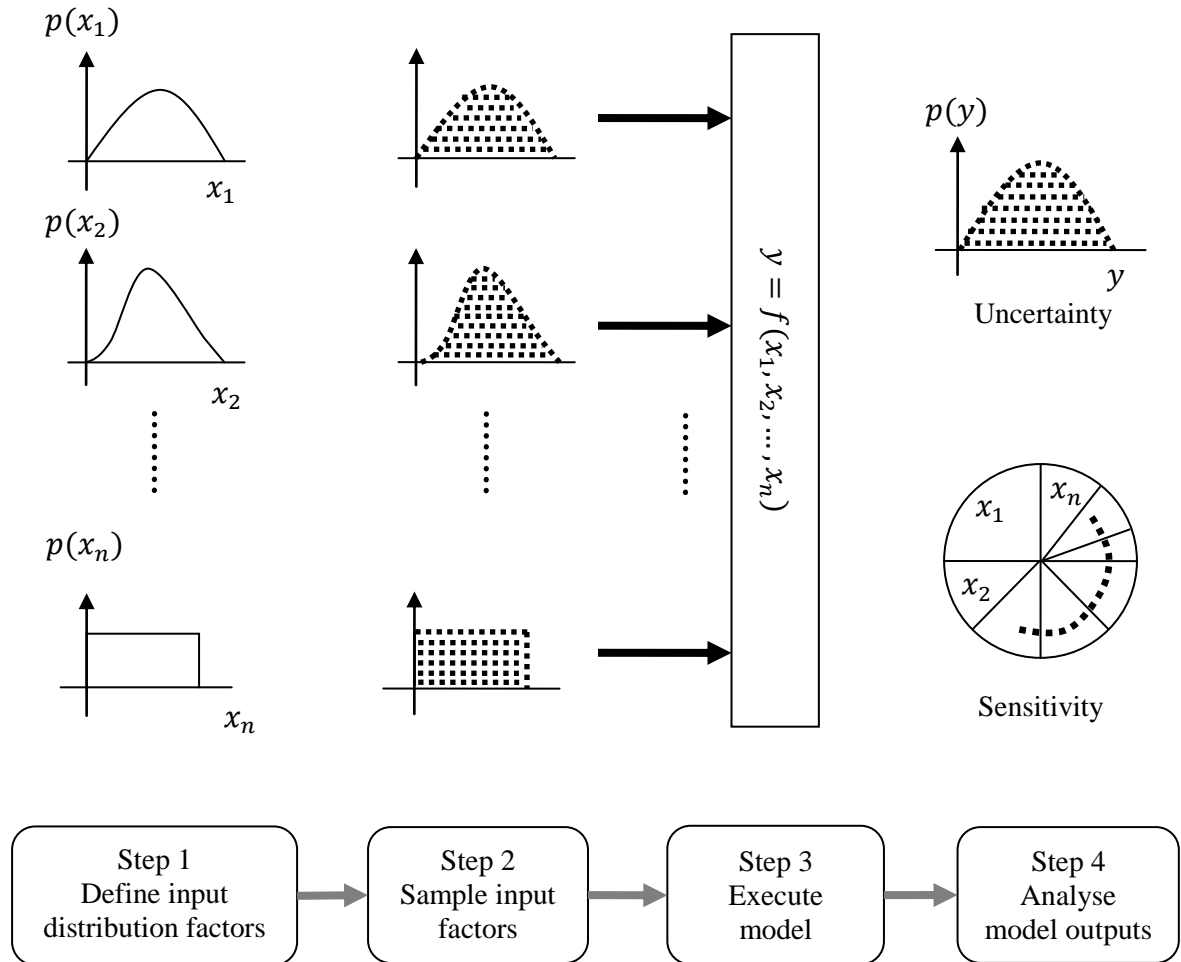
Figure 3.3 Steps for performing global uncertainty and sensitivity analysis

The following provides a detailed description of the four main steps for performing uncertainty and sensitivity analysis.

1. Define input distribution factors

The first step in implementing uncertainty and sensitivity analysis is to define the input factors $(x_1, x_2, ..., x_n)$ that need to be investigated for their influence. These factors

are defined with their uncertainties using appropriate probability distribution functions (PDFs). The selected PDFs of nuisance factors indicate their probability of occurrence, which can be based on expert reviews, scientific literatures or surveys.

2. Sample the input factors

The second step is to produce statistical samples of each input factor within their PDF distributions. The strategy to generate samples and the produced total number of samples is determined by the method of sensitivity analysis used. For example, Morris generates samples based on the percentage variation of factors within their dimensions. This method also produces the lowest number of sample among sensitivity analysis methods that is given by $N(k + 1)$, where $N \sim 10$ and k is the number of factors. Details of the Morris method are described in Section 3.5.

3. Execute algorithm model

The third step is to solve (i.e. execute) the algorithm model. Each sample set produced in the previous step is applied to the input of the model for execution to obtain the model output. The sample set is a set of points from each of the factor samples. Each of the sample sets differs in that it represents a unique case to the model input. The execution of algorithms of the model is repeated until all the sample sets are solved.

4. Analyze the model output

The final step for performing the uncertainty and sensitivity analysis is to obtain its results. The available results depend on the method of the uncertainty and sensitivity analysis used. The Morris method, for example, performs only the sensitivity analysis, and therefore, it produces results of sensitivity of input factors to the model output. A comprehensive sensitivity analysis method, such as the EFAST method, performs both uncertainty and sensitivity analyses. The EFAST method produces results for these two analyses.

3.5. Morris Method

The Morris is a unique type of global sensitivity analysis method although it calculates sensitivity indices based on the One-factor-At-a-Time (OAT) basis. The method is commonly used for the purpose of screening the important (also unimportant) factors. It is widely used because of its efficiency, independence and simplicity [41]. The Morris method requires a low number of samples for its computation. It produces qualitative results, which means it does not calculate the percentage of the influence of each factor to the model output in a numerical way. This method is often used as the preliminary sensitivity analysis before performing more comprehensive sensitivity analysis, which produces detailed (i.e. quantitative) results.

The idea of the sensitivity analysis according to the Morris method is that the most influential factor is determined by the highest output variance of the same percentage of perturbation of its input uncertain factors. To understand how the Morris method works, consider a model described by a function:

$$Y = f(X), \tag{3.1}$$

where $X = x_1, \dots, x_n$ -   model input consisting of n factors

$Y = y_1, \dots, y_m$ -   model output consisting of m output response

Assume that the dimensions of each factor (X) are scaled within $(0 - 1)$. The sample points of each factor are determined by the number of the grid level (L_G) used so that their values are within $(0, \frac{1}{L_G-1}, \frac{2}{L_G-1}, \dots, 1)$. The grid level determines the resolution of the sample points to be produced. A high number of grid levels produce high resolution sample points. Figure 3.4 shows an example of two grid levels: L_G=4 and L_G=8 for three factors.
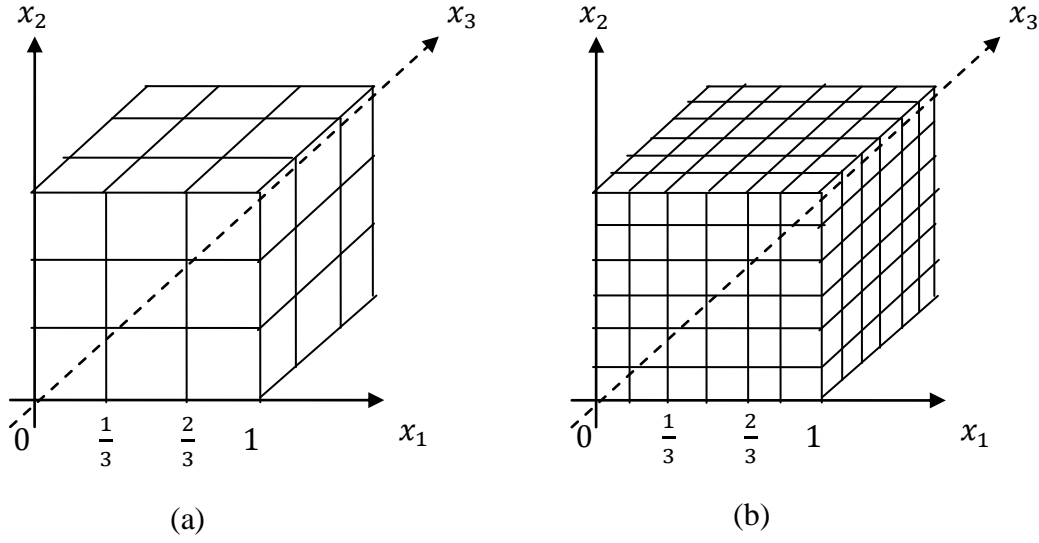
Figure 3.4 Comparison between two grid levels (a) $L_G=4$, (b) $L_G=8$

To obtain a matrix of samples, the Morris method performs a sampling strategy by varying one factor at a time (OAT). The OAT means that only one factor is varied between two consecutive sets of samples. However, the sampling strategy of the Morris method produces samples in a way such that the samples represent complete ranges of multi-dimension uncertain factors through its global sampling approach. Thus, it is considered as a unique global sensitivity method although it is based on the OAT.

Appendix A shows an example of how the Morris method produces the matrix of samples for each input factor for three factor dimensions. Using the matrix samples, the impact of changing the ith input factor on the model output, known as the elementary effect $EE_i(X)$, can be calculated.

$$EE_i(X) = \frac{Y(x_1, \ldots, x_i + \Delta, \ldots, x_n) - Y(X)}{\Delta}.$$ (3.2)

Where Δ -   predetermined perturbation

        $Y(X)$ -   model output without perturbation

        $Y(x_1, \dots, x_i + \Delta, \dots, x_n)$ -   model output with perturbation of $i^{th.}$ factor

Next, the standard statistical mean and standard deviation values (μ, σ) of the set of EE_i are calculated for each input factor. The calculated mean and standard deviation values identify the factor that has the following influence on model output:

- Linear influences

- Non-linear or interaction influences

- Negligible influences

The high mean value indicates the high overall (i.e. linear) influence of the factor. The high standard deviation value indicates the high interaction, or the non-linear factor. In contrast, the mean and standard deviation values that are close to zero indicate the unimportant (i.e. negligible) factors. It should be noted that the calculated mean and standard deviations by the Morris method are qualitative measures. Thus, the percentage of sensitivity among factors is invalid as a means of comparison.

3.6. EFAST Method

The EFAST is a global uncertainty and sensitivity analysis method. The EFAST method was developed by Saltelli et al [8, 42]. This method is a variance-based method. To understand how the EFAST method works, the uncertainty and sensitivity analysis based on the variance-based method is firstly described in general, since the principle of the EFAST method is based on the variance-based method. The section continues to present briefly the variance-based method prior to presenting the detail of uncertainty and sensitivity analysis performed by the EFAST method.

3.6.1. Introduction of Variance-based Method

The variance-based sensitivity analysis measures the uncertainty and sensitivity of the model outputs based on analyzing the output variance. Any variation of input factor results in a variation in the model output. The degree of the output variation, however, is determined by the sensitivity of the model output. Also, the variation of different input factors produces different degrees of variation in the model output. Thus, the most influential factor using the variance-based method is determined by the highest percentage of contribution of the input factor to the total output variance.

In the variance-based method, the only important information is the knowledge of variations in the model input as well as the calculated output variance. These variations are used for estimating the uncertainty and sensitivity of the model output. The mathematical structure, linearity or non-linearity, and complexity of the model algorithms can be unknown. For this reason, the variance-based method is a powerful method for investigating uncertainty and sensitivity of output model.

To understand how the uncertainty and sensitivity are measured by the variance-based method, consider a complex model shown by a response surface in Figure 3.5. For illustration simplicity, assume that only two input factors (x_1, x_2) with their respective PDFs $(p(x_1), p(x_2))$ are studied. The variance-based method estimates the uncertainty and sensitivity of the model output as follows.

To estimate the uncertainty of the model output, the variance-based method randomly samples the input factors within their complete PDFs. In this example, the region of the uncertainty analysis is bound by the area of ABCD, shown in the Figure 3.5. This method then applies the sample of factors to the model input to solve the complex model in order to obtain a model output. The process of applying the samples of input factors is repeated for another sample until all the input sample points are evaluated. Then, this method tabulates the corresponding model outputs using a histogram to obtain an output distribution. The output distribution represents the uncertainty of the model output (i.e. $p(y)$).

Figure 3.5 Response surface using the variance-based method [43]

To estimate the sensitivity of the model output, the variance-based method analyses the produced output variance. The variance-based method calculates the mean value and total variance of the output distribution ($p(y)$) using the standard statistical analysis. The mean ($\bar{y}$) and total output variance (s^2) are described by Equation (3.3) and (3.4), respectively.

$$\bar{y} = \frac{1}{N_s} \sum_{i=1}^{N_s} y_i. \tag{3.3}$$

$$s^2 = \frac{1}{N_s - 1} \sum_{i=1}^{N_s} (y_i - \bar{y})^2. \tag{3.4}$$

Where N_s -   number of samples

          y_i - $i^{th.}$ model output

According to the analysis of variance (ANOVA), the total output variance (V_{total}), where ($V_{total} = s^2$), can be decomposed into the sum of the variance contributed by the uncertain factors of incremental dimensions such that [8]:

$$V_{total} = \sum_{1 \le i \le n} V_i + \sum_{1 \le i < j \le n} V_{i,j} + \dots + V_{1,2,3,\dots,n} \,, \qquad (3.5)$$

where V_i -   variance contributed by $i^{th.}$ input factor

          $V_{i,j}$ -   variance contributed by interaction of factors $i^{th.}$ and $j^{th.}$.

Different variance-based methods use different decomposition techniques. For example, the EFAST method decomposes the variance contributed by the input factors by assigning them different frequencies, and later measures the strength of the assigned frequencies on the model output using the Fourier analysis. Details of the EFAST method are described in the next section.

Equation (3.5) provides useful information to understand sensitivity indices calculated by the variance-based global sensitivity analysis. In Equation (3.5), the first term in the right hand side (i.e. V_i) is the variance contributed by the main (first-order) effects, the second term (i.e. $V_{i,j}$) is the variance contributed by the interactions between two factors (second-order effects), and so on. The sensitivity index of the first- and second-order effects, for example, is given by Equations (3.6) and (3.7), respectively.

$$SI_i = \frac{V_i}{V_{total}} \qquad (3.6)$$

$$SI_{i,j} = \frac{V_{i,j}}{V_{total}} \qquad (3.7)$$

The previous description provides a general procedure for calculating uncertainty and sensitivity indices by the variance-based method. This description serves a basic understanding performed of the variance-based method. Next, the EFAST method, which is one of the variance-based methods, is focused for calculating the uncertainty and sensitivity model output. The EFAST method, as well as the Morris method, is the main global uncertainty and sensitivity analysis used in this thesis.

3.6.2. Details of EFAST Method

The EFAST method, as the name implies, is the extended version of the original Fourier Amplitude Sensitivity Test (FAST) [44-47]. The original FAST method estimates only the first-order sensitivity index, which indicates the contribution of a single factor to the total output variance. The EFAST method, in addition, estimates a total-order sensitivity index. The total-order sensitivity index indicates the contribution of a single factor including its interactions with other factors to the total output variance. Thus, the EFAST method produces two sensitivity indices: the first- and total-order.

The EFAST method works based on the Fourier transformatiom. The process for calculating sensitivity indices by the EFAST method requires four important steps. They can be described as follows [13, 48, 49]:

1. Define a search curve

Consider a similar model described by Equation (3.1). The input uncertain factors of the model are described by $X = (x_1, \dots, x_n)$, where n is the number of factors studied. The

EFAST method assigns all the input factors with sinusoidal functions, known as search curves. The search curves are defined as:

$$x_i(s) = g_i(\sin \omega_i s) \tag{3.8}$$

where g_i - $i^{th.}$ transformation function, $i = 1,2,3, ... , n$

ω_i -   a set of $i^{th.}$ different angular frequencies

s -   scalar variable within $(-\infty < s < +\infty)$

Each input factor is assigned a unique frequency of the search curve in a way that this frequency can be distinguished during analysis of model output using Fourier analysis. Besides using a unique frequency for each input factor, the assigned search curves also consider the input factor distributions [49]. Several papers present effective and efficient search curves to be used in the EFAST method [50]. For example, a search curve that can effectively produce a uniform distribution sample within input factors is described by Equation (3.9) [13].

$$x_i(s) = \frac{1}{2} + \frac{1}{\pi} \arcsin(\sin(\omega_i s)) \tag{3.9}$$

It should be noted that, in this thesis, the uniform distribution functions for all studied factors are used since they are assumed to be equal probability of occurrence.

For an illustration, Figure 3.6 shows the simulated transformation function of Equation (3.9) using two factors; x_1 and x_2 with their respective angular frequencies of $\omega_1 = 11$ and $\omega_2 = 21$. The scalar s is varied within $\left(-\frac{\pi}{2} < s < +\frac{\pi}{2}\right)$ in equispaced intervals.
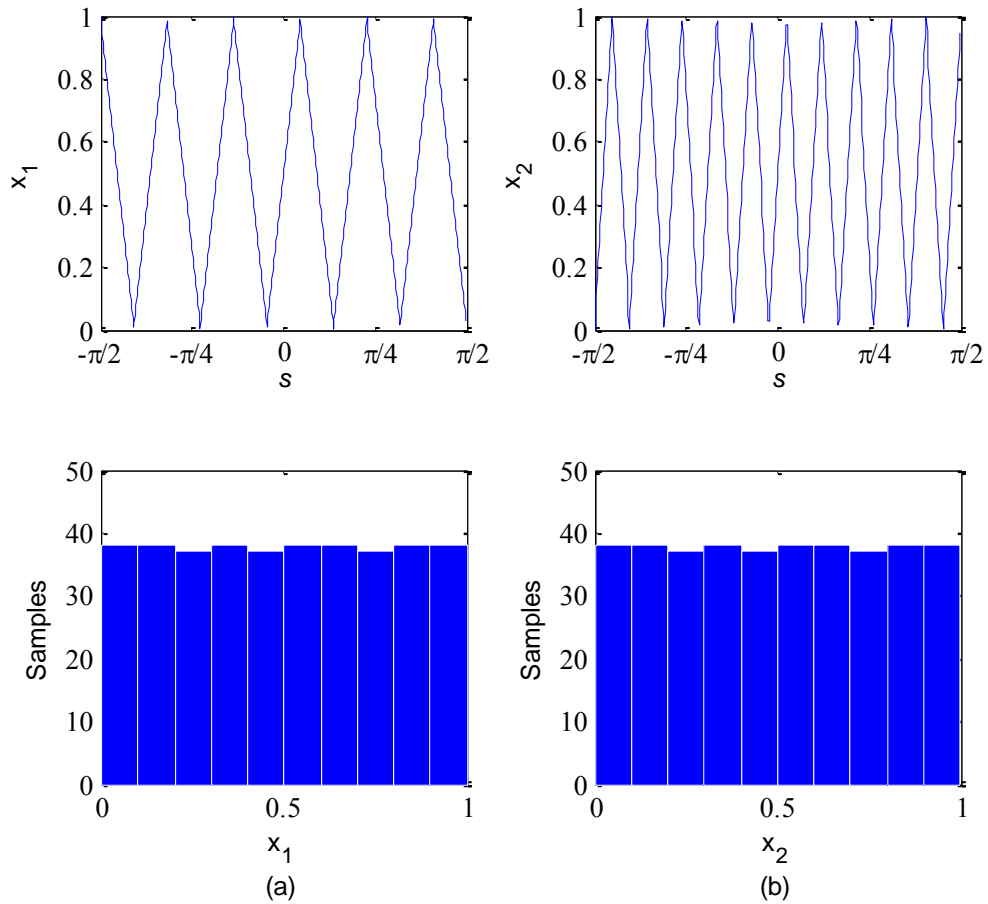
Figure 3.6 Transformation curves and histograms for different angular frequency (a) $\omega_1 = 11$, (b) $\omega_2 = 21$

The corresponding histograms, which are produced using 377 sample points, indicate clearly that the use of the transformation function distributes sample points uniformly within $(0-1)$ for both input factors. The uniformly distributed sample points are important when the investigated input factor is uncertain in a uniform way.

2. Calculate Fourier coefficients

The EFAST method uses the produced sample points (i.e. matrix of samples), in the previous step, for solving the model and produce the model outputs. The model outputs are expanded, using the Fourier analysis, to estimate coefficients of Fourier cosine and Fourier sine (A_j, B_j). These coefficients are calculated as follows:

$$A_j = \frac{1}{2\pi} \int_{-\pi}^{\pi} f(s) \cos(js) \, ds, \qquad (3.10)$$

$$B_j = \frac{1}{2\pi} \int_{-\pi}^{\pi} f(s) \sin(js) \, ds. \qquad (3.11)$$

where
$$f(s) = \sum_{j=-\infty}^{\infty} \left(A_j \cos(js) + B_j \sin(js) \right)$$

$$= f(g_1(\sin \omega_1 s), g_2(\sin \omega_2 s), \dots, g_n(\sin \omega_n s))$$

3. Calculate total variance and variance of each factor

The EFAST method calculates two types of variance. The first is the total variance and the second is the variance contributed by each input factor. These variances are calculated using the Fourier cosine and sine coefficients described in the previous step. Firstly, the variance spectrum (Λ_j), for each integer frequency $(j = 1,2, \dots, \infty)$, is defined as follows:

$$\Lambda_j = (A_j^2 + B_j^2) \qquad (3.12)$$

Secondly, the variance of the $i^{th.}$ input factor (V_i) is calculated by evaluating the variance spectrum at the assigned fundamental angular frequency and its higher harmonics $\left(\Lambda_{p\omega_i} \right)$, where $p = 1,2, \dots, \infty$.

$$V_i = \sum_{p=1}^{\infty} \Lambda_{p\omega_i} \qquad (3.13)$$

Next, the total output variance is calculated using all the frequencies of the assigned sinusoidal function as follows:

$$V_{total} = \sum_{j=1}^{\infty} \Lambda_j \qquad (3.14)$$

4. Calculate sensitivity indices

The EFAST method calculates first-order and total-order effects. The first-order effect of $i^{th.}$ factor (SI_i) is calculated by dividing the variance contributed by the $i^{th.}$ input factors (V_i) to the total variance (V_{total}).

$$SI_i = \frac{V_i}{V_{total}} \qquad (3.15)$$

The calculation of total-order effect of $i^{th.}$ factor $(SI_{i,total})$, however, requires calculation of the variance of $i^{th.}$ factor (V_i) and its complementary variance $(V_{\sim i})$. The complementary factor is defined as the entire set of factors except the $i^{th.}$ factor. The variance of $i^{th.}$ factor (V_i) is calculated by Equation (3.13). The complementary variance is calculated as follows.

First, the EFAST method combines the remaining factors, which are all factors except the $i^{th.}$ factor, as a single group factor (x_{group}). This combination results in only

two factors that are involved in the investigation: $i^{th.}$ factor (x_i) and the group factor (x_{group}). With the two factors, the possible variance can be due to the effect of factor x_i, x_{group} and their interaction $(x_{i,group})$ as illustrated in Figure 3.7.
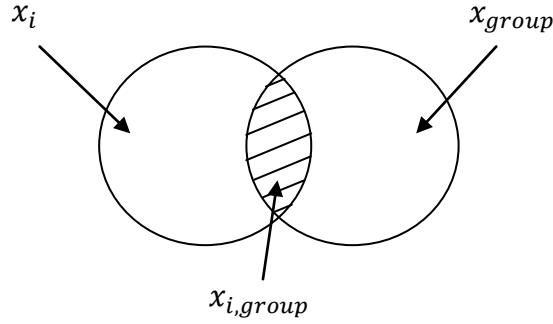
Figure 3.7 Illustration of variance contributed by factor x_i, x_{group} and their interaction $(x_{i,group})$

Second, the EFAST method calculates the variance contributed by the group factor (V_{group}) in a way, described previously, similar to the one it uses to calculate the $i^{th.}$ factor (V_i). Each factor of the group factors is assigned with only one fundamental frequency. Any variance that remains uncalculated is assumed to be due to the interaction of the $i^{th.}$ factor with other factors (i.e. $x_{i,group}$).

The total-order effect of the $i^{th.}$ factor $(SI_{i,total})$, is simply the sum of the variance of the $i^{th.}$ factor and its interaction variance divided by the total output variance.

$$SI_{i,total} = \frac{V_i + V_{i,group}}{V_{total}} \qquad (3.16)$$

3.7. Uncertainty of Nuisance Factor

Uncertainty analysis is a study of how the uncertainty of a model inputs results in the uncertainty of model outputs. In the uncertainty analysis study, the term 'input factors' includes the uncertainty of model parameters, structure, assumptions and specifications [8]. In this study, however, the uncertainty of nuisance signals in the input fault signals to the measurement algorithms of IEDs is considered. The uncertainty of other factors is not considered because the evaluated measurement algorithms have fixed and known parameters. Their fixed parameters (i.e. measurement algorithm coefficients) have been described in Section 2.5

The occurrence of faults initiates a variety of nuisance signals in input fault current and voltage signals. However, the presence of nuisance signals and their amount in the fault current can differ from those in the fault voltage [1, 6]. Their amount is uncertain since it depends on random sources such as the fault location and fault resistance. In general, the uncertainty of nuisance factors is determined by the variability of parameters (i.e. factors) on fault loops.

There are two types of parameter variability in the faulted system. The first is the parameter variability in the network system and the second is the parameter's variability in instrument transformers. Both types of variability produce a variety of nuisance signals that mix with the fundamental frequency component to produce input signal distortion to IEDs. In this thesis, the sources of nuisance factors have been divided into two types: the factors of network systems and the factors of instrument transformers. They are described in the next two sections.

3.7.1. The Factors of Network Systems

The variability of network parameters is commonly produced as a consequence of fault occurence. However, the parameter variability can also be produced in normal conditions. Off-nominal frequency, for instance, is common during normal conditions due to the switching activity of loads. This type of variability produces nuisance components in both

primary fault current and primary fault voltage. However, as mentioned, the produced nuisance components in the primary fault current can differ from the produced nuisance components in the primary fault voltage.

A fault in a transmission line, particularly the single phase-ground fault, is the most common of all faults in power system [51-53]. Such faults represent more than 80% of faults in the power system. The occurrence of a fault on the transmission line can be as a result of bush fires, equipment failure or human error, which are unpredictable. This study focuses on faults that occur in the transmission line. When fault occurs on the transmission line, parameters describing the faulted system are uncertain. Table 3.2 shows the uncertainty sources during faults in transmission lines.

Table 3.2 Source of nuisance signals in the power network

Source or Nuisance Factors	Symbol
▪ Fault inception angle	β
▪ Fault location	F_L
▪ Fault resistance	R_F
▪ Harmonic components*	h_n, n=1,2,3 …
▪ Off-nominal fundamental frequency	δf_1

* - Nuisance components

The sources of the nuisance components and factors describing them are random, due to the following:

a) Fault inception angle

The fault can occur at any time. In the context of signal processing, the time of the fault is related to the fault inception angle on the voltage supply. The fault can incept at

any point from (0 - 2π) radians on the voltage signal. The fault inception angle is related to the amplitude of the decaying DC offset on fault current signals.

b) Fault location

IEDs used in a transmission line are required to detect any fault on the line from the relaying point up to the end of the line. However, the fault location is unpredictable and it can occur at any location of the protected line. Thus, fault location can be uncertain within (0-100) % of the protection zone. The fault location is related to the time constant of the decaying DC offset in the fault current. It also determines the Source to Impedance Ratio (SIR), in which the SIR has a significant impact on the CVT transient [54].

c) Fault resistance

As mentioned, the occurrence of faults may introduce fault resistance. The fault resistance is a sum of three resistance elements: arc resistance, resistance of any path to ground and ground resistance [22]. These elements are unpredictable. For example, the ground resistance depends on the type of soil. Thus, the value of fault resistance (R_F) is uncertain in any fault conditions.

d) Harmonic components

The usage of non-linear loads is increasing due to their high performance, small size and low cost. Non-linear loads and non-linear elements such as instrument transformers, however, produce a variety of harmonic frequencies [55]. Also, arcing fault also produces harmonics. The harmonic frequencies distort the shapes of current and voltage signals to being non-sinusoidal. The magnitudes of harmonic components on the current and voltage signals vary because they are dependent on the number of non-linear loads and non-linear elements used.

e) Off-nominal fundamental frequency

The imbalance between power generation and load demands produces a deviation of the power fundamental frequency (i.e. off-nominal frequency). It is caused by the switching activity (connecting and disconnecting) of loads. The continuous changing of load demands, ideally, requires the power generation to quickly adapt to the changes.

Practically, it is impossible for the power generation to instantly adapt to the load changing. Thus, it is most common that the fundamental frequency shows a small deviation around the power frequency.

3.7.2. The Factor of Instrument Transformers

The sources of nuisance components from instrument transformers can be classified into two types. The first is the source that is uncertain, and the second is the source that is certain (predictable). The remanent flux in the CT core has been identified as the source of nuisance components that are uncertain during fault conditions. The remanent flux distorts the secondary output of CT. It can be produced in two ways. The first is through a field testing of the CT, which is periodically performed, for calibration. The second is after the occurrence of a fault.

The field testing of the CT or the occurrence of faults produces remanent flux that may add or subtract, depending on their relative polarities, to the existing flux produced by the symmetrical current component. Thus, the remanent flux is uncertain and can be as high as 80 % of the saturation threshold [56, 57].

The second type of nuisance component source is result of the different types of configuration used in the CTs and CVTs. These sources are presented since configurations that produce fault test scenarios with the worst case result will be considered. Evaluating measurement algorithms using the worst case scenarios provides a better performance evaluation. Table 3.3 shows the second type of nuisance sources, which is predictable, in the CT and CVT.

The burden of the CT and CVT consists of three elements namely burden resistance; lead resistance that connects between the CT or CVT and the IED; and the IED itself. The burden of the CT and CVT may be uncertain during the initial design stage. However, once the CT, CVT and digital protective relays are installed, the burden values of the CT and CVT are known and fixed. These values are unchanged in fault conditions.

Table 3.3 Source of predictable nuisance signals in instrument transformers

CT	CVT
▪ Types of burden	▪ Types of burden
	▪ Sum of stack capacitance
	▪ Types of Ferroresonance Suppression Circuits

The sum of stack capacitance of the CVT is used to reduce the high voltage level to the intermediate level. The sum of stack capacitance may be classed into three types: high, medium and lower sum of stack capacitance. The CVT with the high sum of stack capacitance shows less transient effect on voltage signals than that of the lower capacitance value [38, 54].

To avoid resonance, CVT uses the Ferroresonance Suppression Circuit (FSC) to create an alternative path to dissipate energy. Two types of FSC can be distinguished: active and passive. The active FSC produces a more severe transient effect on voltage signals than the passive circuit [54, 58]. Figure 3.8 shows the configuration of both the active and the passive circuits.

NOTE:
This figure is included on page 65 of the print copy of
the thesis held in the University of Adelaide Library.

Figure 3.8 Typical FSC (a) active (b) passive [58]

Where R_f, L_f, C_f -   equivalent resistance, inductance and capacitance. Subscript f indicates ferro-resonance

In this thesis, the focus is on the nuisance components with uncertain factors while considering CT or CVT configuration in a way that they produce the most severe input test fault scenarios to the measurement algorithms. Thus, the CVT model that utilizes the low sum of stack capacitance and an active FSC circuit is used.

3.8. Nuisance Components in Fault Signals

In fault conditions, fault currents and voltages contain a variety of nuisance signals. The presence of the nuisance components in fault signals results in distorted input signals to IEDs. These nuisance signals influence the output of the measurement algorithm, and therefore, the output of IEDs. They result in measurement errors on the output of the measurement algorithm during the estimation of fundamental frequency component. Consequently, the IEDs may operate incorrectly.

In the digital protection system, the common nuisance factors studied are the decaying DC offset, low multiple harmonic frequencies and off-nominal fundamental frequency [18, 34, 59]. Nuisance signals of high harmonic frequencies are not studied since the anti-aliasing LPF implemented in IEDs can effectively attenuate these nuisance signals. As an illustration, the effect of the decaying DC offset, third and fifth harmonic components and off-nominal fundamental frequency on the output of Cosine filter algorithm during estimating the amplitude of the fundamental frequency component are presented.

It should be noted, however, that some of these nuisance components may not influence the output of the Cosine filter due to the immunity of the filter. However, as IEDs implement a variety of measurement algorithms, these components may affect other measurement algorithms because different measurement algorithms have different levels of immunity. Therefore, these nuisance components, in general, should be considered as nuisance factors since they may be present in the input fault signals to IEDs.

3.8.1. The Decaying DC offset

The decaying DC offset has two important parameters/factors: amplitude and time constant. Both factors influence the output transient response of the measurement algorithm. Figure 3.9 shows the impact of high amplitude and a long time constant of the decaying DC offset on the output transient response of the Cosine filter for estimating the amplitude of fundamental frequency component. In this Figure, the time constant of $\tau = 100$ milliseconds is simulated. Figure 3.10 shows the simulation of the same parameter except that the time constant is reduced to $\tau = 20$ milliseconds. Both Figures indicate that the output of the Cosine filter shows an overshoot. The definition of the overshoot is described in Section 4.3.3.
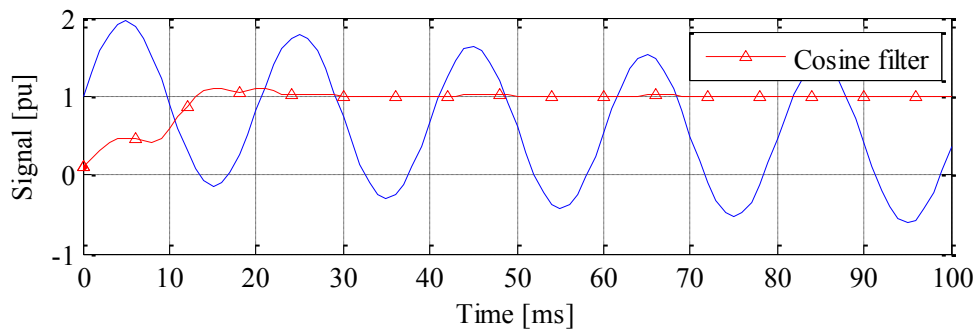
Figure 3.9 Impact of high amplitude of decaying DC offset with time constant of $(\tau = 100\ ms)$ on output transient response of Cosine filter
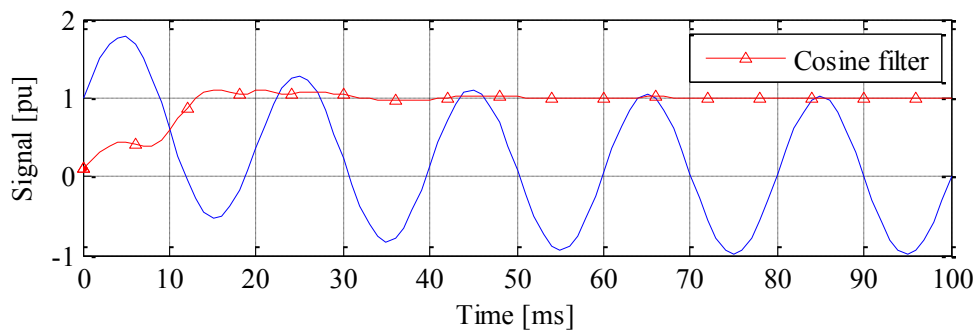
Figure 3.10 Impact of high amplitude of decaying DC offset with time constant of $(\tau = 20\ ms)$ on output transient response of Cosine filter

3.8.2. The Third Harmonic

The impact of the amplitude of the third harmonic component on the output transient response of the Cosine filter is shown in Figure 3.11. It is clearly shown that the output of the Cosine filter is unaffected by the amplitude of the third harmonic component. The Cosine filter estimates accurately 1 (p.u.) the fundamental frequency component after its data window is elapsed.
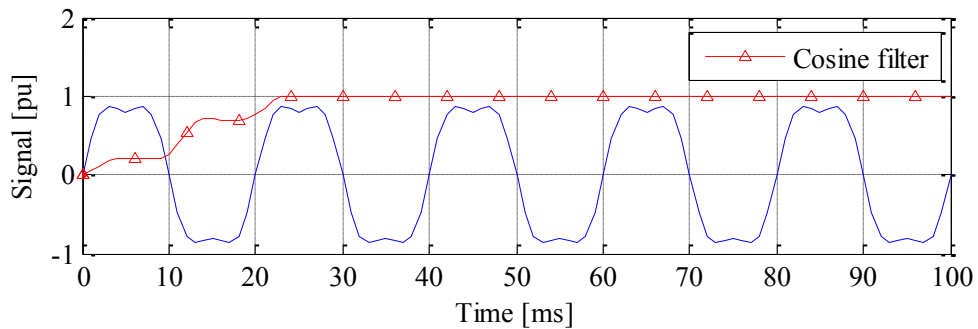
Figure 3.11 Impact of 20%* amplitude of third harmonic component on output transient response of the Cosine filter

3.8.3. The Fifth Harmonic

The impact of amplitude of the fifth harmonic component on the output transient response of the Cosine filter is shown in Figure 3.12. It is clearly shown that the output of the Cosine filter is also unaffected by the amplitude of the fifth harmonic component.
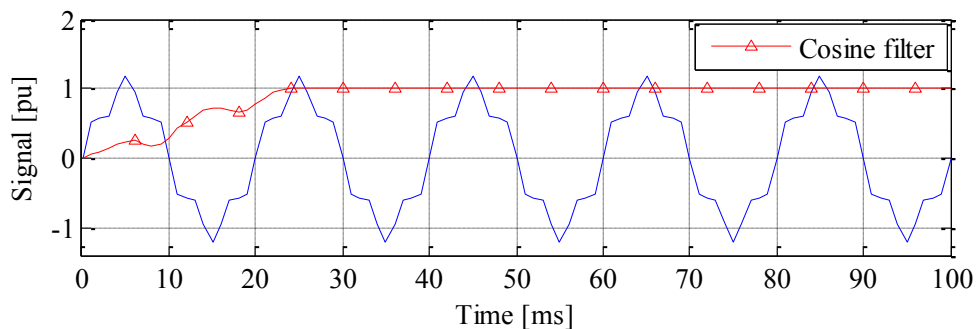
Figure 3.12 Impact of 20%* amplitude of fifth harmonic component on output transient response of the Cosine filter

* - based on the amplitude of fundamental frequency component

3.8.4. The Off-nominal Fundamental Frequency

The impact of the power system frequency of 45Hz on the output transient response of the Cosine filter is shown in Figure 3.13. It indicates that the output of the Cosine filter is oscillating within (0.85 to 1.0) per unit in its steady state response.
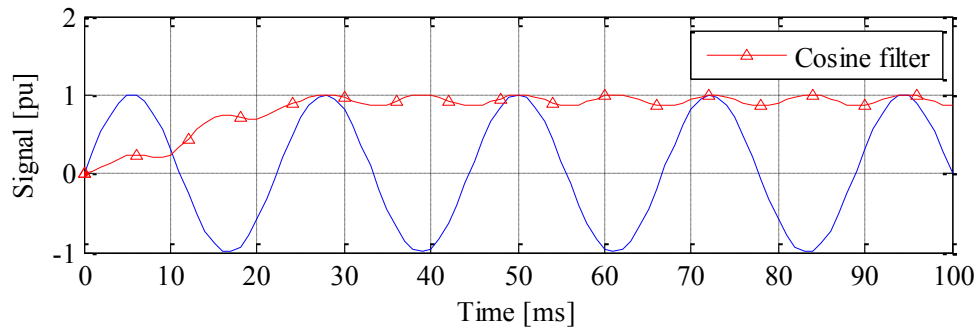
Figure 3.13 Impact of power system frequency of 45 Hz on output transient response of the Cosine filter

As illustrated, two of the nuisance factors, which are the amplitude of third and fifth harmonic components, do not influence the output of the Cosine filter. However, they may influence the output of other measurement algorithms. In fault conditions, the degrees of nuisance factors can be of different amounts. Furthermore, the interactions of nuisance factors can result in high influences on the output of the measurement algorithms. Thus, it is worth to highlight that the sensitivity analysis can be used to investigate the main and interaction effects of nuisance factors to provide more understanding of the output behavior of measurement algorithms.

3.9. Conclusion

The introduction, concept and classification of uncertainty and sensitivity analysis methods have been presented in this chapter. The computation difficulties in performing global uncertainty and sensitivity analysis have been described. Two types of computationaly

efficient methods: Morris and EFAST are presented in detail. These two methods are selected as the main global sensitivity analysis techniques to be used for the performance evaluation of measurement algorithms.

The nuisance signals in fault current and voltage signals have been discussed. The sources of the nuisance signals, which are unpredictable, have also been elaborated. The unpredictable source of nuisance signals is initiated from the fault systems that include instrument transformers. Additionally, other sources of nuisance components that are predictable have also been described. The predictable sources of nuisance signals are initiated by the instrument transformers.

The impacts of commonly studied nuisance signals: the decaying DC offset, harmonic components and off-nominal fundamental frequency on the output of the Cosine filter have been illustrated. The illustration shows how the Cosine filter responds to those nuisance signals while tracking the amplitude of the fundamental frequency component.

Chapter 4. The Design of the Methodology for Performance Evaluation

4.1. Introduction

The previous chapter presented the concept of the uncertainty and sensitivity analysis method. It also presented two global sensitivity analysis methods: the Morris and EFAST. The EFAST method is the main method of global uncertainty and sensitivity analysis used in this thesis. The EFAST method was selected for two reasons. Firstly, the EFAST method provides quantitative, rather than qualitative, results. Secondly, it is model independent, which means that the mathematical algorithm of the model under test can be unknown.

In any global sensitivity analysis method, including the EFAST method, the main limitation is computational time, particularly for practical testing. For this reason, applying only the EFAST method to evaluate the performance of measurement algorithms is prohibitive. Thus, it is important to use the preliminary sensitivity analysis prior to the EFAST method in such a way that the proposed methodology can be implemented not only in simulation but also in practical testing. The Morris method is used as a preliminary

sensitivity analysis for screening important factors among all the studied factors. Then, in the EFAST method only those important factors are considered. The use of the Morris followed by the EFAST method is known as a two-stage sensitivity analysis.

Moreover, the success of implementing global sensitivity analysis using the Morris and the EFAST methods, in the context of testing measurement algorithms in both simulation and practical testing, requires the consideration of several additional requirements. Thus, this chapter continues to discuss details of the global uncertainty and sensitivity analysis method in the context of evaluating the performance of measurement algorithms. The assumptions of the design methodology are also addressed.

A methodology to evaluate the performance of measurement algorithms in the steady state is designed, since this is also important in protection studies. In the steady state, however, the performance of measurement algorithms is evaluated by analyzing their frequency response without performing the uncertainty and sensitivity analysis. The global uncertainty and sensitivity analysis is not used because the input factors, which are measurement algorithm coefficients that used to obtain the frequency response, are fixed. The fixed input factor of a model (i.e. measurement algorithms) does not produce uncertainty in the model output.

Section 4.2 discusses the main design considerations that include strategies for the successfully performing global uncertainty and sensitivity analysis in the context of the performance evaluation of measurement algorithms. The consideration takes into account the implementation of the proposed methodology in simulation as well as practical testing of a commercial IED. Section 4.3 continues to describe how to provide fault test scenarios that are parameterized by the uncertainty of factors. The model of a system consisting of a CT and CVT connected to the network in a fault condition is described. This section also describes the model of IED including measurement algorithms. The performance criteria used to measure the quality of measurement algorithms are described. Next, the main procedure that combines these models to implement global uncertainty and sensitivity analysis are presented. Section 4.4 presents the discussion of the proposed methodology. In Section 4.5, the procedures for evaluating measurement algorithms performance in the steady state are presented. Finally, Section 4.6 provides the conclussion of this chapter.

4.2. Methodology Requirements

The methodology for the performance evaluation of measurement algorithms using the global uncertainty and sensitivity analysis demands several important considerations and requirements. The considerations, requirements and the reasons for their selection are described in the following sections.

4.2.1. Automatic Creation of Extensive Fault Scenarios

In fault conditions, the initiated nuisance signals mix with the fundamental frequency component to produce distorted input signals to measurement algorithms. The influence of the nuisance signals on the output of measurement algorithms can be evaluated by testing those measurement algorithms using test signals parameterized by different nuisance factors. As the factors are uncertain, fault test signals that represent all sample points within the uncertainty of factors should be created.

The complete representation of factors' uncertainties within their distributions requires a high number of sample points. Each sample point, which is representing a unique fault test scenario, is used to execute the measurement algorithms to obtain their output response. The proposed methodology, which is based on the uncertainty and sensitivity analysis, therefore, requires an extensive number of fault test scenarios as well as the execution of measurement algorithms for each scenario.

It is a tedious and impossible task to simulate manually fault test scenarios for a high number of sample points. Thus, a program that interfaces among three software tools: the SIMLAB, MATLAB and ATP/EMTP program has been developed. The developed program automatically and systematically creates fault scenarios, which are influenced by different degrees of uncertainty of input factors. The main tasks of the software tools used are summarized in Table 4.1.

Table 4.1 Functionality of software tools used in evaluating the performance of measurement algorithms

Tools	Functions
SIMLAB	- To provide systematic sample points of nuisance factors for global uncertainty and sensitivity analysis
ATP/EMTP	- To create the template of thefault loop consisting of models of fault network, CT and CVT
MATLAB	- To read sample points from SIMLAB, and then modify and execute fault template in ATP/EMTP - To simulate measurement algorithms - To calculate performance indices - To automate control and record extensive fault simulations

4.2.2. Issue of Unknown Measurement Algorithms Implemented in IEDs

One main aim of this thesis is to evaluate the performance of measurement algorithms implemented in commercial IEDs. Most often, information on the protection algorithms, including the measurement algorithms, of commercial IEDs are unknown since they are the secret property of manufacturers. The main reason for the secrecy is that the performance of IEDs of different manufacturers is mainly distinguished by the implemented mathematical algorithms.

Thus, it is important to use the method of global uncertainty and sensitivity analysis that does not require mathematical algorithms implemented in IEDs to be known, which is model independent. As mentioned in Chapter 3, the variance-based is the model independent sensitivity analysis. The variance-based method such as the EFAST method does not require knowledge of the mathematical algorithms of the model, nor even any assumptions about their linearity and monotonic behaviour. The EFAST method is selected as the main method for the global uncertainty and sensitivity analysis to evaluate the

performance of measuremement algorithms implemented in commercial IEDs. The EFAST method is also the main method used in the computer simulation.

4.2.3. Practical Evaluation

The main method used in this thesis is a global, instead of local, uncertainty and sensitivity analysis method. Indeed, the used of the global method provides the main research gap between the methodology proposed in this thesis and the methodologies of those previously studied for the performance evaluation of measurement algorithms.

As mentioned in the previous section, a global uncertainty and sensitivity analysis that is based on the variance-based method has been selected. However, the variance-based method is a sample based method, which means that the input factors are required to be sampled within their spaces. The popular way to sample is to use the Monte Carlo (MC) sampling method. The MC method randomly samples input factors within their uncertainty distributions to produce sample points.

The main limitation of the sample based method, however, is the high number of sample points that are required to represent the entire input factor distributions. Even the use of the Latin Hypercube Sampling or the Sobol sequence sampling techniques, in which both techniques are the effective sampling method, result in the produced number of sample points still being high. Furthermore, if the number of investigated input factors is high, the number of sample points can be extremely high. Table 4.2 tabulates how many samples of the Sobol sequence sampling method are required to calculate sensitivity indices as a function of the number of factors.

Table 4.2 Number of factors and the corresponding required executions required using Sobol sequence sampling technique

Number of Factor	3	4	5	6	7	8
Number of samples based on SIMLAB implementation	16,384	32,768	65,536	131,072	262,144	524,288

The high number of executions may not be a time constraint in computer simulations since the high-speed processing computer is widely available. However, for the practical testing of measurement algorithms of IEDs, where usually practical testing requires much longer time than its model simulation, the high number of executions can be a time constraint and prohibitive. For example, seven factors require 262,144 samples using the Sobol sequence sampling method in the SIMLAB program. The evaluation process that is based on the QMC simulation with the Sobol sequence sampling method, therefore, can take up to 6.1 months if the practical execution for each sample requires 1 minute to complete the process.

For this reason it is necessary to reduce the high number of executions so the proposed methodology can be implemented for practical testing. One option is to reduce the number of investigated factors by eliminating some of them. However, only factors that have small or no influence (unimportant factors) on the output of measurement algorithms should be identified for the elimination. Thus, a two-stage uncertainty and sensitivity analysis method has been designed in which the Morris method is the first-stage. The aim of the Morris method is to identify unimportant factors among the investigated factors. Only important factors are then used to investigate their influence on output of In the second-stage, the EFAST method is used. Although the QMC simulation with the Sobol sequence sampling method is one of the variance based methods, this method, as tabulated in Table 4.2, requires a high number of samples and therefore it is computationally expensive. The QMC simulation with the Sobol sampling technique measures the first-order and all the higher-order effects of the input factors. The EFAST method, however, only measures the first- and total-order effects of the input factors. Thus, the computation by the EFAST method is less expensive than the QMC simulation with the Sobol sampling technique. The minimum recommended sample points per factor for the EFAST method are 65 [8]. The results of the first- and total-order effects by the EFAST method have agreed well with the QMC with the Sobol sampling technique [42]. Thus, for the second-stage, the EFAST method is selected instead of the QMC with the Sobol sampling technique. By using the EFAST method, after the Morris in first-stage, the computation burden is further reduced.

4.2.4. Quantitative Results

The sensitivity analysis methods can be classified based on the result of outcomes: qualitative or quantitative [8]. Both results show the influence of input factors of a model to the model output. However, the qualitative result cannot be used to numerically compare the influence of the input factors to one another. In contrast, the quantitative result can be used to numerically compare among them. The quantitative result shows the percentage of influence of the input factors to the model output. This study aims to compute the influence of the input factors on the output of measurement algorithms in a quantitative way.

For this reason, the main analysis method is based on the global uncertainty and sensitivity analysis that can produce quantitative results. Although both the QMC with either the Sobol sampling technique or the EFAST method produce the quantitative results, the EFAST method is selected for the reason described in the previous section.

4.3. Design Stages

Section 3.4 describes the four basic steps for performing the global uncertainty and sensitivity analysis method for any fields of study. In the context of the evaluation of measurement algorithms' performance, the first two steps aim to provide the input fault test scenarios that are influenced by different degrees of nuisance signals. The third step is to solve the measurement algorithms by executing them, in order to produce the output estimation of the fundamental frequency component. Finally, the fourth step is to compute the uncertainty and sensitivity in the output estimation of the fundamental frequency component. This section details these steps.

4.3.1. Fault Test Scenarios

This thesis focuses on faults in a transmission line network. Faults in the transmission line can be classified into many types such as phase-to-phase or three-phase faults. The basic mathematical algorithms to identify the types of fault are well known [60].

From a signal processing point of view, different types of faults produce a fundamental frequency component that changes its amplitude and phase angle; and nuisance components. Therefore, a model of the ideal network that is connected to a model of either a CT or CVT is used to create fault test currents and voltages. The produced fault test signals are adequately representing the input test signal to the measurement algorithms for protection studies [61]. Fault scenarios using a model of a single phase-ground fault are generated, with this type of fault being the most common in the power system [51-53]. In the model, the necessary nuisance signals, such as the third harmonic that is required for this study, are also injected.

4.3.1.1. The Power Network Fault Model

Figure 4.1 shows the model of a fault using an ideal network. It consists of a voltage source, resistor, inductor and simple switch. This model is used to generate primary fault currents and fault voltages to feed the input of the CT and CVT model, respectively.

$$v = \sum_{m=1}^{H} V_m \sin(\omega_m t + \theta_m)$$
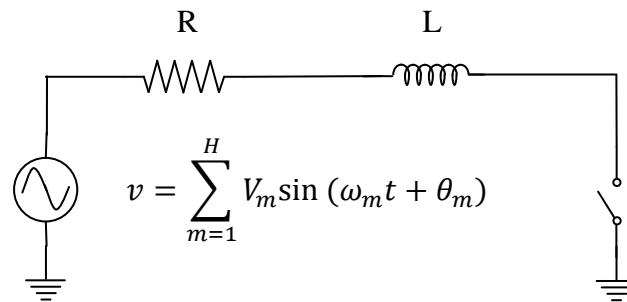
Figure 4.1 Ideal fault network

where V_m, ω_m, θ_m -   voltage amplitude, angular frequency and initial angle of mth harmonic components

   R, L -   equivalent resistance and inductance

   H -   the highest harmonic order in the model

The value of R and L are the equivalent sum of source impedance, fault resistance and fault location in fault conditions. The parameters of R and L, fundamental angular frequency, time constant$(\tau = L/R)$ and the amplitudes of third and fifth harmonics (V_3, V_5) are considered as variables during simulation. However, the phase angle of those harmonic components is not considered. Furthermore, harmonic components that are higher than the fifth harmonic are also not considered since they are assumed to be attenuated by the anti-aliasing LPF of IEDs. Closing the switch, the fault model simulates primary fault signals: currents and voltages. The primary current and voltage signals are applied to the input of the CT or CVT model respectively, to produce output secondary signals to IEDs.

4.3.1.2. The CT Model

The function of the CT is to replicate and scale down a high primary current into a low level secondary current, which is suitable for the operation of IEDs. Figure 4.2 shows a typical CT equivalent circuit.

NOTE:
This figure is included on page 79 of the print copy of the thesis held in the University of Adelaide Library.

Figure 4.2 A CT equivalent circuit [62].

Where R_P, L_P -   primary winding resistance and leakage inductance

R_S, L_S -   secondary winding resistance and leakage inductance

$N1:N2$ -   turn ratio

All the illustrated basic elements of the CT are known and predictable during fault conditions. As described in Section 3.7.2, the only source of nuisance signals in the CT that is unpredictable is the remanent flux. The remanent flux is considered as one of the uncertainty factors for generating fault current test signals.

Many researchers have been investigating the impact of CT saturation on the measurement algorithms and the protection algorithms of IEDs [61-63]. The investigation shows that the CT accurately replicates the primary current in normal or abnormal fault conditions if the CT is unsaturated. However if the CT is saturated, in particular during fault conditions, the secondary current is no longer an accurate replication of its primary. The secondary current signal is distorted and this signal affects all elements of IEDs.

A model of the CT based on paper [63] is used. The parameters of the CT are given in Appendix B. Extensive single phase-ground fault current scenarios are generated, using a fault system that couples between the ideal transmission line network and the CT model. The current scenarios (U_{CT}) are parameterized by the uncertainty of six factors. They are described by Equation (4.1).

- Amplitude of decaying DC offset (α)

- Time constant of decaying DC offset (τ)

- Amplitude of the third harmonic (h_3)

- Amplitude of the fifth harmonic (h_5)

- Off-nominal fundamental frequency (δf_1)

- Remanent flux in the core of CT (λ)

$$U_{CT} = f(\alpha, \tau, h_3, h_5, \delta f_1, \lambda). \tag{4.1}$$

4.3.1.3. The CVT Model

The function of a CVT is to replicate and scale down a high primary voltage at relaying point into a low level secondary voltage. A CVT is commonly used in protection systems due to its lower cost compared to other technologies, small space requirement and simple construction.

Figure 4.3 shows a typical model of a CVT equivalent circuit. The basic configuration of the CVT consists of an equivalent capacitive voltage divider (C_1, C_2), a compensation reactor, a step-down voltage transformer (VT) and a Ferro-resonant Suppression Circuit (FSC).
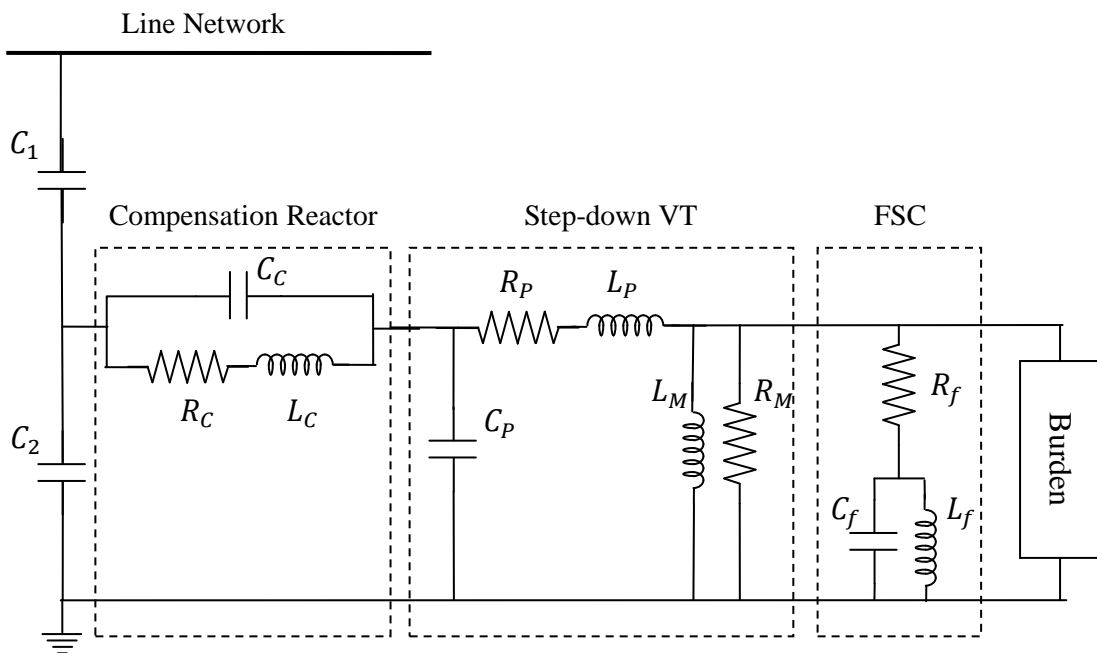
Figure 4.3 A CVT equivalent circuit

where R_x, L_x, C_x -   equivalent resistance, inductance and capacitance. Subscript $x \in (c, p, f)$ is for compensation reactor; primary winding and ferro-resonance

       R_M, L_M -   magnetizing resistance and inductance

The operation of each block forming the CVT is well documented [54]. Unlike the CT, the secondary voltage of the CVT is an accurate replication of the primary voltage only during normal conditions. In fault conditions, although the CVT may be unsaturated, its secondary voltage can be distorted due to the behavior of energy storage elements of the CVT [38]. The energy storage elements such as the compensation inductor (L_C) cannot dissipate their energy instantly. These elements require an amount of time, which is a few cycles, to dissipate their energy. Thus, the secondary voltage is often distorted in the first few cycles following a fault [54].

A fault that incepts on the peak of a voltage signal results in the secondary voltage being distorted by several high frequency components [64]. However, these components have an insignificant impact on the IEDs since the relay uses the anti-aliasing LPF to attenuate these high frequency components. However, some manufacturers use an LPF that is purposely designed to pass a few of high frequency components in order to achieve a balance between the accuracy and speed of the IEDs. Also, the high frequency components can be presented due to non-ideal (i.e non-sharp) transition characteristic between the pass- and stop-band of the LPF.

In contrast, if a fault incepts at a zero voltage crossing, the secondary voltage contains low frequency components [64]. The anti-aliasing LPF, in this case, is unable to attenuate these low frequency components, particularly sub-synchronous frequencies. The sub-synchronous frequency is a frequency that is lower than the cut-off frequency of the designed LPF. As a result, the estimation of the fundamental component is highly impacted by the presence of the low frequency components in the fault voltages.

Extensive papers investigating the distorted secondary voltage of the CVT and its impact on IEDs have been published [38, 51, 65-67]. These papers show that other factors contributing to the worst transient errors are the type of burden, types of FSC circuit (active or passive) and capacitive voltage divider. As described in Section 3.7.2, these factors are considered such that measurement algorithms of IEDs are evaluated in worst case scenarios. Using the worst case scenarios, a better methodology for performance evaluation is provided.

A model of an ideal transmission line network is used. The model is connected to a simplified CVT equivalent circuit that uses a low stack capacitance (i.e. < 100nF) and an active FSC to simulate fault voltage test signals. Such a CVT circuit produces the worst case scenarios. The simplified CVT equivalent circuit provides an acceptable model for use in protection studies. Figure 4.4 shows a typical simplified CVT equivalent circuit [38].
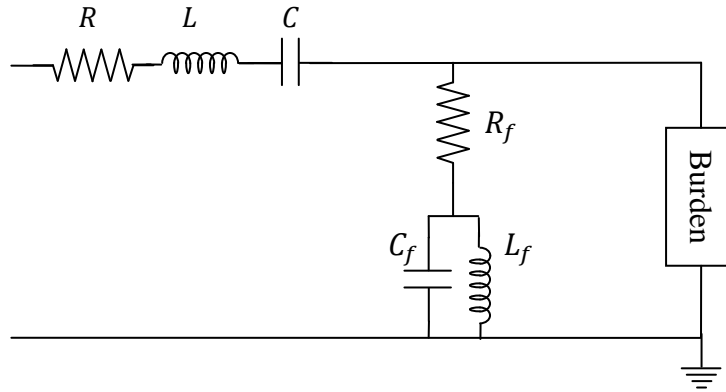
Figure 4.4 A simplified CVT equivalent circuit

where R, L, C -   equivalent resistance, inductance and capacitance from the sum of stack capacitance, compensation reactor and step-down VT

The simplified circuit is used to simulate single phase-ground fault voltage scenarios. The parameters of the CVT are given in Appendix B. The voltage scenarios (U_{CVT}) are parameterized by the uncertainty of five factors. They are described by Equation (4.2).

- Fault inception angle (β)

- Amplitude of the third harmonic (h_3)

- Amplitude of the fifth harmonic (h_5)

- Off-nominal fundamental frequency (δf_1)

- Amplitude of voltage collapse (ΔV)

$$U_{CVT} = f(\beta, h_3, h_5, \delta f_1, \Delta V). \tag{4.2}$$

4.3.2. IED Digital Protective Relay Model

The model of the IED used for the evaluation of the measurement algorithm performance is based on paper [63]. The main elements of the IED are shown in Figure 4.5.

NOTE:
This figure is included on page 84 of the print copy of
the thesis held in the University of Adelaide Library.
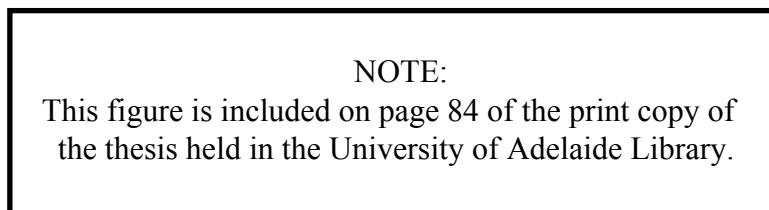
Figure 4.5 An IED block diagram [63]

This IED model, which has been used for studying overcurrent protection, consists of five elements. In this thesis, however, the important elements of the IED for the purpose of the performance evaluation of measurement algorithms are the first to the fourth element, which is the block for amplitude estimation of the fundamental frequency component produced by the Cosine filter. The comparator element (50 Element) is not used.

4.3.2.1. The Analog LPF

The first element of the IED model is the analog LPF. It is used to avoid the aliasing effect and to attenuate the high order frequency components in the input signals. A second-order Butterworth LPF with cut-off frequency of 300Hz is used. The selected cut-off frequency

allows the third and fifth harmonic nuisance components to be parts of the simulated fault test scenarios. In this way, the performance of the Cosine filter in the presence of those harmonic components can be evaluated. The frequency response of the Butterworth LPF used is shown in Appendix C.

4.3.2.2. The A/D Converter

Output analog signals from the anti-aliasing LPF that have eliminated high frequency components are required to be converted to the digital samples. This is because the operation of the IED is based on digital samples. These samples are used by measurement algorithms and various protection functions for their execution. Noise introduced during the quantization process of analog to digital converter (A/D) is not modeled.

4.3.2.3. The Cosine Filter Algorithm

The mathematical algorithms of the Cosine filter is based on paper [36]. The Cosine filter is required to estimate the fundamental frequency component from the output samples of current and voltage produced by the A/D. In this study, the fundamental frequency component is 50Hz. The Cosine filter processing the input samples for calculating the real and imaginary parts of the fundamental frequency component is described by Equations (2.7) and (2.8), respectively. The algorithms of the Cosine filter are implemented using the MATLAB program.

It is worth mentioning that the performance of algorithms other than the Cosine filter can be evaluated by replacing the Cosine filter block in Figure 4.5 with another measurement algorithm.

4.3.2.4. The Amplitude Estimation

This element is used simply to calculate the amplitude of the fundamental frequency component estimated by the Cosine filter. The mathematical equation to calculate the amplitude is described by Equation (2.3).

4.3.3. Transient Response Performance Criteria and Indices

The measurement algorithms of IEDs perform two important functions while processing input fault signals. The first is to estimate the fundamental frequency component, and the second is to filter non-fundamental frequency components such as the DC offset and multiple harmonic components. A good performance of measurement algorithms have the following characteristics [1]:

- Band-pass response around the power system frequency

- DC and decaying DC attenuation

- Harmonics attenuation

- Accurate and fast transient response

- Simplicity of design

These characteristics, except design simplicity, distinguish these performance criteria into two types: criteria in the transient response and criteria in the steady state. Next, performance indices in both criteria are defined to measure the performance of the measurement algorithms. The next section describes the selected criteria on the transient response of measurement algorithms and their respective performance indices.

4.3.3.1. Transient Response Performance Criteria

The occurrence of faults changes several characteristics of the current and voltage signals in the power system. The IEDs use the change of characteristics to detect the fault. The most common characteristics used for fault detection are the amplitude and phase angle of the fundamental frequency component of the current and voltage signals.

In a transmission line protection, the fault occurrence increases the amplitude of current signal from a low level in the pre-fault to a higher level amplitude in the post-fault (step-up change). In contrast, the fault occurrence decreases the amplitude of the voltage signal from a high level in the pre-fault to lower level in the post-fault (step-down change).

The measurement algorithms that respond to these step changes (i.e. step-up or step-down) for estimating the amplitude change only show high accuracy in their estimation output if the fault signal contains only the fundamental frequency component. As pointed out, this is not the case in fault conditions, since many nuisance components are initiated and mixed with the fundamental frequency component. The measurement algorithms that estimate the fundamental frequency component from those distorted fault signals may show errors in their output transient response.

Many papers have proposed performance criteria to calculate the errors in the output of measurement algorithms. In this thesis, the calculations of errors are listed in Table 4.3. These quantities (i.e. criteria) are the most widely used criteria for measuring the performance of the algorithm that responds to the step input signals. Other criteria can be the Percentage of Maximum Overshoot, Percentage Mean Absolute Error or Percentage Root-Mean-Square Error [18, 68, 69].

Table 4.3 The criteria in step-response for the evaluation of the measurement algorithm performance

Step-up	Step-down
- Overshoot - Settling time - Steady state error	- Undershoot - Settling time - Steady state error

The performance of the measurement algorithms when their inputs are the fault current and voltage signals is selected based on those criteria in the step-up and step-down, respectively. The calculated overshoot index identifies the safety margin for the pick-up setting of the IED. The settling time and steady state error correspond to the speed and accuracy of the estimated fundamental frequency component by the measurement algorithms respectively.

Figure 4.6 and 4.7 illustrate a typical step response of the measurement algorithm to step-up (fault current) and step-down (fault voltage) signals. The measured performance criteria, i.e., overshoot (O_s), undershoot (U_s), settling time (T_s) and steady state error (S_{se}) are also illustrated in those Figures.
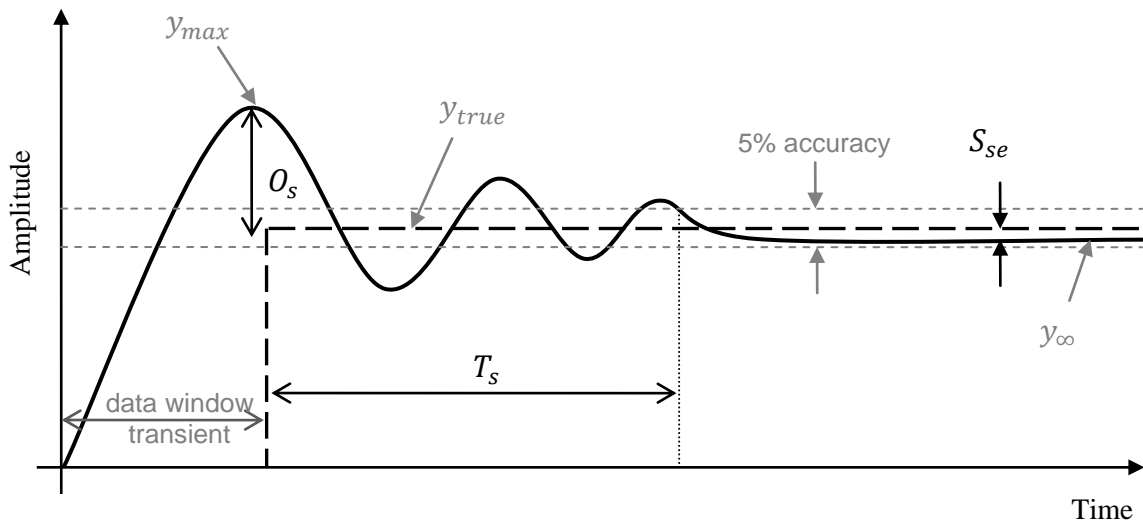
Figure 4.6 Typical response of measurement algorithm to step-up signal
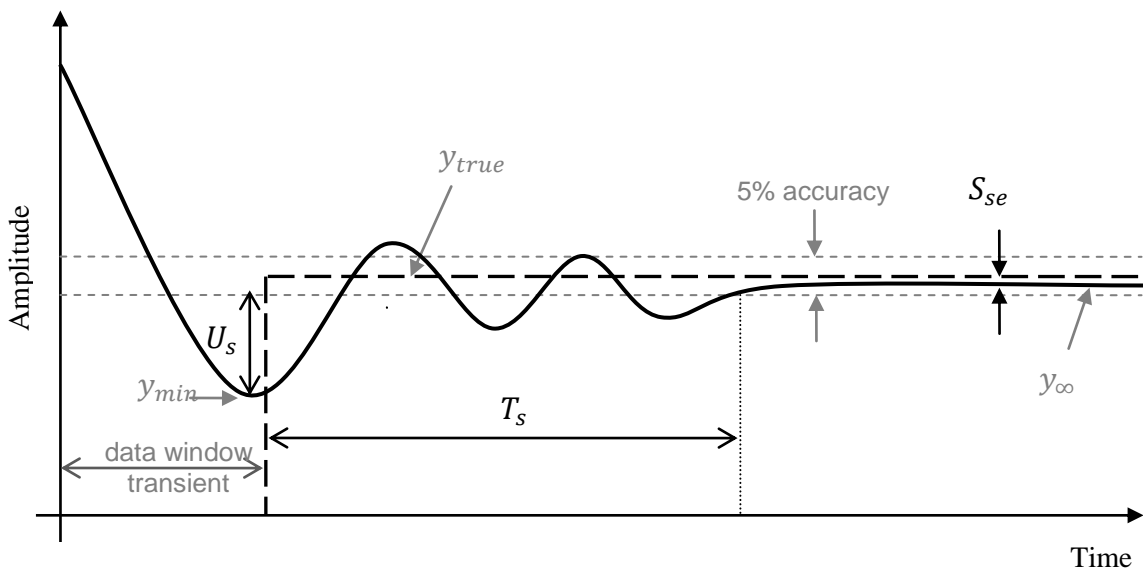
Figure 4.7 Typical response of measurement algorithm to step-down signal

A transient period for the data window of measurement algorithms is considered. The data window transient is a time required by measurement algorithms to completely fill their data window with samples of currents or voltages. During this transient period, the output of the fundamental frequency component estimation is not an effective value, which means that any estimation value during this period should not be used for fault detection or other protection functions. The estimated value is only valid after the data window of the measurement algorithms is completed.

To access the quality output of the measurement algorithms on those selected criteria, transient response performance indices are introduced. The performance indices are described next.

4.3.3.2. Transient Response Performance Indices

The performance criteria on output transient response of measurement algorithms are measured using numerical indices based on the recommendation in [70]. The numerical indices are calculated as follows:

1.   Overshoot, O_S

Overshoot is a measurement of the difference between the highest peak (y_{max}) and the estimated steady state (y_∞) values. The overshoot, expressed as a percentage, is calculated on the output transient response of the measurement algorithm when its input is the fault current signal.

$$O_S(\%) = \frac{y_{max} - y_\infty}{y_\infty} \, X \, 100.$$

(4.3)

2. Undershoot, U_S

Undershoot is a measurement of the difference between the lowest peak (y_{min}) and the estimated steady state (y_∞) values. The undershoot value, which is expressed as a percentage, is calculated on the output transient response of the measurement algorithm when its input is a fault voltage signal.

$$U_S(\%) = \frac{y_{min} - y_\infty}{y_\infty} \; X \; 100. \tag{4.4}$$

3. Settling time, T_S

Settling time is generally defined as a time required for the output of the model to settle down within specific steady state accuracy, starting from the rapid change of the unit step. Two accuracy values, 2% or 5%, are often used. As described previously, the length of the data window of measurement algorithms is considered since the effective output of the measurement algorithms is after their data window has elapsed. Thus, the settling time in this thesis refers to a time required by the output of the measurement algorithms to settle within a selected steady state accuracy starting after the data window has elapsed. A 5% steady state accuracy is selected.

4. Steady state error, *Sse*

Steady state error is a measurement of the difference between the true/ideal value (y_{true}) and the estimated steady state value (y_∞) of the measurement algorithm. The steady state error, which is expressed as a percentage, is measured as follows:

$$Sse(\%) = \frac{y_\infty - y_{true}}{y_{true}} \; X \; 100. \tag{4.5}$$

Each numerical index of Equations (4.3) to (4.5) shows the quality of output of measurement algorithms that response to the single fault test signal. Ideally, an index value that is close to zero indicates the good performance output of the measurement algorithm for estimating fundamental frequency component, and vice-versa.

As the global uncertainty and sensitivity analysis method requires extensive evaluations, the overall performance is accessed using statistical indices. The common statistical indices: mean (μ_{error}), standard deviation (σ_{error}), minimum (min_{error}) and maximum (max_{error}) of error are used to calculate overall performance indices. The statistical indices are given by Equations (4.6) to (4.9).

$$\mu_{error} = \frac{1}{N_S} \sum_{k=1}^{N_S} PI_k \, , \tag{4.6}$$

$$\sigma_{error} = \frac{1}{(N_S - 1)} \sum_{k=1}^{N_S} (PI_k - \mu_{error})^2 \, , \tag{4.7}$$

$$min_{error} = minimum(PI_k) \text{ and} \tag{4.8}$$

$$max_{error} = maximum(PI_k). \tag{4.9}$$

The N_S is the number of samples and PI_k is the calculated transient response performance indices of the kth sample.

4.3.4. Two-Stage Global SA

The main limitation for implementing global uncertainty and sensitivity analysis for the evaluation of measurement algorithms performance is that it is a time computationally expensive, particularly in practical testing. The limitation is because of two factors:

1.   The first is that the global uncertainty and sensitivity analysis method that is based on variance-based requires a high number of sample points. As the number of input factors increases, the number of sample points can be unmanagable and therefore require high computational time even though during in a simulation-based in which a high-speed processor is used.

2.   The second is that a commercial IED that is used to evaluate its measurement algorithms, on average, requires 1 minute for processing a single fault test scenario. The required time period is impractical for this study to use a Quasi-Monte Carlo simulation with a Sobol sampling sequence method. As described in Equations (4.2) and (4.3), the number of investigated factors is six factors for fault test current and five factors for fault test voltage. If the QMC with Sobol sampling sequence method (Table 4.2) is performed, this method requires approximately 90 and 45 days to complete evaluation using those six and five factors, respectively.

To minimize the described limitation, a two-stage global sensitivity analysis has been designed. The first-stage is the Morris method. It is used as a preliminary sensitivity analysis that identifies important factors among the studied factors. Then sensitivity analysis using the EFAST method, which is the second-stage, is performed.

In the second-stage, only important factors are used to further investigate their influence on the output of measurement algorithms. Unimportant factors can be fixed at any values within their uncertainty, such as at their nominal values. The aim of the EFAST method is to obtain the comprehensive results of the global uncertainty and sensitivity analysis. Figure 4.8 shows the block diagram of the two-stage method using the Morris and EFAST methods.
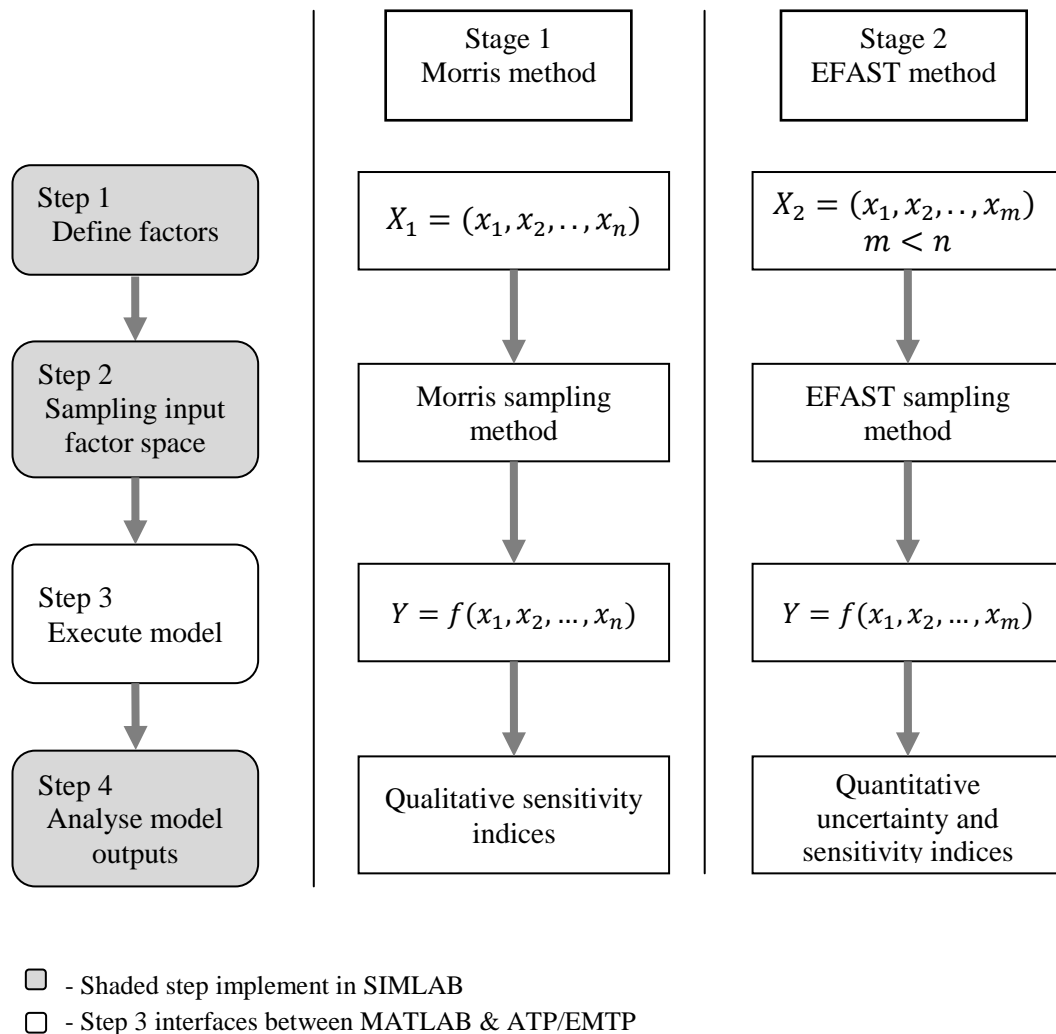
Figure 4.8 Block diagram of two-stage global sensitivity analysis

In simulation, the model of IED consists of the anti-aliasing LPF, A/D and Cosine filter algorithm. The characteristics of LPF are assumed to be a second-order Butterworth LPF with the cut-off frequency of 300Hz, and Cosine filter of 80 samples per cycle. However this study assumes an ideal A/D converter. In practice, the A/D converter can affect the performance of measurement algorithms of the IEDs.

4.4. Limitations and Assumptions

The main limitation of the proposed methodology is that it can be only used in practical testing to evaluate the measurement algorithms of IEDs that provide input and output access nodes. Most available commercial IEDs, however, provide these access nodes. The performance of measurement algorithms is systematically tested even if details of the measurement algorithms are unknown. Test signals are applied to the input of unknown measurement algorithms of IED and their corresponding output is recorded and analysed.

The second limitation is that the EFAST global uncertainty and sensitivity analysis method is able to measure only the effect of first- and total-order effect. This method is unable to measure the effect of factor interactions. However, in this thesis, the proposed methodology using two platforms: simulation and practical testing, provides the basic principle that can be used with other methods of global uncertainty and sensitivity analysis. In the case when factor interaction effects are required to be computed, a recommendation is provided in Chapter 7. However, it should be noted that computation of factor interaction effects usually requires expensive computations.

4.5. Methodology for Steady State Performance Evaluation

A feasible way to evaluate the performance of measurement algorithms in the steady state is by analyzing their frequency responses. The frequency response shows how measurement algorithms respond to the input signal of different frequencies in the steady state [9]. Ideally, the high performance of measurement algorithms shows a frequency response of a unity-amplitude gain at the fundamental frequency and a complete attenuation (zero-amplitude gain) at non-fundamental frequencies.

Figure 4.9 shows the ideal amplitude ($|y_{ideal}|$) frequency response of measurement algorithms for estimating a 50Hz fundamental frequency component. This ideal response is most commonly used as a benchmark frequency response.

In practice, a fundamental frequency often shows a small variation in electrical network due to the switching of loads. The switching of loads is a continous process. For

this reason, the performance of measurement algorithms in the steady state for estimating the fundamental frequency considers a small off-nominal fundamental frequency.
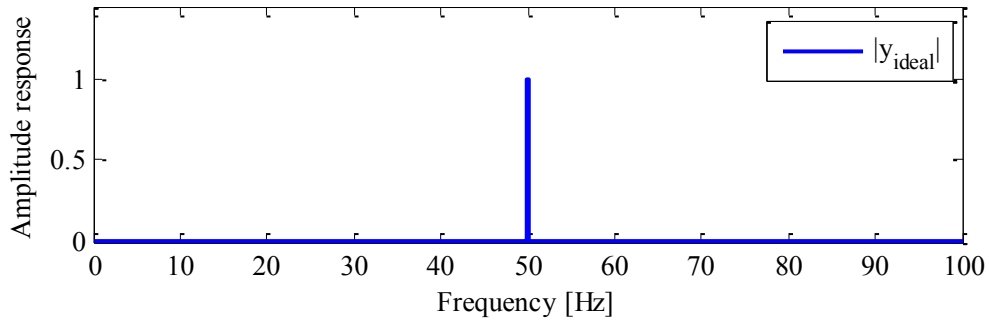
Figure 4.9 Ideal amplitude frequency response

It is also the task of measurement algorithms to attenuate any nuisance signals that may be present in the ouput of the anti-aliasing LPF. These nuisance signals are present because the LPF is unable to attenuate signals that are lower than the cut-off frequency of the LPF such as the DC offset. Moreover, as previously mentioned, the third and fifth harmonic components may also be presented to achieve a balance between the accuracy and speed of the IED's output. Thus, for the steady state evaluation, the performance of measurement algorithms for attenuating the amplitude of the DC offset, third and fifth harmonics are evaluated. Those performance criteria are important in the protection application testing.

4.5.1. Steady State Performance Criteria and Indices

The performance criteria for steady state evaluation are adopted based on the recommendation of papers [1, 70]. The criteria and their respective calculated indices are calculated as follows:

1. Fundamental aggregate index, PI_{FA}

The first performance criterion is the fundamental aggregate index. This index is used to measure the performance of measurement algorithms for estimating the

fundamental frequency component considering the small variation around it. This is because, as mentioned, the network system commonly operates with a small variation around the fundamental frequency component.

A new frequency response benchmark that considers a small variation around the fundamental frequency, known as the ideal frequency response (*FRI),* has been introduced. Figure 4.10 illustrates the benchmark of the ideal frequency response.
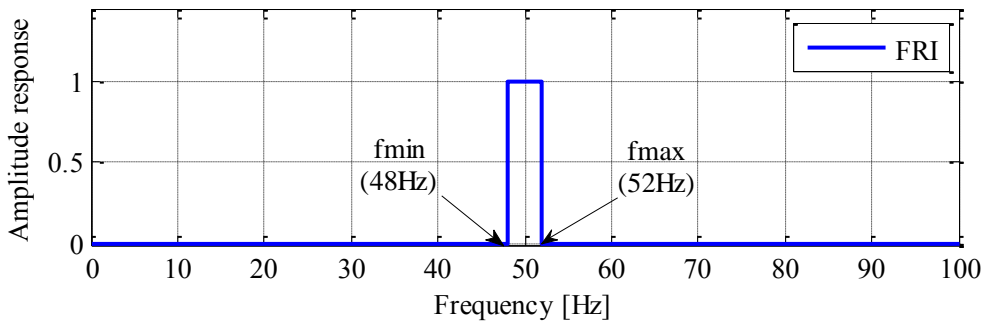
Figure 4.10 Benchmark of ideal frequency response (*FRI*)

A ±2 Hz tolerance around the fundamental frequency component, which is 50Hz, is assumed. The used tolerance frequency indicates that measurement algorithms should estimate the fundamental frequency component with unity amplitude gain for the frequency variation within a range of ($f_{min} = 48Hz$) to ($f_{max} = 52Hz$). The PI_{FA} index is calculated as:

$$PI_{FA} = \left(\frac{1}{f_{max} - f_{min}}\right) \int_{f_{min}}^{f_{max}} \left(FRI - \acute{f}\right)d\acute{f}. \tag{4.10}$$

Where *FRI* - ideal/benchmark frequency response

$\acute{f}$ - frequency response of measurement algorithm

The PI_{FA} index indicates an average of errors that are produced by measurement algorithms within the frequency variation boundaries.

2. DC amplitude attenuation, PI_{DC}

The second performance criterion for steady state evaluation is the DC amplitude attenuation (PI_{DC}). This criterion measures the ability of measurement algorithms to attenuate the DC component. This index is calculated directly from the frequency response of the evaluated measurement algorithm at 0Hz.

3. Third and fifth harmonic amplitude attenuation, PI_{H3} and PI_{H5}

The third and fourth criteria measure the ability of measurement algorithms to attenuate the amplitude of third and fifth harmonic components, respectively. The practical LPF has a non-ideal transition between the pass- and stop-band. Thus, several higher harmonic components, which are above the cut-off frequency of the LPF, can be expected in the sample of fault currents and voltages. Moreover, as mentioned previously, IEDs may be designed to pass certain harmonic components to balance between their accuracy and speed. In a steady state, two harmonic components: the third and fifth harmonic; are considered. The performance indices for these two components are also calculated directly from the frequency response at 150Hz and 250Hz, respectively.

An indicator for the good performance of measurement algorithms is shown by a lower calculated steady state performance index for each criterion (i.e. PI_{FA}, PI_{DC}, PI_{H3} and PI_{H5}). It is worth noting that the steady state performance indices are calculated from frequency responses, whereby these frequency responses are produced using fixed coefficients of the measurement algorithms. The fixed coefficients indicate that the frequency responses of the measurement algorithms are fixed. Thus, the calculated performance indices are not further analyzed using the uncertainty and sensitivity analysis method since they are certain.

The methodology for evaluation of the performance of measurement algorithms in the steady requires three steps. Figure 4.11 shows these steps for the proposed methodology.

```
┌─────────────────┐      ┌─────────────────┐      ┌─────────────────┐
│  Measurement    │      │  Plot frequency │      │  Calculate steady│
│  algorithms     │ ───► │  responses      │ ───► │  state PIs      │
│  coefficients   │      │                 │      │                 │
└─────────────────┘      └─────────────────┘      └─────────────────┘
```
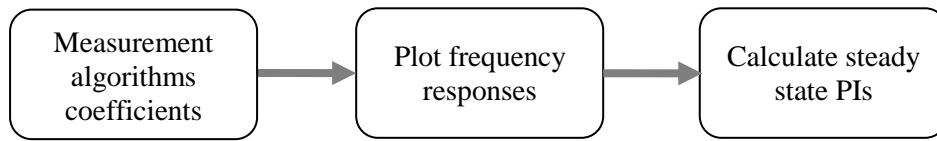
Figure 4.11 Methodology to evaluate performance of measurement algorithms in steady state

The first step is to calculate the coefficients of the measurement algorithms. Next, these coefficients are used to plot the frequency response of the measurement algorithms. Finally, the performance indices in a steady state are calculated.

For the steady state performance evaluation, the performance of measurement algorithms is only evaluated in simulation. This is because the proposed methodology requires the coefficients of measurement algorithms to be known. The DFT measurement algorithms, which are the half-, full-cycle DFT and Cosine filter can be calculated their coefficients as described in Section 2.5.

For practical testing, the performance of measurement algorithms in the steady state is not evaluated for the following two reasons. Firstly, the focus of this thesis is on the new methodology that is based on the global uncertainty and sensitivity analysis. Secondly, the coefficients of a commercial IED are unknown. However, if needed, their frequency response can be measured by applying the known amplitude and phase angle of the sinusoidal input signal (test signal) at a certain frequency, and then recording its output response. This approach requires a variation of test signal frequency over a range of evaluated frequencies. Then the gain in amplitude; and the difference in phase angle between the known test signal and the corresponding recorded output response; are calculated.

4.6. Conclusion

The design requirements for the successful implementation of the proposed testing methodology to evaluate performance of the measurement algorithms using global uncertainty and sensitivity analysis method has been presented in this chapter. The design takes into account that the proposed methodology can be implemented not only in simulation but also in the practical testing of IEDs.

The appropriate models of CT and CVT connected to the model of transmission line for modeling fault test scenarios have been illustrated and described. These models are used to generate systematic fault test signals for the performance evaluation of measurement algorithms. Furthermore, the model of IED that includes mathematical measurement algorithms has been described. The performance criteria and the corresponding indices required for measuring the quality on the output of measurement algorithms have been elaborated.

The idea of a two-stage global sensitivity analysis has been presented. The first-stage is the Morris method for preliminary sensitivity analysis. The second-stage is the EFAST method for comprehensive global uncertainty and sensitivity analysis. The limitations and the assumptions of the proposed methodology using the global uncertainty and sensitivity analysis have been presented.

The methodology to evaluate the performance of measurement algorithms in the steady state has also been described. It is based on the analysis of the frequency response of measurement algorithms.

Chapter 5. Implementation of the Proposed Methodology

5.1. Introduction

The previous chapter presented the design of the methodology for the performance evaluation of measurement algorithms in the transient response. The chapter also presented the methodology for the performance evaluation of measurement algorithms in the steady state. The performance of the measurement algorithm in transient and steady state are evaluated using corresponding performance indices. However, only the performance indices in transient response are further analyzed using the global uncertainty and sensitivity analysis. In this chapter, the implementation of those methodologies is detailed.

In the transient response, the proposed methodology is demonstrated by evaluating the performance of measurement algorithms implemented in IEDs. The methodology is implemented using two platforms. The first is simulation–based and the second is practical testing.

In the simulation-based platform, the methodology has been demonstrated by evaluating the performance of the Cosine filter. However, in practical testing, the

performance of the unknown measurement algorithms of a commercial IED has been demonstrated. For both platforms: simulation and practical, the same input fault test scenarios are simulated using the ATP/EMTP program. Thus, the procedures to create the fault test scenarios, which are parameterized by a variety of nuisance factors, are identical in both platforms. Most often, the practical evaluation requires much more complex procedures than the evaluation using the model simulation. For this reason, the implementation of the methodology in the transient response is presented in two separate platforms.

It should be noted that the aim of demonstrating the methodology as two separate platforms is to show their implementation rather than to compare their results. The main reason is that some information of commercial IEDs is the secret property of the relays manufacturer. The detailed information of the IED elements may be unknown (i.e. grey box). Thus, the model of the IED used in the simulation-based may not accurately represent a physical device. However, the results, which are obtained in each platform using the proposed methodology, are valid.

The SIMLAB program is used to perform a two-stage global sensitivity method: the Morris and EFAST. The SIMLAB is the specific software for the uncertainty and sensitivity study [8]. However, this program should be interfaced with the ATP/EMTP program to produce accurate fault test signals in a systematic way such that the uncertainty and sensitivity of measurement algorithms' output can be analysed. As mentioned in Chapter 4, the global uncertainty and sensitivity analysis requires extensive evaluation. Thus, to automate the process of evaluation, a script in the MATLAB program is developed. The script provides an iinterface among the MATLAB, SIMLAB and ATP/EMTP programs.

For practical testing, beside those three software tools, a commercial SEL-421 relay, SEL-AMS, SEL-5401 and AcSELerator Quickset software are used for testing and analyzing the output of the relay (i.e. IED). The fault test signals are simulated using the ATP/EMTP program and these test signals are injected to the server of Remote Relay Test System (RRTS) [71]. The RRTS provides a command to a Remote Test System module, which consists of the SEL-AMS and SEL-5401, to run and trigger the SEL-421 relay. Once the SEL-421 relay is tripping, all the results of testing are stored in the server of the

RRTS system. A developed script in the MATLAB program is used to automatically process all the results of testing.

The methodology for the performance evaluation of the measurement algorithms in the steady state uses the frequency response in which the steady state performance indices are calculated. As mentioned in the previous chapter, these indices are calculated without further analyzing their uncertainty and sensitivity to the variation of the input factors. This is because the coefficients of the evaluated measurement algorithm, which are used to plot their frequency responses, are fixed and known. The fixed and known coefficients mean that their input factors do not involve uncertainties.

Section 5.2 presents the implementation of the proposed global uncertainty and sensitivity analysis to evaluate the performance of the measurement algorithm of the IED. The fault system is modeled in the ATP/EMTP program in order to produce the extensive fault test scenarios that are influenced by the different degrees of uncertainty of the nuisance factors. The created fault test scenarios are used to evaluate the performance of measurement algorithms in both the simulation and practical testing. In simulation, the model of the IED including the Cosine filter algorithm is modeled in the MATLAB program. For practical testing, the IED SEL-421 relay is used. Section 5.3 presents the implementation of the methodology in the steady state to evaluate the performance of measurement algorithms when details of the measurement algorithms are known. Finally, Section 5.4 provides the conclusion to this chapter.

5.2. Evaluation in Transient Response

This thesis uses a two-stage approach: the Morris and EFAST global sensitivity analysis method. The two-stage approach is implemented in two platforms: computer simulation and practical testing. In both platforms, the same input fault test scenarios are used to evaluate the performance of the measurement algorithms. In simulation, the performance of the Cosine filter is evaluated, whereas in practical testing the performance of the unknown measurement algorithms of a commercial IED are evaluated.

Regardless of the platforms used, global uncertainty and sensitivity analysis requires four main steps. The first two steps are aimed to provide systematic fault test scenarios that are influenced by the uncertainty of the nuisance factors. The performance of measurement algorithms is evaluated using two types of input fault test signals: fault currents and fault voltages. Both the fault current and voltage signals are generated using the ATP/EMTP program.

5.2.1. Generating Current Scenarios

Fault current test scenarios are generated considering six nuisance factors including the decaying DC offset, which is the most common nuisance signal in the fault current. The six nuisance factors are described by Equation (4.1). To produce the nuisance factors within their uncertainties, these factors are varied within their PDFs. The amplitude of the decaying DC offset is varied from none to 100% of the amplitude of the fundamental frequency component. The time constant of the decaying DC offset is assumed to vary within (0.5 to 15) cycles.

The amplitudes of the third and fifth harmonic components are considered as the input factors. The phase angles of these harmonic components, however, are not considered. Harmonic components that are higher than the fifth order are also not considered since they are assumed to be attenuated by the anti-aliasing LPF of the IED. The fundamental frequency component used is 50Hz and it is assumed to vary within ±4Hz. The remanent flux in the CT core is assumed to vary within (-0.8 to 0.8) of the flux saturation threshold.

All these input factors are assumed to be distributed by a uniform distribution function since no information about their distributions has been systematically studied and published. The uniform distribution indicates that each of the sample points within its distribution has an equal probability of occurrence.

The aim of the proposed uncertainty and sensitivity analysis method is to quantify the uncertainty and sensitivity output of the measurement algorithms in a global way. Thus, each nuisance factor (i.e. parameter) is varied within their complete range rather than

around their nominal value. Table 5.1 summarizes the nuisance factors under study and their ranges of uncertainty.

Table 5.1 Nuisance factors on fault current scenarios

Nuisance factors	Variable	Uniform distribution (minimum maximum)
Decaying DC Offset amplitude	α	(0-100)%*
Decaying DC Offset time constant	τ	(10-300)ms
Third harmonic amplitude	h_3	(0-20)%*
Fifth harmonic amplitude	h_5	(0-10)%*
Off-nominal fundamental frequency	δf_1	(46-54)Hz
Remanent flux	λ	(-80 to 80)% of flux saturation threshold

* - the value is based on the percentage of the fundamental frequency amplitude.

To produce fault current test scenarios influenced by a variety of the nuisance factors, a fault system in the ATP/EMTP program is modelled and simulated. The fault system consists of models of an ideal transmission line network that is connected to a model of a CT. Figure 5.1 shows the equivalent fault system modeled in the ATP/EMTP program to produce the fault current scenarios.

CT model   Transmission line fault model
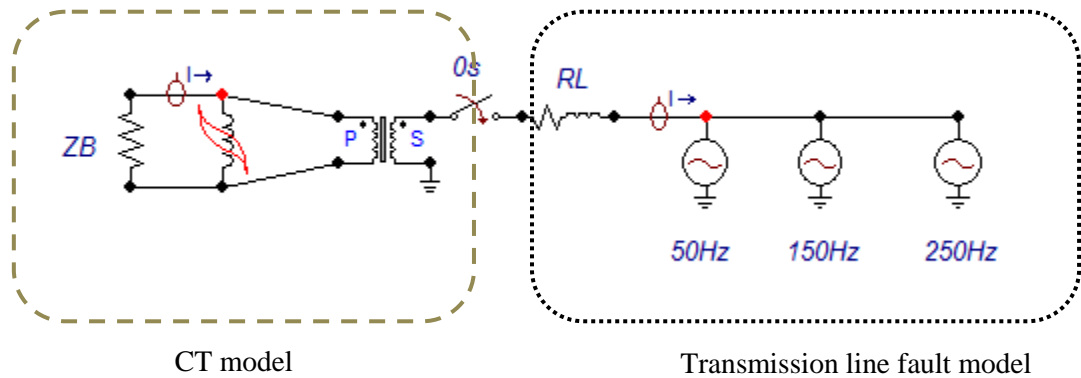
Figure 5.1 System model to produce current test scenarios

The model of the line network is represented by the resistive and inductive (R-L) elements. The model of the CT used has been described in Section 4.3.1. The parameters of the CT are based on paper [63].

In Figure 5.1, the 150Hz and 250Hz elements are used to inject the amplitude of the third and fifth harmonic component respectively. The RL element controls the time constant (τ) of the decaying DC offset. The 50Hz element controls the fundamental frequency variation within (46 to 54) Hz. This element is also used to control the amplitude of the decaying DC offset by varying phase angles within (0 – 90)°. Figure 5.2 shows an example of setting the 50Hz element in the ATP/EMTP program.
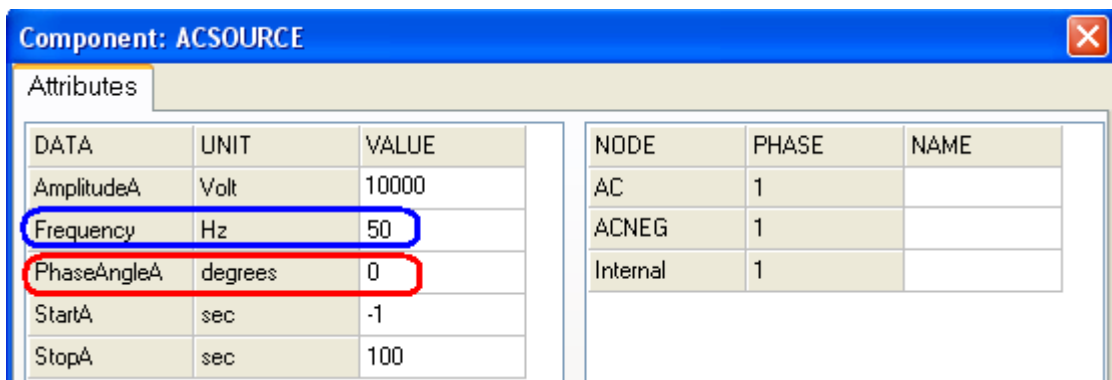
Figure 5.2 Example of 50Hz element setting in the ATP/EMTP program

The non-linear inductor (type-96 element) is used to model the V-I characteristic of the CT. The V-I characteristic and the parameters of the CT used are shown in Appendix B. The non-linear inductor of the ATP/EMTP element is also used to vary the remanent flux of the CT core. The CT burden (ZB) is selected in a way that any selected combination of nuisance factors will produce the fault current signal with distortion.

To simulate the single phase-ground fault, the switch is triggered by closing it at t=0 second. The simulation generates the fault current test signal of zero amplitude during the pre-fault, and higher level amplitude during the post-fault current. Extensive fault test signals are generated based on the method of the global sensitivity analysis used, namely the Morris and EFAST method. The duration for each simulated fault current test signal is 0.32 seconds.

Figure 5.3 shows an example of the fault current test scenario simulated in the ATP/EMTP program. The true amplitude of the fundamental frequency component is 5kA. In this example, the produced fault test scenario is influenced by the remanent flux that has 60% of the flux saturation threshold.
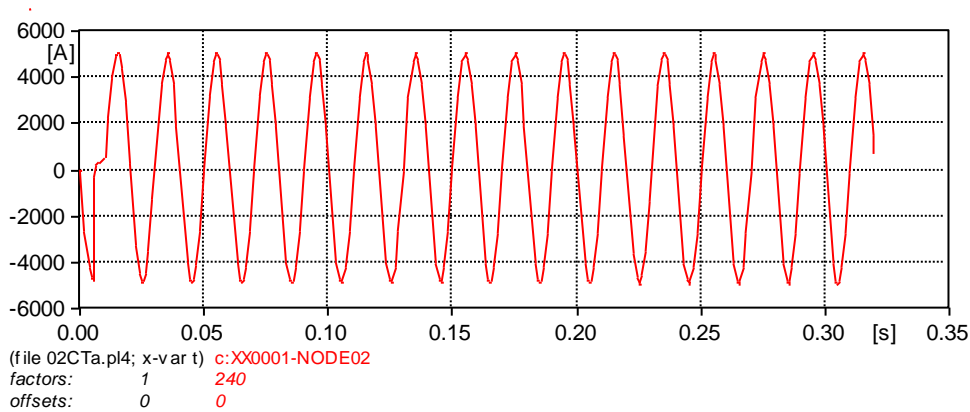
Figure 5.3 Fault current test scenario in ATP/EMTP

5.2.2. Generating Voltage Scenarios

Fault voltage test scenarios are generated considering five nuisance factors. These nuisance factors have been described by Equation (4.2). Three of these nuisance factors, the

amplitude of third and fifth harmonic, and the off-nominal fundamental frequency, have similar varying values, as they are used to generate fault current test scenarios. These three nuisance factors have been described in the previous section.

The amplitude and the time constant of the decaying DC offset are omitted since these factors have less influence on the fault voltages than fault currents during fault conditions. Instead, the influence of amplitude of the voltage collapse is investigated. The voltage collapse amplitude is one of the important factors that influences the fault voltage signals, and hence, it has a significant impact on the IEDs [38]. The amplitude of the voltage collapse represents the uncertainty of fault resistance, fault location and Source to Impedance Ratio (SIR).

Table 5.2 summarizes the considered nuisance factors for generating the fault voltage test scenarios. A uniform PDF is used to represent the uncertainty of all these factors for producing the fault voltage test scenarios.

Table 5.2 Nuisance factors on fault voltage scenarios

Nuisance factors	Variable	Uniform distribution (minimum maximum)
Fault inception angle	β	(0-90)°
Third harmonic amplitude	h_3	(0-20)%*
Fifth harmonic amplitude	h_5	(0-10)%*
Off-nominal fundamental frequency	δf_1	(46-54)Hz
Voltage collapse amplitude	ΔV	(0-100)% of pre-fault voltage

* - the value is based on the percentage of the fundamental frequency amplitude.

Figure 5.4 shows the fault system modeled in the ATP/EMTP program to simulate the fault voltage scenarios. The system consists of a model of the representing transmission network connected to the model of a CVT. In the transmisson model, the pre-fault element

is used to provide the ideal pre-fault voltage level for the first 60 milliseconds (3 cycles). Fault conditions are simulated by closing a switch at t=60 milliseconds.

After the fault is incepted, the elements of 50Hz, 150Hz and 250Hz are used to vary the fundamental frequency; amplitude of the third harmonic; and amplitude of the fifth harmonic respectively. Their variations, which have been described for generating the fault current test scenarios in the previous section, are performed in the similar way.

The representation of transmission fault model

CVT model
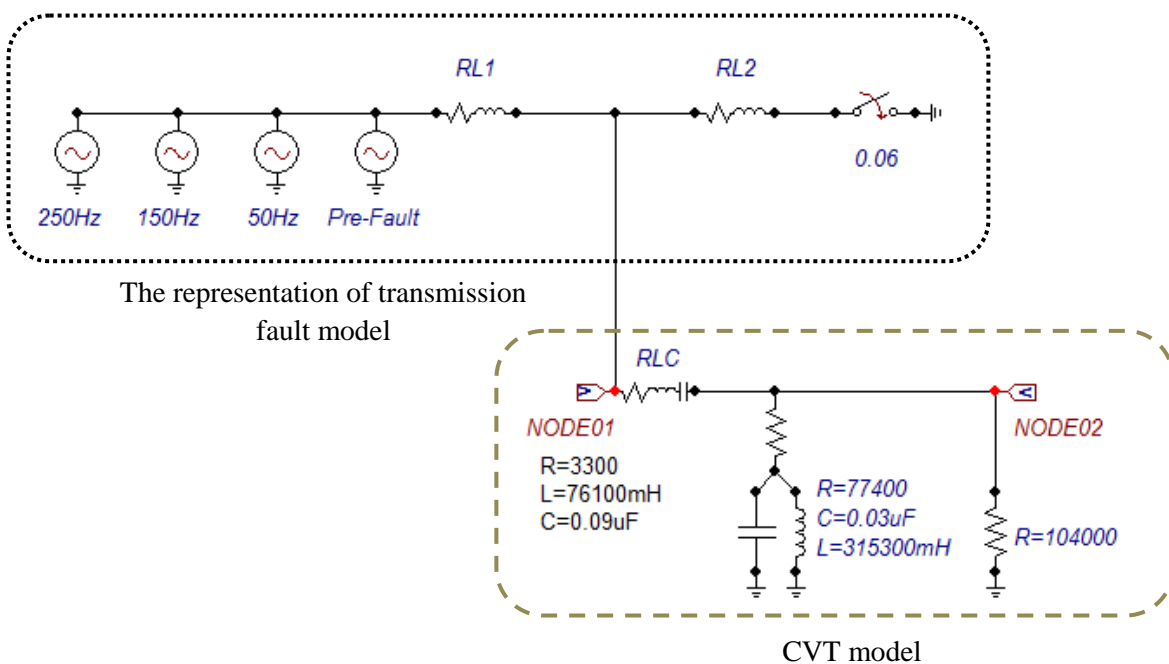
Figure 5.4 System model to produce voltage test scenarios

A pre-fault voltage is simulated since one of the studied factors is the amplitude of the voltage collapse (ΔV). This factor is the difference in amplitude between the post-fault and the pre-fault. Thus, it is necessary to simulate the pre-fault signal in a way that its initial amplitude is known. The amplitude of the voltage collapse is controlled by varying the two RL elements (RL1 and RL2) in the model of the transmission network. The CVT equivalent circuit used is based on paper [38].

Figure 5.5 shows an example of the fault voltage test signal simulated in the ATP/EMTP program. The true peak amplitude of the pre-fault and post-fault voltages of the simulated fundamental frequency component is 10kV and 5kV, respectively. The fault is incepted at 60 milliseconds. Note that the subsidence transient occurs at t=60ms up to t=100ms, which is 2 cycles. In most cases, the voltage subsidence transients last for 2-3 cycles [54]. In this study, however, 8 cycles (0.16 seconds) are simulated following the fault inception to ensure the complete occurrence of a subsidence transient.
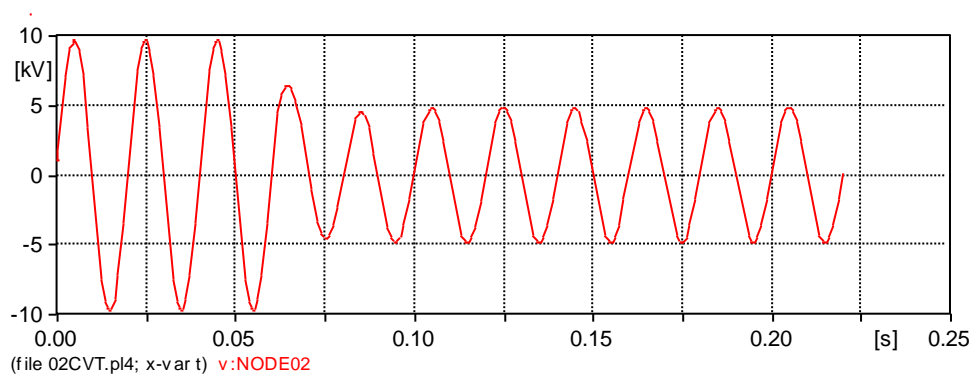
Figure 5.5 Fault voltage test scenario in ATP/EMTP

5.2.3. The IED Model

The operation of IEDs is based on the mathematical algorithms for processing the samples of the input signals. Thus, it is important to use a program that can easily script these mathematical algorithms. A MATLAB program is selected to script the measurement algorithms. Also, as the MATLAB program has extensive functions for signal processing, it can be used to model the anti-aliasing LPF of the IEDs; and to calculate the performance indices of the measurement algorithms.

The model of IED used is based on paper [63], and it has been described in Section 4.3.2. The MATLAB scripts for modeling the second-order anti-aliasing LPF and the Cosine filter are described in Appendix C. As an illustration, Figure 5.6 and 5.7 show the amplitude transient response of the Cosine filter to the simulated fault current and voltage signals of the previous examples.
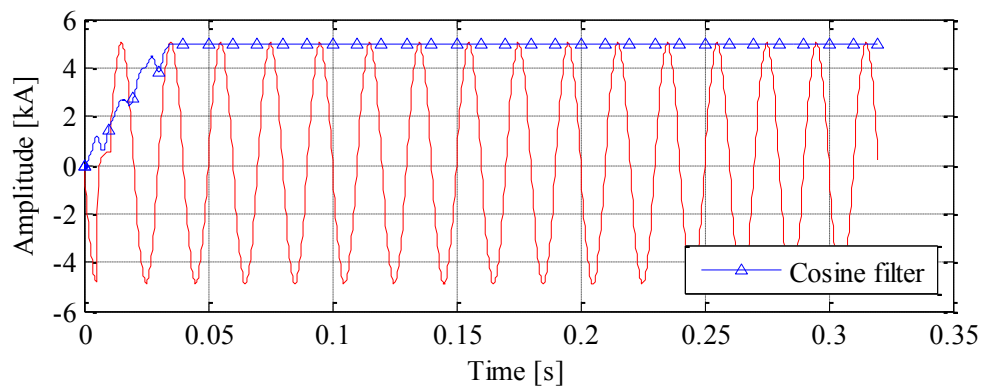
Figure 5.6 The amplitude tracking of Cosine filter to the fault current
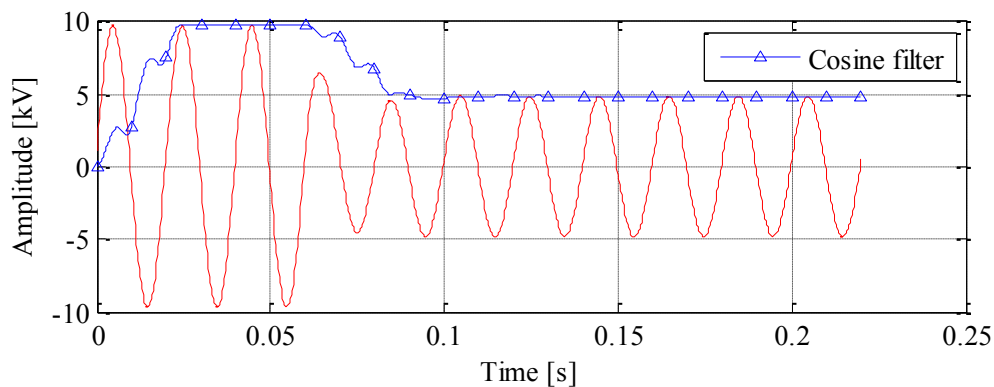
Figure 5.7 The amplitude tracking of Cosine filter to the fault voltage

5.2.4. The Simulation Methodology

The implementation of the proposed methodology in computer simulation uses a combination of three software programs: the ATP/EMTP, SIMLAB and MATLAB programs. The proposed methodology that is based on global uncertainty and sensitivity analysis requires four main steps. Three of these steps, which are steps 1, 2 and 4, are performed in the SIMLAB program. The third step involves an interface between the ATP/EMTP and MATLAB programs.

A two-stage method is performed. The first-stage uses the Morris method and the second-stage uses the EFAST method. The aim of the Morris method is to identify the important factors among all the investigated factors whereas the EFAST method aims to produce comprehensive uncertainty and sensitivity results in a quantitative way. Each method, however, requires the same process for its implementation.

Figure 5.8 shows the block diagram for the implementation of the proposed method to evaluate the uncertainty and sensitivity output of the measurement algorithm in simulation. The block diagrams of Figure 5.8 will be described using four basic steps of the global sensitivity analysis method, as follows:
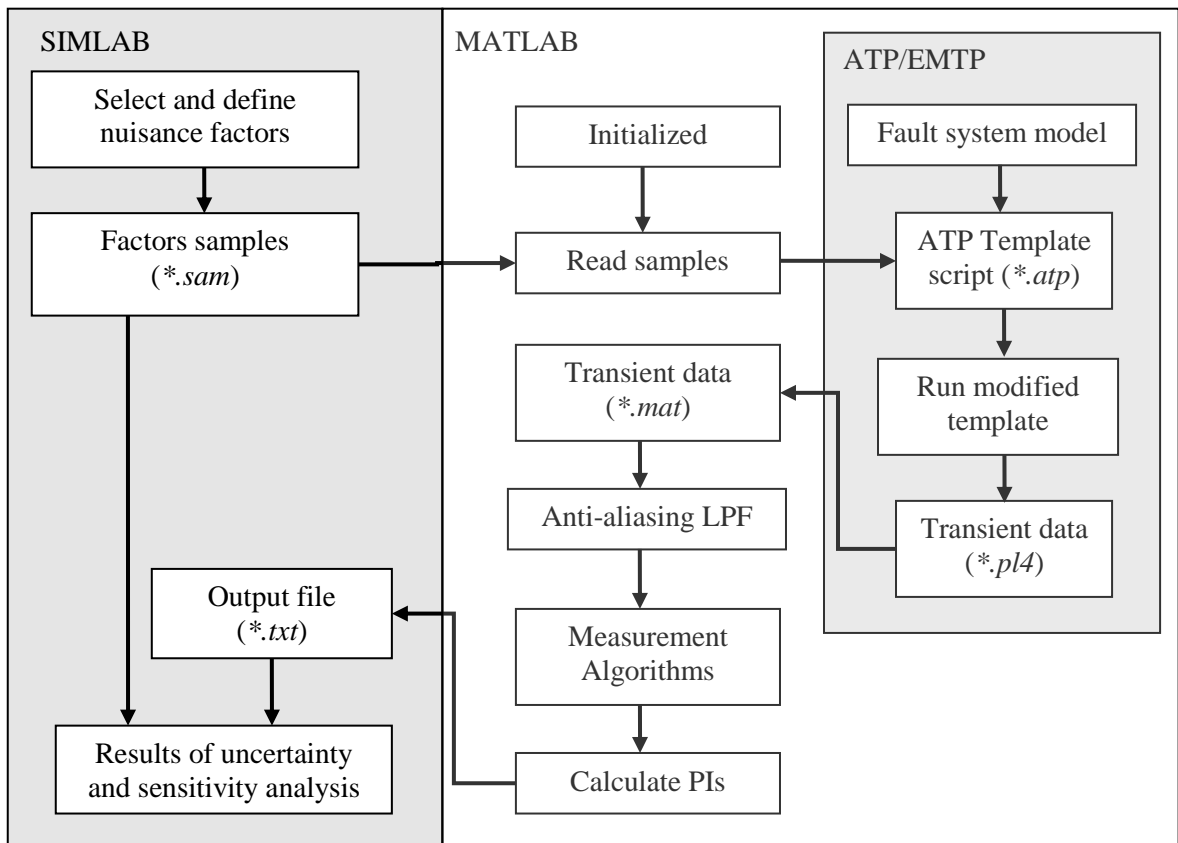
Figure 5.8 Block diagram for evaluation measurement algorithms uncertainty and sensitivity output using the simulation

1. Select and define input uncertainty factors

The first step in implementing the uncertainty and sensitivity analysis is to select and define all the investigated nuisance factors in fault signals. Six nuisance factors in the fault current signal and five nuisance factors in the fault voltage signal, shown in Table 5.1 and 5.2 respectively, are selected. The distribution of these nuisance factors is defined using a uniform distribution due to their equal probability of occurrence during the fault conditions. This first step is performed in the SIMLAB program.

In the first-stage of the sensitivity analysis, which is the Morris method, all the nuisance factors from the fault signals: current and voltage are used to evaluate their influence on the output of the measurement algorithm. The Morris method then identifies the unimportant factors through the screening process. The result of the Morris method will be used to eliminate those unimportant nuisance factors.

Thus, in the second-stage of the sensitivity analysis, only the subsets of all nuisance factors (i.e. important factors) are selected. These important factors are used in the EFAST method for obtaining comprehensive results of the global uncertainty and sensitivity.

2. Statistical sample of the input factors

The second step is to generate statistical samples for all nuisance factors by sampling them within their uniform distributions. The sampling technique is based on the method used for the uncertainty and sensitivity analysis. As mentioned, two methods of sensitivity analysis: the Morris and EFAST are used. The Morris method generates the samples based on varying one factor at a time (OAT) (see Appendix A). The EFAST method generates the samples through the transformation of uncertain factors using different frequencies based on the Fourier theory (see Section 3.6). For both methods, the SIMLAB program is used to generate statistical samples of the input factors.

In the first-stage, the statistical samples required by the Morris method are generated using eight levels of grids $(L_G = 8)$. The selected grid levels, which are the maximum grids available in the SIMLAB, produce high resolution statistical samples for simulating fault current test signals. Besides selecting the maximum levels of grids, the highest number of executions, which are $N_S = 70$, is also selected.

Figure 5.9 shows an example of the parameters'setting of the Morris sensitivity method in the SIMLAB environment. This selection allows the Morris method of the SIMLAB program to create 70 sets of samples. Each sample set represents a unique fault current test signal. It contains a sample point for each nuisance factor described by Equation (4.1).
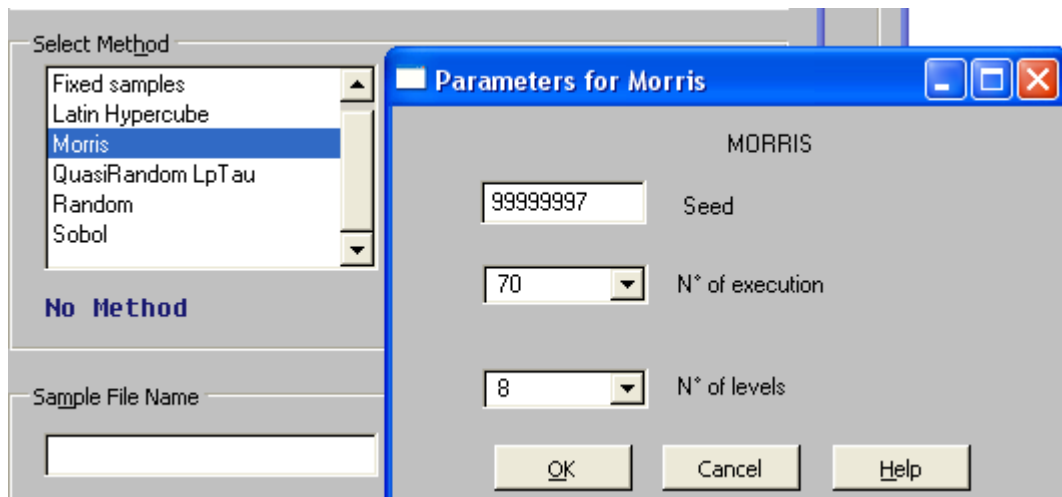
Figure 5.9 Parameters setting for the Morris method in SIMLAB

Similarly, the maximum eight levels of grids ($L_G = 8$) are also selected to produce the statistical samples for generating the fault voltage test signals. However, the highest number of executions is $N_S = 60$ since the number of investigated nuisance factors in the fault voltages is less than that in the fault currents. Note that for the both types of the input test signals: fault current and voltage, the highest number of sample sets is selected due to their low computation in the first-stage.

In the second-stage, which is the EFAST method, the user has to enter a number of the required executions (i.e. N_S). A minimum requirement is 65 samples for each uncertain factor studied [8]. A number of required samples of 2000 is selected and the EFAST method produces the optimal number of sample set according to its sampling strategy. Note that the Morris method is performed to eliminate the unimportant factors prior to the EFAST method, which means that the number of investigated factors is reduced in the

latter. With a smaller number of the factors used in the EFAST method, the selected number of sample set (i.e. 2000 samples) produces the acceptable results for the uncertainty and sensitivity analysis study.

Table 5.3 summarizes the selected number of samples for the Morris and EFAST methods, as well as the corresponding sample files (*.*sam*) used in this thesis. For the EFAST method, although the minimum sample required is 65 per factor (i.e. a total of $N_S = 195$ simulations for 3 factors), $N_S = 1995$ simulations (i.e. optimal sample sets produced by the EFAST method) is selected to achieve high accuracy results.

The sample file that produced by the SIMLAB program contains information on the number of factors, number of samples and the matrix of sample points of the nuisance factors. Appendix D shows an example of a created sample file, which is the *02SampleM.sam*.

Table 5.3 Sample files created in SIMLAB for creating fault scenarios in the Morris and EFAST method

Sensitivity Method	Type of fault scenario	Number of factors	Minimum sample required	Selected number of samples	Sample file (*.sam*)
Morris (1st stage)	Current	6	28	70	*01SampleM*
	Voltage	5	24	60	*02SampleM*
EFAST (2nd stage)	Current	4	260	1988	*01SampleE*
	Voltage	3	195	1995	*02SampleE*

3. Execute measurement algorithms

This step consists of several stages. The initial stage is to create the ATP template script of the fault system. The template is produced by representing the systems of Figure 5.1 and 5.4 in the ATP/EMTP program. An example of the generated template and the identified nuisance factors are illustrated in Appendix E. Using the template script, parameters of nuisance components (i.e. factors) are modified and then the script is executed in the ATP/EMTP platform. As the number of samples required to be executed is high, a script in the MATLAB program is developed to automate the process.

The developed MATLAB script reads the the matrix samples sample file (*.*sam*) generated by the SIMLAB. Then the script modifies the template of the fault system and simulates them in the ATP/EMTP platform. A row of matrix samples (a single scenario) is represented by a set of varying nuisance factors. The MATLAB script controls the simulation process in the ATP/EMTP until all sets of test scenarios are executed and the corresponding fault test signals are stored in the file with extension (*.*pl4*).

The developred script also convert the produced input fault transient scenarios in (*.*pl4*) to the matrix file (*.*mat*) format. A converter program *pl42mat.exe* is used [10]. The conversion to the matrix file (*.*mat*) format is important because, in the next process, the model of the IED and all the necessary calculation will be performed in the MATLAB program. Using the MATLAB program, the transient response performance indices can be easily scripted since the MATLAB has an extensive signal processing library.

Next, the fault transient signals, both current and voltage, are applied to the model of anti-aliasing LPF. The second-order Butterworth LPF with cut-off frequency of 300Hz is used. The output of the LPF is applied to the input of the measurement algorithm (the Cosine filter) for tracking the amplitude of the fundamental frequency component. For each output response of the measurement algorithm, the transient response performance indices are calculated and recorded.

Finally, the developed script creates an output text file (*.*txt*) that is readable by the SIMLAB program. The output text file contains the corresponding calculated transient response performance indices from each row of the matrix sample in the sample file. All

the stages of step 3, except creating ATP template, are performed in an automatic way using the script that is developed in the MATLAB program.

4. Calculate uncertainty and sensitivity indices

The final stage in the implementation of the proposed methodology is to calculate the uncertainty and sensitivity indices. To calculate these indices, two files are used: the samples file (*.sam) generated by the SIMLAB program; and the output text file (*.txt) created by the MATLAB program. These two files are loaded to the SIMLAB program again. The sample file is loaded through a load sample file, whereas the output text file is loaded using an external model, as illustrated in Figure 5.10. Then, the methods of sensitivity analysis: the Morris and EFAST are selected to analyze the uncertainty and sensitivity of the transient response performance indices.
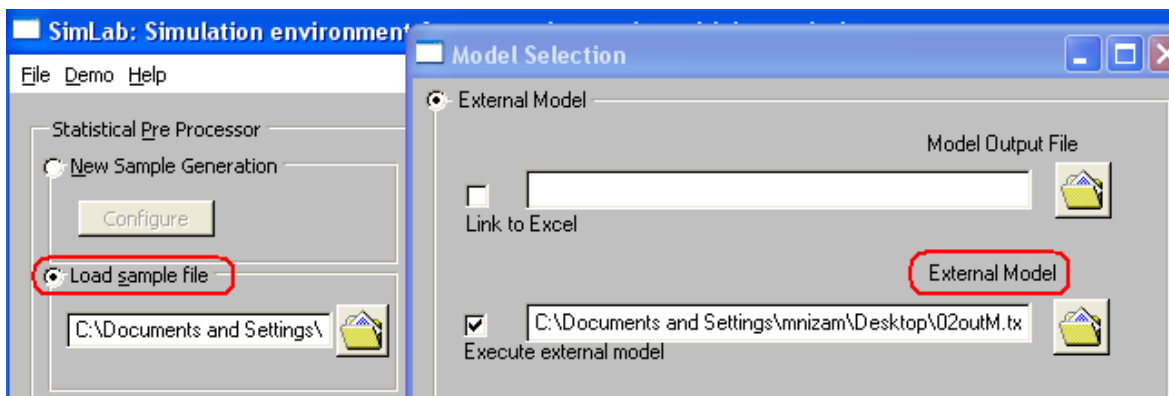
Figure 5.10 The sample file and the output text file in SIMLAB

As previously mentioned, a two-stage sensitivity analysis method is performed. The first-stage is the Morris method and the second-stage is EFAST method. Similar procedures are then repeated using the second-stage sensitivity method.

5.2.5. Practical Methodology

The global uncertainty and sensitivity analysis method requires four main steps. Three of these steps, which are steps 1, 2 and 4, are identical to the steps used in the simulation platform. These three steps are performed in the SIMLAB program. As these steps are identical as those in the simulation, this section will present the implementation of the proposed methodology with greater focus on the third step. The third step involves more complex procedures than those used in the simulation platform.

The implementation of the proposed methodology for practical testing requires additional software tools to those used in the simulation, in addition to the software tools used in the simulation. Three additional software programs as well as equipment for testing IEDs are required.

1. A SEL5401 software [72]

This software provides a (*RTA*) file that is required in testing a commercial IED. The file provides a configuration of the input channels of the IED where the first three input channels are used for the voltage signals and the next three channels for the current signals. The file also contains the duration of the generated fault test signals and their scales.

2. An AcSELerator Quickset program [73]

This program is used to analyze the output files produced from the evaluated IED. The program is used to read the result of compressed files (*C4.*txt*). The compressed files are the main files required in this study since they show the amplitude tracking of the fundamental frequency component of the implemented measurement algorithms.

3. A remote relay testing web account

Power Laboratory at the University of Adelaide provides a remote relay testing platform for power electrical students and researchers [71]. The performance of the available commercial IED in the laboratory can be tested in a remote way. This platform

provides a safe platform for users to test the IED since there is no direct contact between the users and the test system: IED device and instrument transformers.

Figure 5.11 shows the block diagram for the implementation of the proposed global uncertainty and sensitivity analysis method for practical testing. The dash-dot blocks indicate the evaluation process that is similar to the process used in the simulation, which are steps 1, 2 and 4 of the four main steps for performing the global sensitivity analysis. The dash-dot blocks include all the process blocks in the SIMLAB and the ATP/EMTP programs. Their functions have been explained in the previous section.
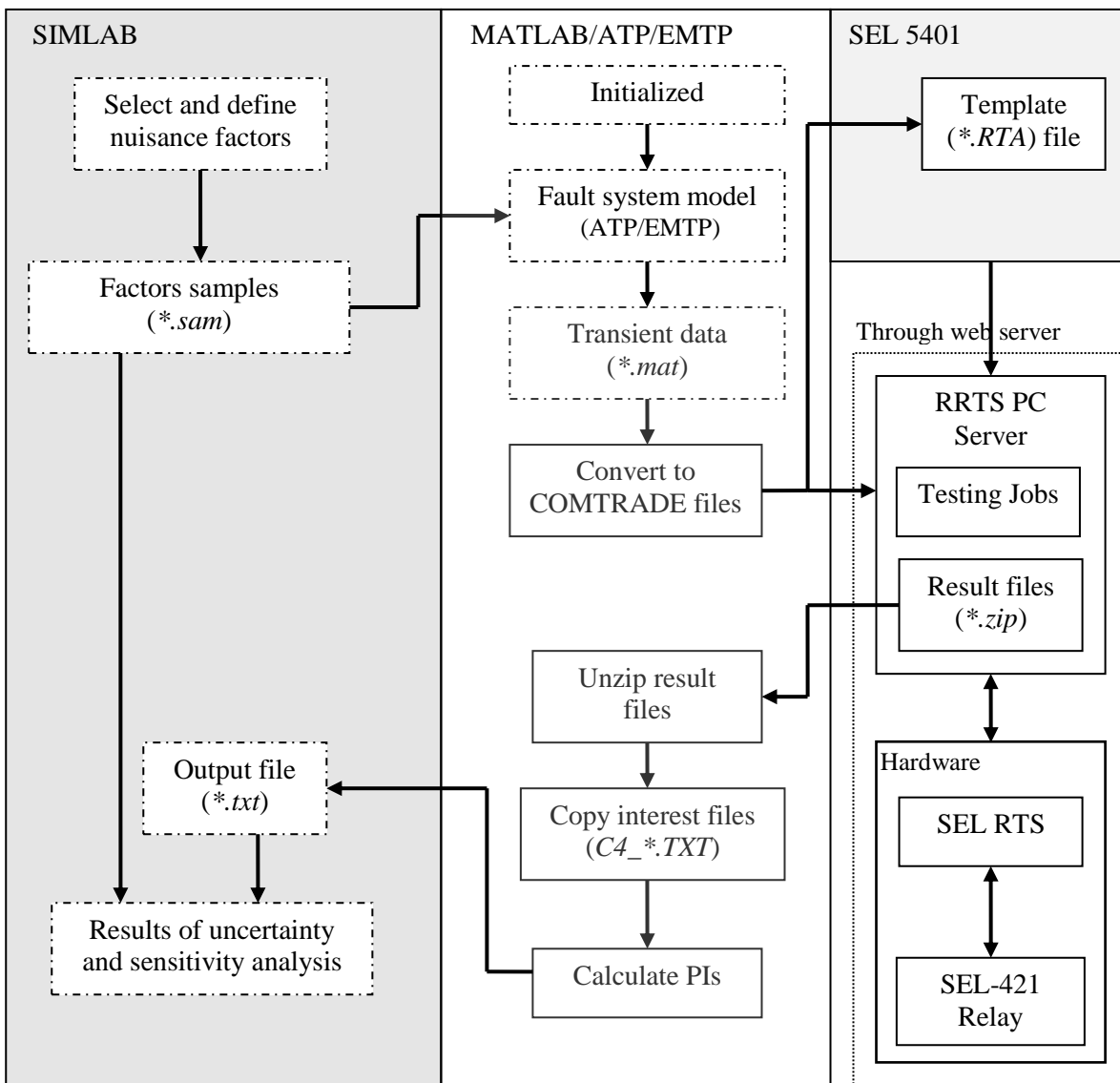
Figure 5.11 Block diagram for the evaluation measurement algorithms' uncertainty and sensitivity output in practice

As previously mentioned, the third step in the practical testing requires a more complex procedure than the implementation of the methodology during the simulation. Thus, the implementation of the proposed practical methodology for this third step will be described in detail.

Once the the sample file (*.*sam*) is created, a developed MATLAB script is used to read the matrix of the sample file; to modify and then execute the fault system template in the ATP/EMTP platform; and finally to convert the fault transient signals (*.*pl4*) to a matrix file (*.*mat*).

Next, a MATLAB script is further developed to convert those transient signals to the Common Transient Data Exchange (COMTRADE) files' format [74]. The COMTRADE consists of two files namely the configuration file (*.*cfg*) and the data file (*.*dat*). Since the test scenarios are a variety of single phase-ground faults of a same period of simulation, only the information in the data file is changed for each scenario. The configuration file remains unchanged.

The SEL-5401 software is used to define the input channels of the test set. This software creates (*.*RTA*) file and reads both the (*.*cfg*) and the (*.*dat*) of the COMTRADE files. Since the same configuration file of the COMTRADE and the same setting of the input channels for all the generated fault test scenarios are used, the relay testing assistant file (*.*RTA*) also remains unchanged.

Those three types of files: (*.*RTA*), (*.*cfg*) and up to ten different (*.*dat*) files are automatically zipped using a script developed in MATLAB program. The produced zipped files create a batch of testing jobs. The zipped files are uploaded to the Remote Relay Test System (RRTS) server at the University of Adelaide [71].

Then, each scenario is processed by the hardware devices, which consists of the SEL RTS Test Set and the IED SEL-421 relay. The SEL-421 relay is tested by means of a low-level test. This type of test bypasses the input of the isolation transformers in the SEL-421 [75, 76]. The PC server is used to control and execute series of the testing jobs to the SEL-421 relay via SEL RTS Test Set. This server also stores the transient response results of the measurement algorithm in the form of the compressed files (*.*zip*).

In all tests that have been performed, the SEL-421 is configured as an overcurrent protection. Note that this configuration will not affect the outcome of the results since the interested characteristics are on the output behavior of the measurement algorithm instead of the protection functions.

One minute, on average, is required to process each fault signal. Once all the test signals are executed, all the result files are stored in the RRTS server in the form of the zipped folders. Each folder represents a single test scenario. It may contain the compressed of the event files (*C4_*.txt*), raw event files, breaker report file and the setting file. Thus, it is important to unzip the zipped folders and analyse the file of interest.

For this study, the file of interest is the compressed (*C4_*.txt*). This file contains samples of the transient response of the evaluated unknown measurement algorithms of the IED for the estimation of the fundamental frequency component.

Since an extensive number of result folders are required to be unzipped and then the compressed (*C4_*.txt*) files are searched to be unzipped as well, a script in the MATLAB program is developed to automatically unzip these result folders and files. The developed script search in each folder and copy the compressed (*C4_*.txt*) files to our local computer for further analysis.

Then, the AcSELerator Quickset program is used to read the sample data from the compressed (*C4_*.txt*) for plotting the output transient responses of the implemented measurement algorithms. However, it should be noted that the AcSELerator Quickset is only suitable for the used of investigating a small number of test scenarios because this software works manually. The manual investigation of a large number of scenarios, which is the case for the global sensitivity analysis method, may lead to the errors and it is impractical.

In this study, a total of 4113 scenarios (currents and voltages) are required to be analysed in order to calculate the performance indices in the transient response. To automate the plot and analyze the results from SEL-421, a script in the MATLAB program is developed. Appendix F shows the application of the developed script by providing the comparative examples between the plots using the AcSELerator Quickset and the plots

using the developed script in the MATLAB program. The developed script produces an identical plot as in the AcSELerator Quickset program.

Next, the MATLAB script is used to automate the calculation of transient response performance indices: overshoot, undershoot, steady state error and settling time. The calculated transient response performance indices are tabulated and saved as the output text file (*.txt*), which is created using the MATLAB script. The produced output text file is in a format that is readable by the SIMLAB software. Finally, the SIMLAB program is used to read again the sample file (*.sam*) and the output file (*.txt*) for uncertainty and sensitivity analysis.

5.3. Steady State Evaluation

This section presents the implementation of the proposed methodology to evaluate the performance of measurement algorithms of IEDs in the steady state. A script in the MATLAB program, which has an excellent library function for signals processing, is developed to automatically calculate the performance of the full- and half-cycle DFT and Cosine filter. Figure 5.12 shows the block diagram to evaluate the performance of the measurement algorithms in the steady state. The implementation of the proposed methodology requires three main steps.
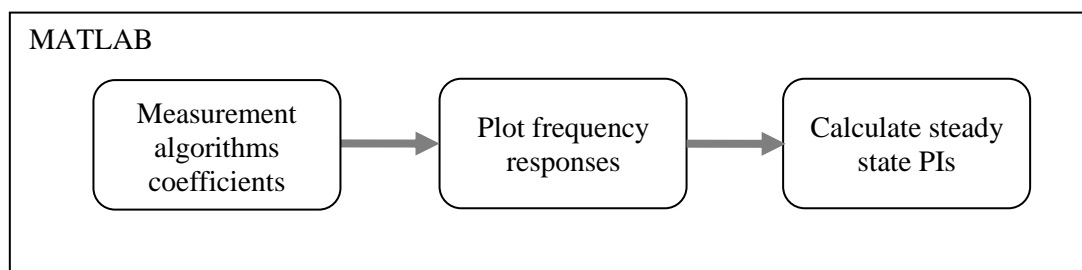
Figure 5.12 Block diagram for evaluation measurement algorithms performance in the steady state

The first is to obtain the coefficients of the measurement algorithms: the real and imaginary parts. These coefficients are calculated from the cosine and the sine terms of Equations (2.1) and (2.2) for the full-cycle DFT; Equations (2.5) and (2.6) for the half-cycle DFT and Equation (2.7) for Cosine filter. Appendix G shows the calculated numerical coefficients of the evaluated measurement algorithms.

The second step is to plot the frequency response of the measurement algorithms using their respective coefficients. Appendix H shows the MATLAB scripts used to plot the frequency response of the three measurement algorithms. In the next step, the performance indices in the steady state are calculated using a developed script in the MATLAB program. All these three steps for calculating measurement algorithms performance indices in the steady state are automatically executed. The results of the performance evaluation of the measurement algorithms in the steady state are presented in the next chapter.

5.4. Conclusion

The implementation of the proposed methodology for the performance evaluation of measurement algorithms in the transient response and steady state has been described in this chapter. In the transient response, the proposed methodology is implemented in two platforms: simulation-based and practical testing. In both platforms, the necessary software tools that are required for the success of the implementation are described in detail.

In simulations, the proposed methodology in the transient response is demonstrated by evaluating the performance of the Cosine filter. In practical testing, the proposed methodology is demonstrated by evaluating the performance of the unknown measurement algorithms of a commercial IED. In both platforms, however, the same input fault test scenarios are used. There is a description of the details of the simulation of the fault test scenarios using the ATP/EMTP program; and the model of IED including the Cosine filter, whereby both are implemented in the MATLAB program.

The implementation of the proposed methodology for the performance evaluation of the measurement algorithms in the steady state is described as well. The proposed methodology is demonstrated on measurement algorithms when details of their coefficients are known. The coefficients of the three popular DFT algorithms: the full- and half-cycle DFT and Cosine filter are calculated and then are used to plot their amplitude frequency responses. Next, the steady state performance indices are calculated. The evaluation process in the steady state, which is performed automatically using the script in the MATLAB program, is presented in detail.

Chapter 6. The Results of Performance Evaluation

6.1. Introduction

This chapter presents the results of the performance evaluation of measurement algorithms in the transient response and the steady state using the proposed methodologies. In the transient response, the performance of measurement algorithms based on the global uncertainty and sensitivity analysis method is evaluated. This method measures the uncertainty and sensitivity on the outputs of the measurement algorithms due to the uncertainty of input factors.

A two-stage global sensitivity analysis method is performed. The Morris method is performed first with the EFAST method being performed second.. The main reason for using the two-stage method is to increase the possibility for the implementation of the proposed methodology, particularly in practical testing. This is because the global uncertainty and sensitivity analysis requires extensive evaluations. Such extensive evaluations can be impossible in practical testing due to time limitations as described in Chapter 4.

The two-stage global sensitivity analysis method is successfully performed in two different platforms: simulation and practical testing. In each platform, the performance of measurement algorithms receiving the input fault current and voltage signals is evaluated. These signals are influenced by the uncertainty of nuisance signals in fault conditions.

The proposed global sensitivity analysis method is demonstrated by evaluating the performance of the Cosine filter in simulation platform. A model of an IED, which includes the mathematical algorithm of the Cosine filter, is used. In practice, the proposed methodology is demonstrated by evaluating the performance of the unknown measurement algorithms of a commercial IED.

However, the aim of the practical evaluation is to demonstrate the implementation of the proposed methodology in a practical way rather than to compare the results between the simulation and practical testing. The main reason for an invalid comparison is that some of the IED elements, particularly the measurement algorithms, can be unknown due to their secret property of the manufacturers. It is interesting to note, however, that the obtained results show a close similarity between the simulation and practical testing.

In the steady state, the performance of the Cosine filter is demonstrated. Also, the performance of the full- and half-cycle DFT measurement algorithms is demonstrated. The results of the performance evaluation in the steady state show the capability of these measurement algorithms to estimate the fundamental frequency component during off-nominal frequency, as well as their capability to attenuate the amplitude of DC offset, third and fifth harmonic components.

The methodology in the steady state for evaluation performance of the measurement algorithms is based on analyzing their frequency response. The methodology automatically calculates coefficients of the measurement algorithms and plots their frequency responses. As these coefficients are fixed and known (i.e. not involving the uncertainty of factors), only the performance indices in the steady state are calculated without further analysis t using the global sensitivity analysis method. Furthermore, as the coefficients of the measurement algorithms of the commercial IED are unknown during practical testing, the proposed methodology is only performed in simulation.

Section 6.2 presents the results of the applied global sensitivity analysis: the Morris and EFAST methods on the output of the Cosine filter in the simulation and the unknown measurement algorithms of the IED SEL-421 relay in the practical testing. The result of the Morris method shows the identified unimportant (non-influential) nuisance factors on the output of both the Cosine and unknown measurement algorithms. The result of the EFAST method shows the uncertainty of the outputs of those measurement algorithms, as well as the contribution of the nuisance factors to the outputs uncertainties.

Section 6.3 presents the results of the performance evaluation of the full-, half-cycle DFT and Cosine filter in the steady state. Frequency responses of these measurement algorithms, for which their coefficients are known, are plotted and their performance indices in the steady state are calculated and presented. Finally, Section 6.4 provides the conclusion to this chapter.

6.2. Transient Response Evaluation Results

The two-stage sensitivity analysis has been performed to evaluate the performance of measurement algorithms implemented in IEDs. Their performance, in the transient state, is accessed by analyzing the output transient response of the measurement algorithms for estimating the amplitude of the fundamental frequency component. The calculated transient response performance indices are: the overshoot, undershoot, steady state error and the settling time. These indices, which are used to indicate the performance of the measurement algorithms, can be uncertain due to the uncertainty of nuisance factors in the input signals to the measurement algorithms.

The evaluation results in the transient response are organized as follows. The result of sensitivity analysis using the Morris method will be presented first followed by the EFAST method. For each method, Morris or EFAST, the first sensitivity results is the case when the input to measurement algorithms is the fault current test signals; and the second case is when the input to measurement algorithms is the fault voltage test signals.

6.2.1. The Morris Method

The Morris method is used to identify the unimportant input nuisance factors on the output transient response of the Cosine filter in simulation; and of the unknown measurement algorithms in practical testing. The unimportant factor is a factor that shows a small or no influence on the output of measurement algorithms. The investigated nuisance factors are six factors in input fault current $(\alpha, \tau, h_3, h_5, \lambda, \delta f_1)$; and five factors in input fault voltage $(\theta, h_3, h_5, \delta f_1, \Delta V)$.

Figure 6.1 shows the result of the applied Morris method on the output of the Cosine filter (i.e. simulation-based) when its input is the fault current signals. Figure 6.2 shows the result of the applied Morris method on the output of the unknown measurement algorithms (i.e. practical testing) for the similar input fault current signals.

The red dash circles on both Figures indicate a cluster of unimportant factors, which have the mean (μ) and standard deviation (σ) values close to the origin (0). This cluster is separated from other factors, which are the important factors. The result shows that the amplitude of the third and fifth harmonics (h_3, h_5) are the two factors that show the least influence on all the calculated performance indices: the overshoot, steady state error and settling time. These two factors show the least influence on both the evaluated measurement algorithms: the Cosine filter and the unknown measurement algorithms.

For the steady state error and settling time, the remanent flux is also a factor that shows less influence on the output of both the measurement algorithms. The common unimportant nuisance factors for all calculated performance indices, therefore, are the third and fifth harmonic components. These two factors (h_3, h_5) are assumed to be the unimportant factors to the input of the measurement algorithms when their input is fault current signals. These two factors will be eliminated in the next comprehensive EFAST method for both the simulation and practical testing.
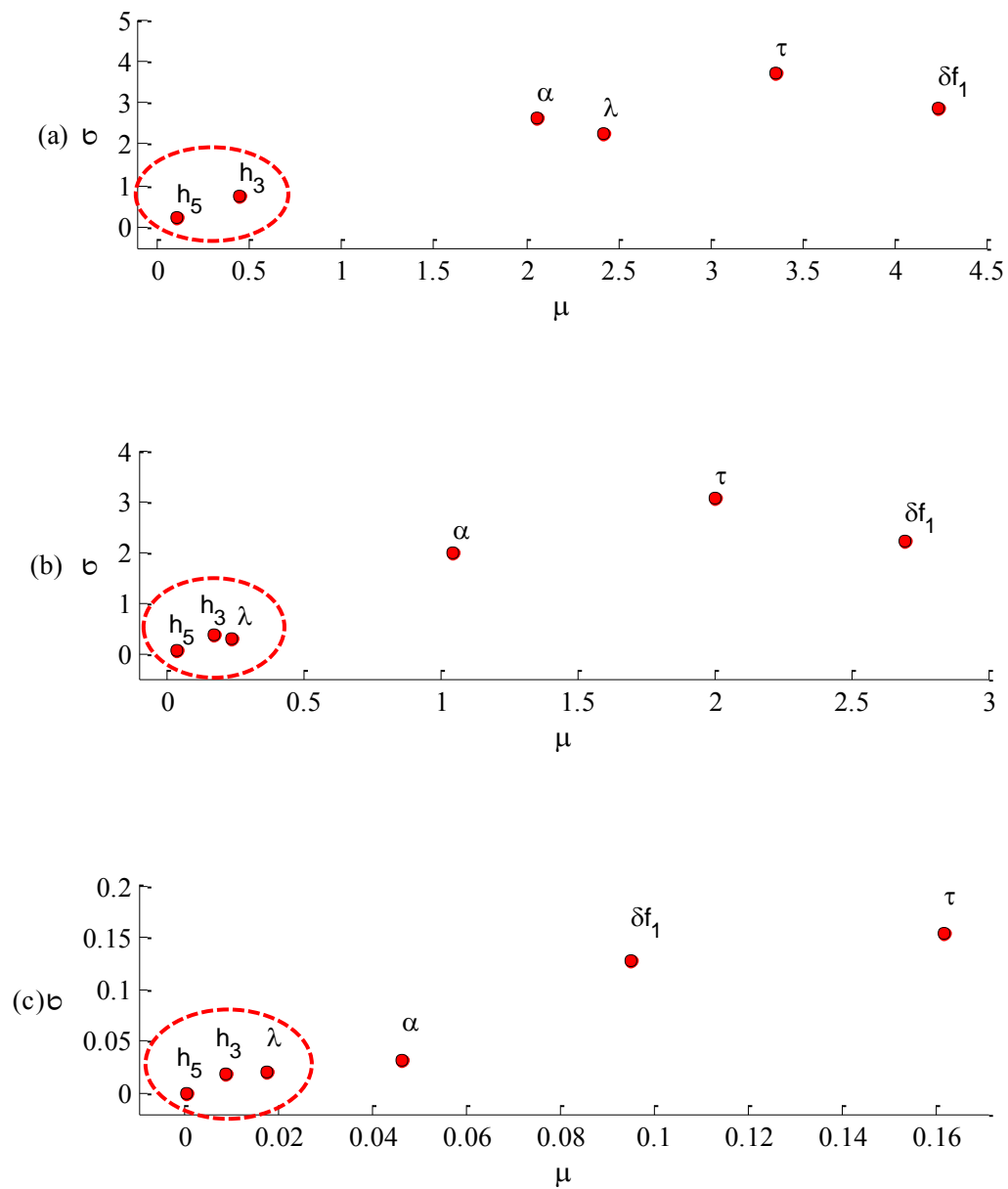
Figure 6.1 Sensitivity results of the output of the Cosine filter when its input is fault current signals (a) overshoot (b) steady state error (c) settling time
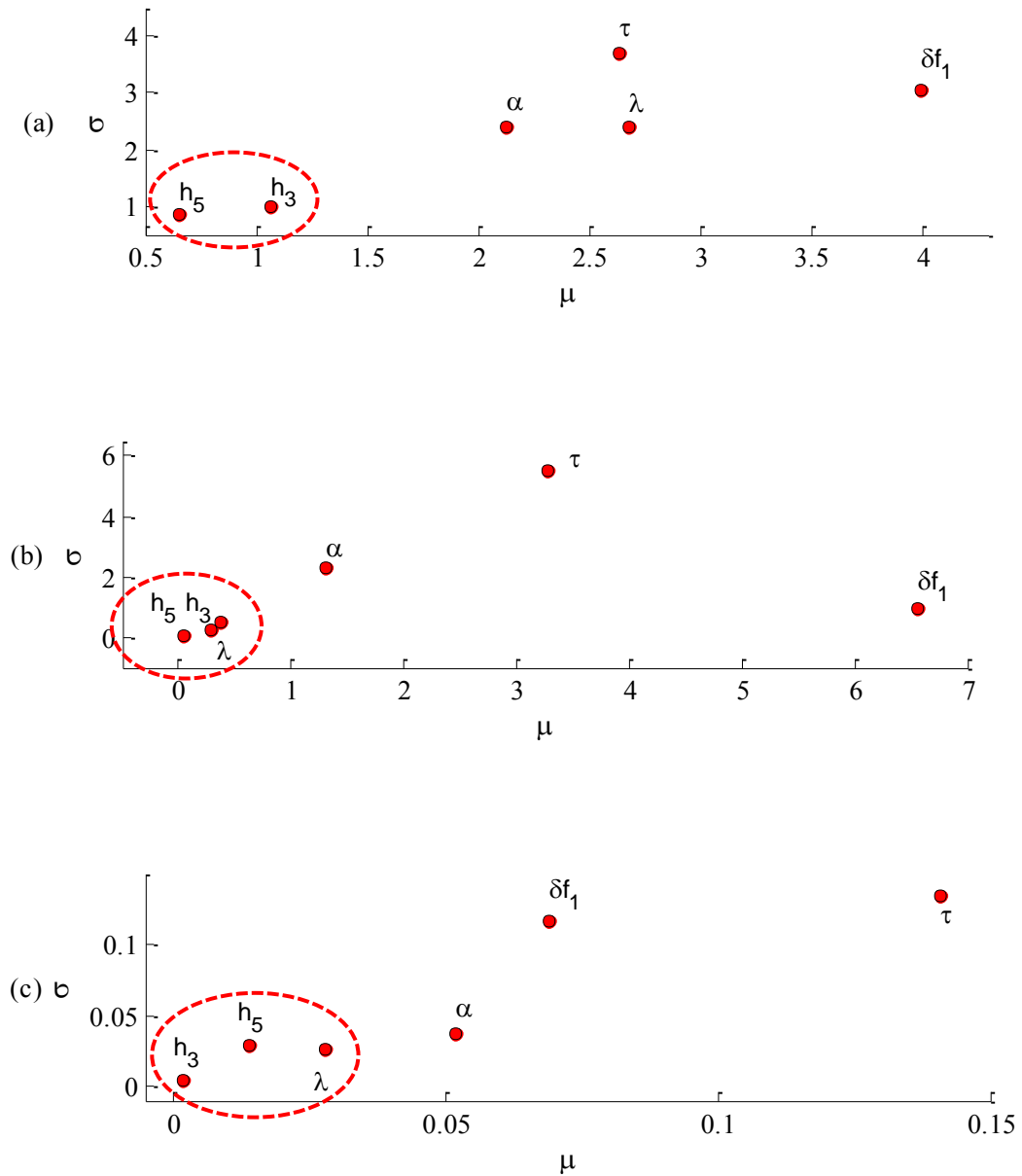
Figure 6.2 Sensitivity results of the output of the unknown measurement algorithms when its input is fault current signals (a) overshoot (b) steady state error (c) settling time

Next, Figure 6.3 and 6.4 show the results of the applied Morris method on the Cosine filter (i.e. simulation-based) and unknown measurement algorithms (i.e. practical testing), respectively. In this case, the input to the measurement algorithms are the fault voltage signals. The calculated performance indices are the undershoot, steady state error and settling time.
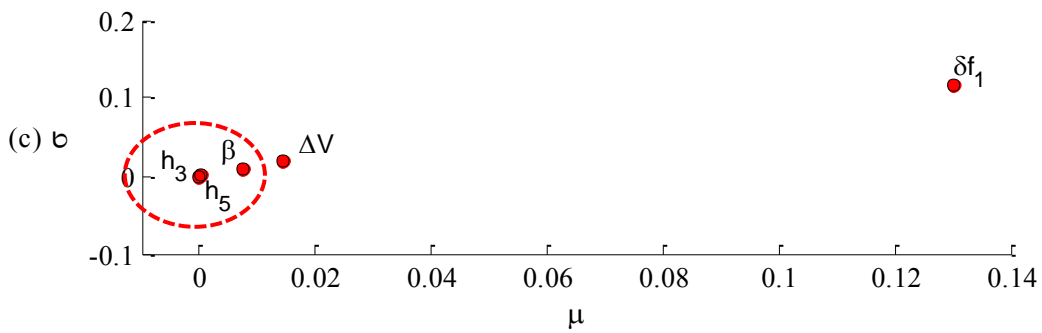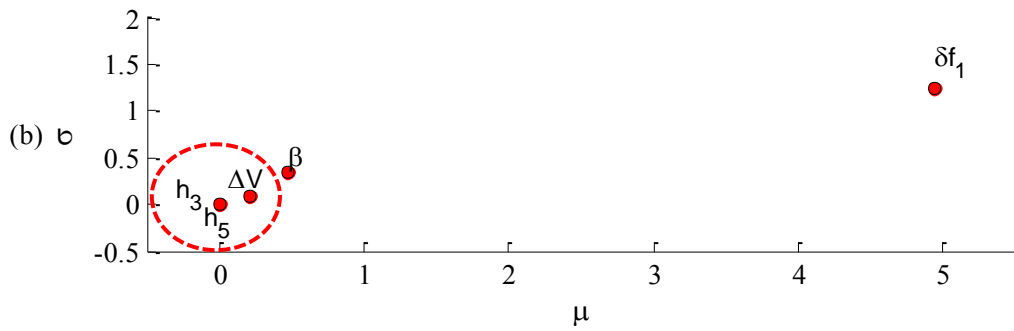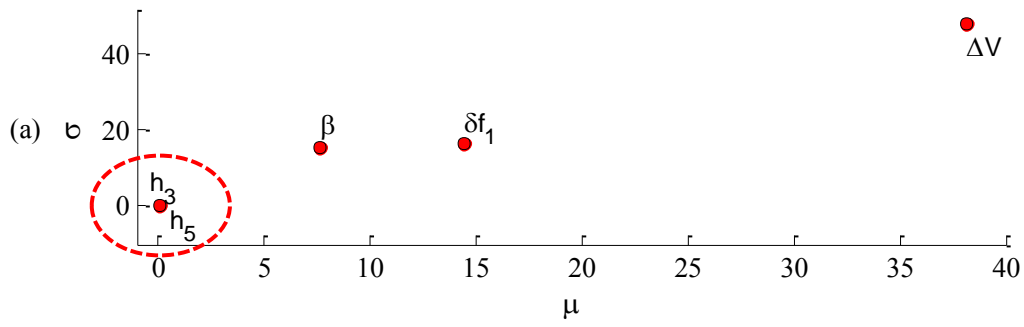
Figure 6.3 Sensitivity results of the output of the Cosine filter when its input is fault voltage signals (a) undershoot (b) steady state error (c) settling time
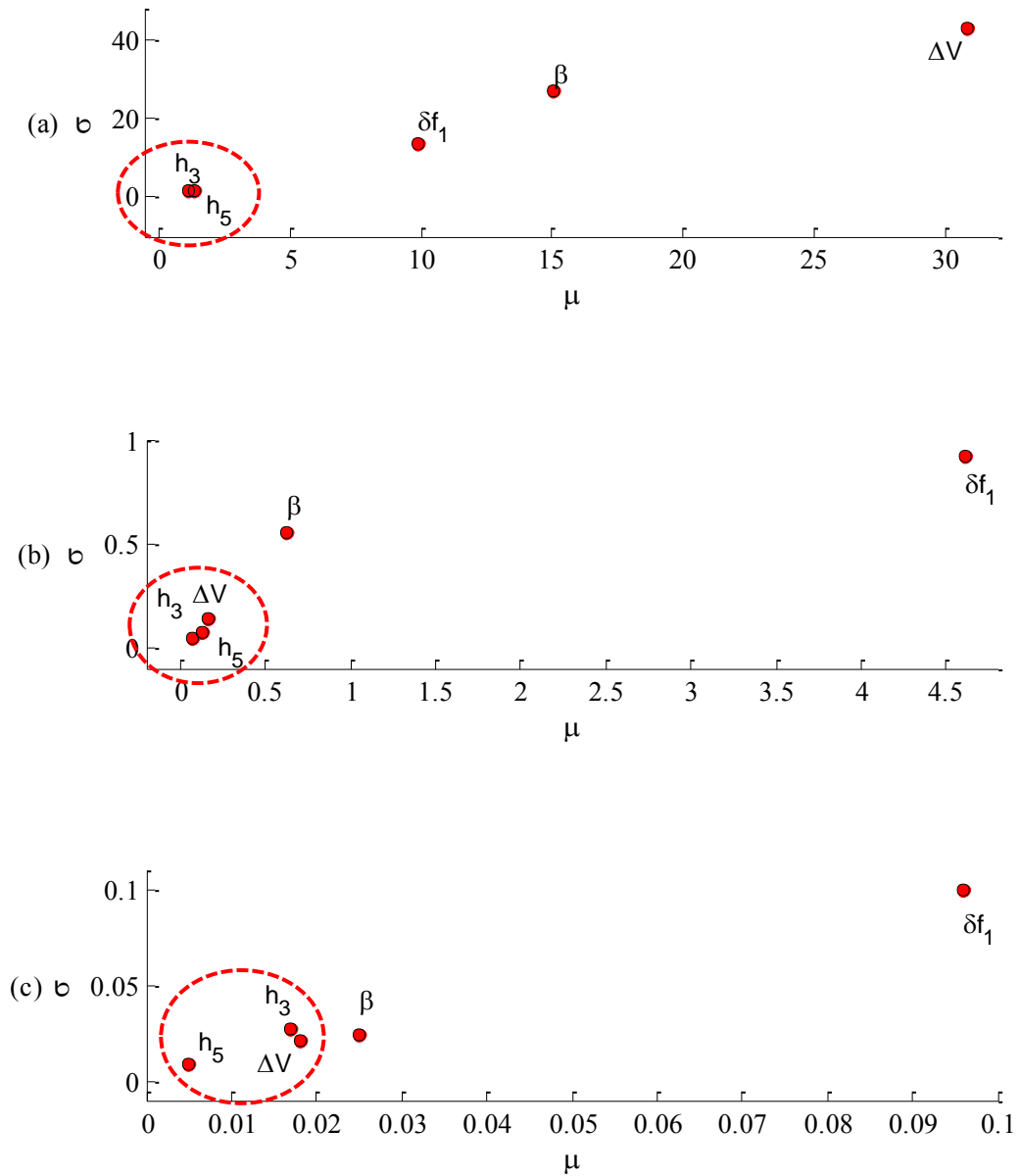
Figure 6.4 Sensitivity results of the output of the unknown measurement algorithms when its input is fault voltage signals (a) undershoot (b) steady state error (c) settling time

As previously described, the red dash-dot circles are used to indicate the clusters of unimportant factors. The results show that the unimportant factors that are common for all the calculated performance indices: the undershoot, steady state error and settling time are the amplitude of the third and fifth harmonics components (h_3, h_5). These two factors are

the common unimportant factors for the output of both the Cosine filter and unknown measurement algorithms.

Beside, the steady state error and settling time of the Cosine filter is also sensitive to the voltage amplitude change (ΔV) and fault inception angle (β), respectively. For the unknown measurement algorithms, the steady state error and settling time are both also sensitive the voltage amplitude change (ΔV).

Similarly, analyzing the common unimportant factors to all the calculated transient response performance indices, the amplitude of the third and fifth harmonic components are the unimportant nuisance factors to the input of the measurement algorithms when their input is fault voltage signals. Thus, these two factors (i.e. h_3, h_5), which are the similar results for unimportant factors on the fault current signals, will be eliminated in the next EFAST method.

It is worth to note that the results from the Morris method that identifies the third and the fifth harmonics components (h_3, h_5), which are the less influential factors on the output of the Cosine filter, agrees well with the published literature. This is because it is well known that the Cosine filter is an effective measurement algorithm to attenuate multiple harmonic components. However, the result presented here provides an alternative and a more insightful investigation of the Cosine filter.

6.2.2. The EFAST Method

The amplitude of the third and fifth harmonic components (h_3, h_5), identified by the Morris method, are the unimportant factors for both types of input test signals: fault current and fault voltage. These factors will be eliminated in the second-stage (i.e. EFAST method) since they show a small influence on the output of measurement algorithms. Therefore, in the EFAST method, the number of the studied factors is reduced to four factors in the fault current ($\alpha, \tau, \lambda, \delta f_1$); and three factors in the fault voltage ($\theta, \delta f_1, \Delta V$).

Next, the EFAST method is performed on the output of the Cosine filter in the simulation and the unknown measurement algorithms in the practical testing using the new

set of the nuisance factors. The EFAST method is performed for two purposes. The first is to estimate the uncertainty on the output of the measurement algorithms due to the uncertainty of the new set of nuisance factors using the EFAST uncertainty analysis. The second is to identify the most influential factor on the output uncertainty of the measurement algorithms using the EFAST global sensitivity analysis. As mentioned in Chapter 3, the EFAST method produces quantitative results in a way that the sensitivity indices can be used for comparing among them. Thus, the results of the EFAST method are presented in a numerical way.

6.2.2.1. Results of Uncertainty Analysis

Four statistical performance indices: minimum, maximum, mean and standard deviation values are used to measure the uncertainty on the output of the Cosine filter. These indices are calculated on each performance criterion, namely the overshoot, steady state error and settling time on the output transient response of the measurement algorithms: the Cosine filter in simulation, and the unknown measurement algorithms in practical testing. Table 6.1 and 6.2 show the calculated uncertainty indices on the output of the Cosine filter and unknown measurement algorithms, respectively; using the EFAST method.

Table 6.1 Result of the uncertainty analysis on the output of the Cosine filter using the EFAST method. (Fault current signals)

Statistic Index	Transient response performance index		
	O_S (%)	S_{se} (%)	T_S (s)
Minimum	0.04	-44.20	0.00
Maximum	79.49	3.17	0.30
Mean	4.04	-1.61	0.12
Standard Deviation	4.59	4.75	0.11

Table 6.2 Result of the uncertainty analysis on the output of unknown measurement algorithms using the EFAST method. (Fault current signals)

Statistic Index	Transient response performance index		
	O_S (%)	S_{se} (%)	T_S (s)
Minimum	0.01	-49.81	0.00
Maximum	89.68	1.72	0.27
Mean	4.21	-3.38	0.10
Standard Deviation	5.21	5.01	0.11

The level of performance of measurement algorithms, such as 'very good, 'good', 'average', can be based on the desired requirements of the protection functions as well as the requirements from the protection engineer. The level of this performance can be of several levels, with each level possibly being of a different range.

For the purpose of discussion, assume that there are only two performance levels: 'good' and 'poor'. Furthermore, assume that the 'good' performance of measurement algorithms is characterized by the following performance index:

- the mean value of the overdershoot is less than 5%,
- the mean value of the steady state error is less than 5%, and
- the mean value of the settling time is less than 0.2 seconds.

The results indicate that the Cosine filter is a 'good' measurement algorithm. The unknown measurement algorithms implemented in the IED are also a 'good' measurement algorithm. The mean values on the calculated performance indices in both the simulation and practical testing fall within the limits of the assumed 'good' characteristic.

It is interesting to note that a close similarity between the results in simulation and practical testing is obtained for the calculated statistical indices. The negative value on the steady state error indicates that the estimated amplitude of the fundamental frequency

component is less than the true value. Moreover, the obtained pattern of the output uncertainty distribution in the simulation is almost similar to that of the practical testing. Figure 6.5 and 6.6 illustrate the overshoot distribution of the Cosine filter and unknown measurement algorithms during the analysis of uncertainty in the SIMLAB.

Figure 6.5 Distribution of overshoot in the output of the Cosine filter
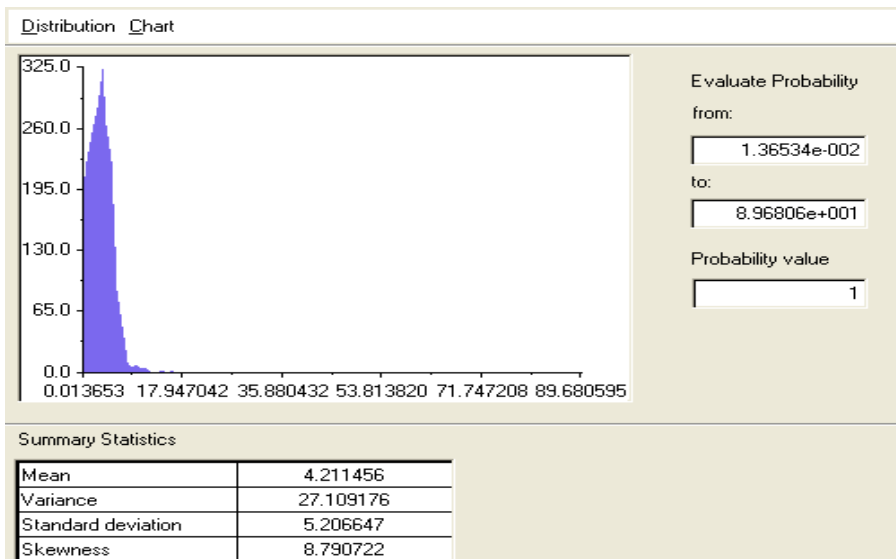
Figure 6.6 Distribution of overshoot in the output of the unknown measurement algorithms

Next, Table 6.3 and 6.4 show the results of uncertainty analysis using the EFAST method, calculated on the output of the Cosine filter and unknown measurement algorithms respectively, when their input is the fault voltage signals.

Table 6.3 Result of the uncertainty analysis on the output of the Cosine filter using the EFAST method. (Fault voltage signals)

Statistic Index	Transient response performance index		
	U_S (%)	S_{se} (%)	T_S (s)
Minimum	0.13	-10.00	0.00
Maximum	90.87	0.20	0.20
Mean	10.63	-3.28	0.10
Standard Deviation	13.73	1.43	0.05

Table 6.4 Result of the uncertainty analysis on the output of unknown measurement algorithms using the EFAST method. (Fault voltage signals)

Statistic Index	Transient response performance index		
	U_S (%)	S_{se} (%)	T_S (s)
Minimum	0.09	-11.31	0.00
Maximum	94.81	-0.86	0. 13
Mean	10.52	-4.89	0.04
Standard Deviation	13.63	1.48	0.04

A 'good' performance of measurement algorithms is assumed when their input voltage signals have the following performance index:

- the mean value of the undershoot is less than 5%,
- the mean value of the steady state error is less than 5%, and
- the mean value of the settling time is less than 0.2 seconds.

The results indicate that both the Cosine filter and unknown measurement algorithms are 'good' measurement algorithms for the steady state error and settling time performance indices only.

Note that the Cosine filter and unknown measurement algorithms produce a faster performance in the settling time index when their input signals are voltage signals in comparison with input current signals. The settling time is faster because the decaying DC offset factor in the fault voltage signals is omitted. This decaying DC offset, particularly its time constant, has a significant impact on the duration of the transient of the fault signals, and thus, the settling time of the measurement algorithms. However, as previously described, the decaying DC offset in the fault voltage signals is omitted, since the presence of this nuisance signal is less pronounced.

For the undershoot, the performance of both the Cosine filter and the unknown measurement algorithms is poor. These measurement algorithms show that their mean value of the undershoot is higher than the assumed 'good' performance. However, this poor performance may be improved by knowing the contribution of the nuisance factors to this undershoot and then reducing the uncertainties of those nuisance factors. The factor that contributes the most to the uncertainty of the undershoot is first factor that needs to be explored (i.e. the priority factor). As described in Chapter 3, the fractional contributions, including the highest contributing factor, can be measured using the sensitivity analysis. Thus, the next section will present the results of the applied EFAST method for identifying the most influential factors on the output of measurement algorithms.

Similar to the previous case, a close distribution pattern on the uncertainty of the calculated performance indices is obtained. Figure 6.7 and 6.8 illustrate an example of the obtained undershoot distribution pattern during the analysis of uncertainty using the EFAST method in the SIMLAB program for the Cosine filter (simulation) and unknown measurement algorithms (practical testing) respectively.
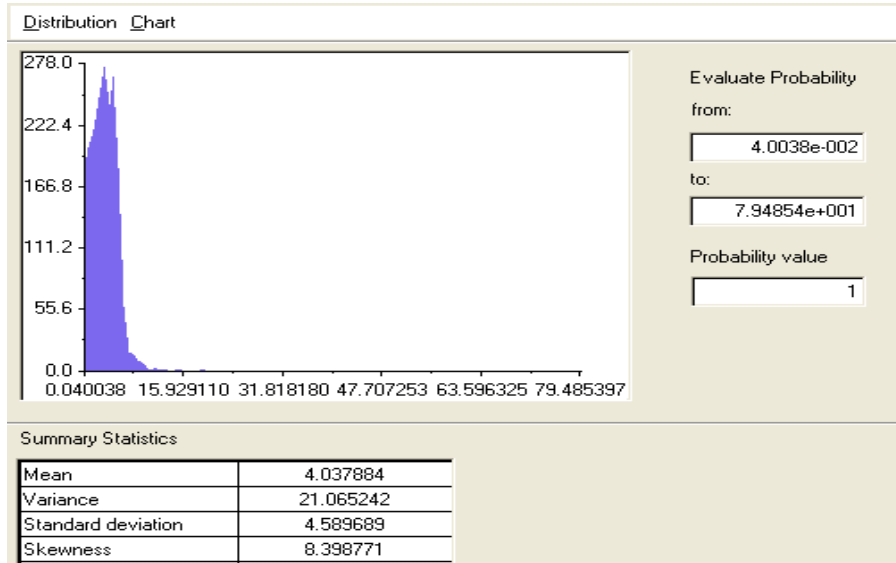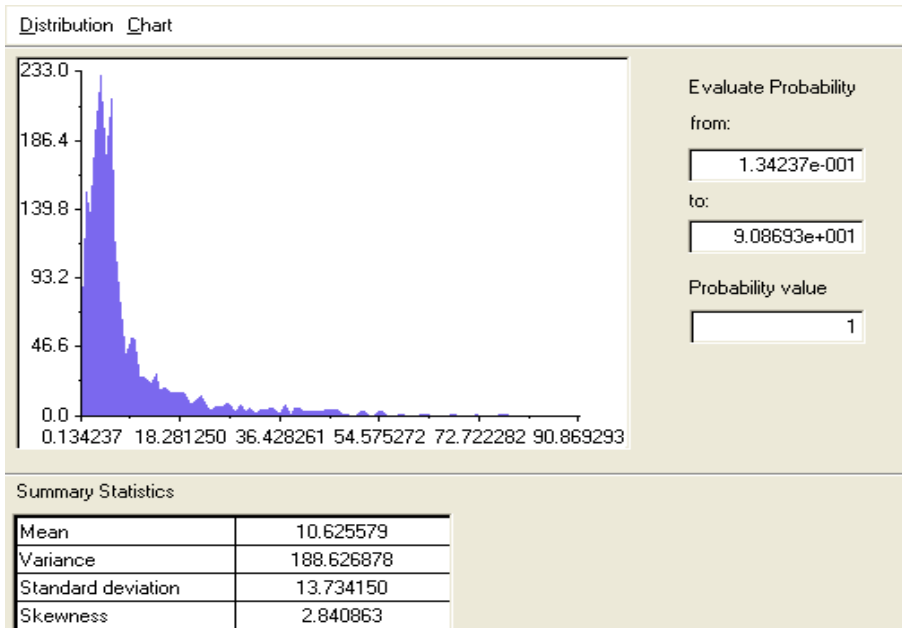
Figure 6.7 Distribution of undershoot in the output of the Cosine filter
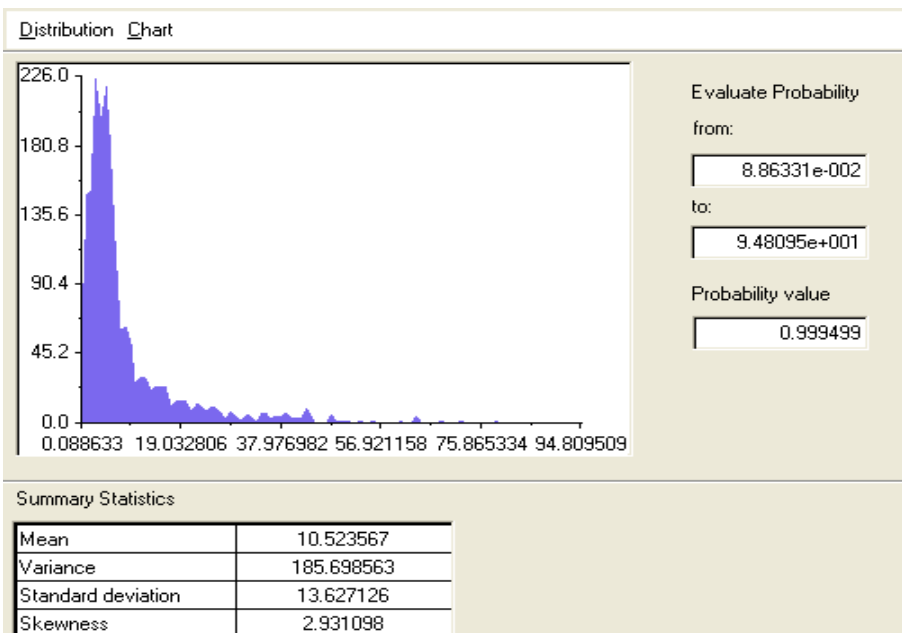
Figure 6.8 Distribution of undershoot in the output of the unknown measurement algorithms

The presented performance of the Cosine filter and the unknown measurement algorithms is assumed to show a 'good' performance if the calculated performance indices meet a certain level of the requirements. In general, if many measurement algorithms are required to be evaluated, the uncertainty results can be used to compare their performance, either in the simulation or in the practical testing so as to choose the 'good' measurement algorithms for the implementation in IEDs for specific protection applications.

6.2.2.2. Results of Sensitivity Analysis

A. Fault Current Test Signals

The EFAST method measures the first- and the total-order effects. The first-order effect indicates the contribution of a single factor to the total output uncertainty of the measurement algorithms. The total-order effect indicates the total contribution of a single factor, that includes its interaction with the other factors, to the total output uncertainty. Table 6.5 shows the numerical results of the EFAST sensitivity analysis method on the output transient response of the Cosine filter when its input is the fault current test signals.

The bold values in the first- and total-order effects for each calculated performance index are highlighted to indicate the highest values. This value, therefore, represents the corresponding input factor that shows the most influencial on the calculated performance indices. For example, the overshoot of the Cosine filter for the calculated first-order effect is most sensitive to the time constant of the decaying DC offset factor (τ), where the index value is 0.1630.

The result indicates that both the overshoot (O_S) and steady state error (S_{se}) of the Cosine filter are the most sensitive, indicated by the first-order effect, to the time constant of the decaying DC offset (τ). The settling time (T_S), however, is most sensitive to the off-nominal fundamental frequency (δf_1). These factors are also the most influential factors in the same performance indices calculated for the total-order effects.

Table 6.5 Results of the sensitivity analysis on the output of the Cosine filter using the
EFAST method. (Fault current signals)

Factor	First-order effect		
	O_S (%)	S_{se} (%)	T_S (s)
α	0.0121	0.0177	0.0306
τ	**0.1630**	**0.3083**	0.1653
λ	0.0335	0.0014	0.0034
δf_1	0.0924	0.2523	**0.6309**
	Total-order effect		
α	0.1977	0.2509	0.1748
τ	**0.7962**	**0.7818**	0.3431
λ	0.6213	0.2829	0.1317
δf_1	0.4777	0.5229	**0.7679**

The second most influential factor on both the overshoot and steady state error of the Cosine filter is the off-nominal fundamental frequency (δf_1). The second most influential factor on the settling time of the Cosine filter is the time constant of the decaying DC offset (τ).

Thus, it can be concluded that the two most influential factors on the calculated transient response performance indices of the Cosine filter, without rank, are the time constant of the decaying DC offset (τ) and the off-nominal fundamental frequency (δf_1). The other nuisance factors can be considered to be less influential on the calculated performance indices.

Table 6.6 shows the result of a similar sensitivity analysis except that it is obtained for the unknown measurement algorithms (i.e. practical testing). Although the numerical

values in the practical evaluation are slightly different than that in the simulation, the most influential factors identified, indicated by the corresponding bold values, are identical as in the simulation for all the calculated performance indices.

Table 6.6 Results of the sensitivity analysis on the output of the unknown measurement algorithms using the EFAST method. (Fault current signals)

Factor	First-order effect		
	O_S (%)	S_{se} (%)	T_S (s)
α	0.0066	0.0182	0.0271
τ	**0.1509**	**0.3336**	0.1729
λ	0.0452	0.0012	0.0069
δf_1	0.0664	0.2324	**0.5579**
	Total-order effect		
α	0.3114	0.2736	0.1698
τ	**0.8203**	**0.8049**	0.3622
λ	0.6559	0.2775	0.1438
δf_1	0.4422	0.4933	**0.7280**

Indeed, the ranking from the most to least influential factors is in the correct order. It should be noted, however, that the aim of the applied sensitivity analysis in this thesis is to identify the most influential factor rather than ranking factors. However, this additional information that the results of the sensitivity analysis applied on the Cosine filter in the simulation and the unknown measurement algorithms in practical testing have a good agreement.

B. Fault Voltage Test Scenarios

This section presents the results of sensitivity analysis using the applied EFAST method on the output of the Cosine filter in simulation and unknown measurement algorithms in practical testing when the input is the fault voltage signals.

Table 6.7 shows the sensitivity result of the output of the Cosine filter. As previously mentioned, the bold values in first- and total-order effects are used to highlight the highest calculated values on the performance indices. The result indicates that the undershoot (U_S) of the Cosine filter is the most sensitive, indicated by the first-order effect, to the amplitude of voltage collapse (ΔV) factor. The steady state error (S_{se}) and the settling time (T_S) of the Cosine filter are both most sensitive to the off-nominal fundamental frequency (δf_1).

Table 6.7 Results of the sensitivity analysis on the output of the Cosine filter using the EFAST method. (Fault voltage signals)

Factor	First-order effect		
	U_S (%)	S_{se} (%)	T_S (s)
θ	0.0092	0.0004	0.0030
δf_1	0.0231	**0.8910**	**0.7054**
ΔV	**0.7241**	0.0000	0.0829
	Total-order effect		
θ	0.2140	0.0433	0.0722
δf_1	0.2379	**0.9838**	**0.9080**
ΔV	**0.9415**	0.0494	0.2877

Moreover, these two factors ($\Delta V, \delta f_1$) also show a significant difference to their second most sensitive factors. In the steady state error, for example, the most sensitive

index value is 0.8910, whereas the second most is 0.0004. The great difference between the highest and the second highest index value means that the identified most important factor not only serves as the most influential but also as the dominant factor. Other nuisance factors can be considered as non-influential factors since they show small influential effects in all the calculated performance indices.

For the total-order effects, a similar result to the first-order effect is achieved. The result shows that the undershoot (U_S) of the Cosine filter is the most sensitive to the amplitude of voltage collapse (ΔV), and the steady state error (S_{se}) and settling time (T_S) are both the most sensitive to the off-nominal fundamental frequency (δf_1).

Next, Table 6.8 shows the result of the similar sensitivity analysis except that it is obtained for the unknown measurement algorithms (i.e. practical testing).

Table 6.8 Result of the sensitivity analysis on the output of the unknown measurement algorithms using the EFAST method. (Fault voltage signals)

Factor	First-order effect		
	U_S (%)	S_{se} (%)	T_S (s)
θ	0.0098	0.0001	0.0015
δf_1	0.0329	**0.8563**	**0.7503**
ΔV	**0.7036**	0.0026	0.0608
	Total-order effect		
θ	0.2357	0.0446	0.0649
δf_1	0.2571	**0.9696**	**0.9309**
ΔV	**0.9379**	0.0591	0.2519

The result indicates that the undershoot (U_S) of the unknown measurement algorithms is the most sensitive, indicated by the first-order effect, to the amplitude of the voltage collapse (ΔV) factor. The steady state error (S_{se}) and the settling time (T_S) of the unknown measurement algorithms are both most sensitive to the off-nominal fundamental frequency (δf_1).

For the total-order effects, a similar result to the first-order effect is achieved. The result indicate that the undershoot (U_S) of the unknown measurement algorithms is the most sensitive to the amplitude of voltage collapse (ΔV), whereas the steady state error (S_{se}) and settling time (T_S) are both the most sensitive to the off-nominal fundamental frequency (δf_1).

It is interesting to note that the factors which are influential on the output of the Cosine filter and the unknown measurement algorithms have the same order of rank for the total-order effect in all the calculated transient response performance indices. However, for the first-order indices, the order of rank is the same for the undershoot and settling time. For the steady state error only the most sensitive factor is identical. Although the second and third factors are in different ranks, this difference can be explained by the numerical error. The difference of index values between these factors is also relatively very small, being close to zero.

6.3. Steady State Response Evaluation Results

The performance of the Cosine filter in the steady state is evaluated. Additionally, the performances of the full- and half-cycle DFT are also evaluated. However, the performance of the unknown measurement algorithms (i.e. practical testing) is not evaluated for the reasons that have been described in Section 4.5.1.

Figure 6.9 shows the plots of the magnitude response of these measurement algorithms. The plot shows their response to the steady state input sinusoidal for frequency ranges of (0-300) Hz. Each subplot shows responses of their real and imaginary parts. As mentioned in Chapter 2, the imaginary part of the Cosine filter uses the same data of its

real coefficients. Thus, the produced frequency response plot for the imaginary part of the Cosine filter is the same as its real part.
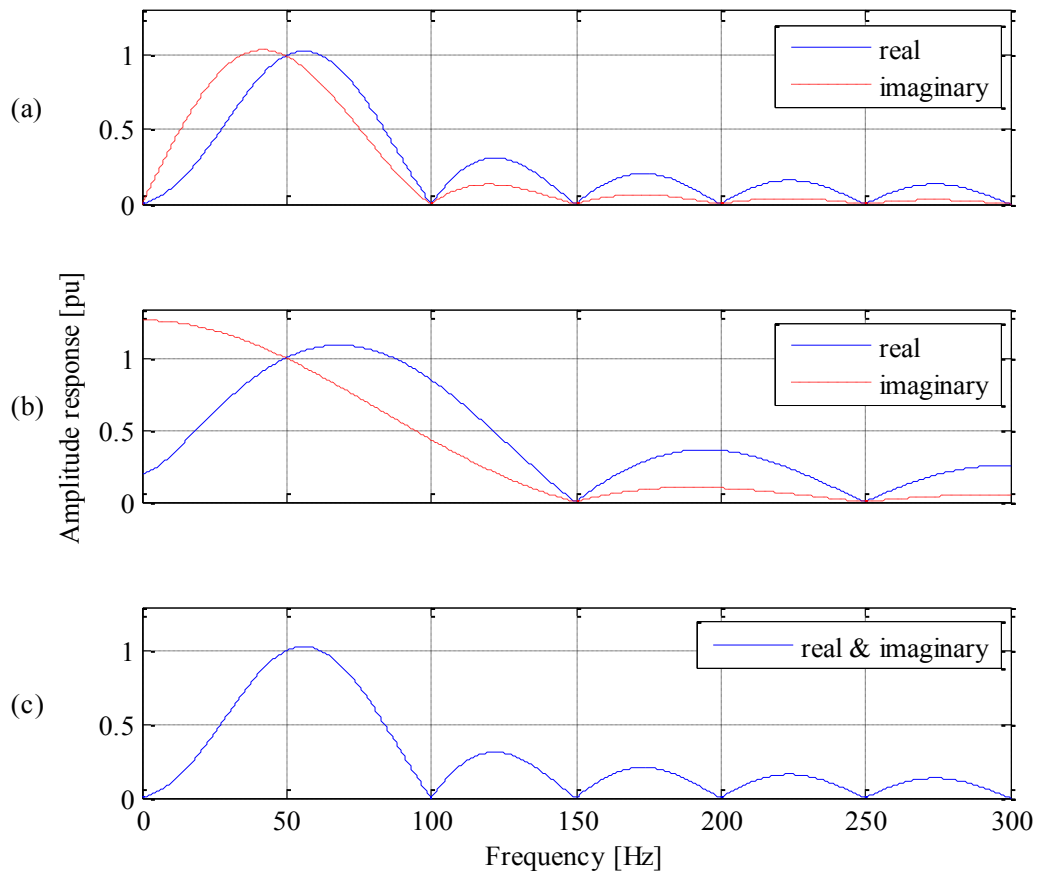
Figure 6.9 Magnitude responses of measurement algorithms from $(0 - 300)$Hz (a) full-cycle DFT (b) half-cycle DFT (c) Cosine filter

Figure 6.9 shows that all the evaluated algorithms have a good frequency response at the fundamental frequency component (50Hz) since the produced amplitude response is 1 p.u. Moreover, all these algorithms also show a good attenuation on the third and fifth harmonic frequencies (150Hz and 250Hz). These two harmonic frequencies are completely attenuated by those evaluated measurement algorithms in the steady state.

The full-cycle DFT and Cosine filter, however, show more advantages over the half-cycle DFT by further attenuating the even harmonic components (100Hz and 200Hz) and the DC offset component. Furthermore, the advantage of the Cosine filter over the full-cycle DFT is exhibited if the input signal contains frequencies that are less than the fundamental frequency. The attenuation of those frequencies by the Cosine filter is more effective since the imaginary amplitude response characteristic of the Cosine filter is superior to the imaginary amplitude response of the full-cycle DFT, while both measurement algorithms have identical real amplitude response characteristics.

The calculation of the proposed steady state performance indices described in Section 4.5.1 requires the overall magnitude response. The overall magnitude response is calculated by averaging the real and imaginary response characteristics in each measurement algorithm.

Both the full- and half-cycle DFT have different frequency response characteristics for their real and imaginary responses. However, the Cosine filter has the identical frequency response between its real and imaginary since it has the similar coefficients. Figure 6.10 shows the overall magnitude responses of these measurement algorithms.
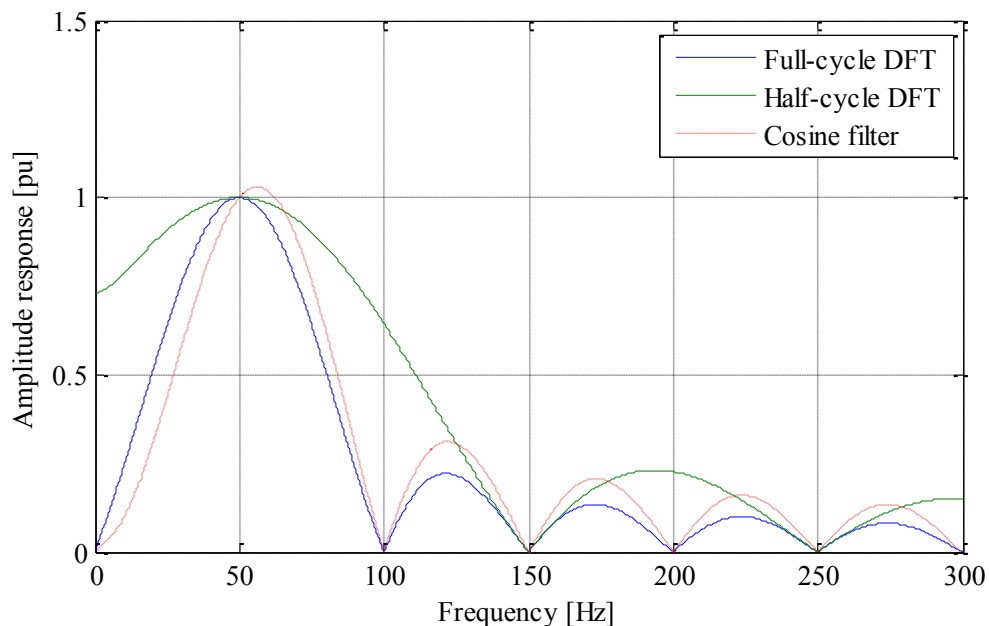
Figure 6.10 Overall magnitude responses of the full-cycle DFT, half-cycle DFT and Cosine filter algorithms

Next, Table 6.9 summarizes the steady state performance indices that are calculated from the overall magnitude responses. The results indicate that all measurement algorithms have good attenuation on the amplitude of third and fifth harmonics, as shown by the zero values in the calculated PI_{H3} and PI_{H5} indices respectively.

Table 6.9 Numerical results of the measurement algorithms performance in the steady state

Measurement Algorithm	PI_{FA}	PI_{DC}	PI_{H3}	PI_{H5}
Full-cycle DFT	0.00091	0.00000	0.00000	0.00000
Half-cycle DFT	0.00022	0.73138	0.00000	0.00000
Cosine filter	0.00989	0.00000	0.00000	0.00000

However, the measurement algorithms show different performances for DC offset (PI_{DC}) attenuation. While the full-cycle DFT and Cosine filter show good DC offset attenuation, the half-cycle DFT is unable to attenuate completely the DC offset component. The half-cycle DFT attenuates the magnitude of the DC offset to about 73% of the input signals.

For calculating PI_{FA} index, the half-cycle DFT shows the best performance, as indicated by its smallest PI_{FA} index value, due to a more flat overall amplitude response around the frequency of 50Hz than the other two measurement algorithms. Note that this index is calculated based on the fundamental frequency variation within (48 – 52) Hz as described in Section 4.5.1. The full-cycle DFT is ranked as the second best measurement algorithm's performance, followed by the Cosine filter.

6.4. Conclusion

The results of the performance evaluation of the measurement algorithms in the transient response and the steady state have been presented in this chapter. In the transient response,

the results of performance evaluations using two platforms: simulation and practical testing are discussed. In simulation, the performance results of the Cosine filter; and in practical testing, the performance results of the unknown measurement algorithms implemented in the IED are presented.

Two methods of the sensitivity analysis: the Morris and EFAST method are successful applied on the output transient responses of those measurement algorithms receiving two types of input fault test signals. The first is fault test currents and the second is fault test voltages. These input fault test signals are influenced by uncertainty of nuisance signals initiated during fault conditions.

The analysis results with uncertainty and sensitivity indices are tabulated graphically for the Morris method; and numerically for the EFAST method. The results from the Morris method indicate that the output of the Cosine filter and unknown measurement algorithms are both insensitive to the amplitude of the third and fifth harmonic components regardless of the types of input fault test signals: currents or voltages.

The uncertainty results from the EFAST method indicate that both the Cosine filter and the unknown measurement algorithms have good performance characteristics when their input is the fault current signals. However, when their input is the fault voltage signals, both measurement algorithms only show good performance in the steady state error and settling time. These measurement algorithms show poor performance for the undershoot.

Next, the sensitivity results from the EFAST method indicate that the overshoot and steady state error on the output of the Cosine filter are both most sensitive to the time constant of the decaying DC offset when its input is the fault current test signals. The settling time of the Cosine filter, however, is most sensitive to the fundamental frequency variation.

If the input to the Cosine filter is the fault voltage test signals, its undershoot is the most sensitive to the amplitude of voltage collapse. The steady state error and settling time on the output of the Cosine filter are both most sensitive to the fundamental frequency variation.

In the steady state performance evaluation, the full-, half-cycle DFT and Cosine filter show good performance in the attenuation of the third and fifth harmonic components. For the attenuation of the amplitude of the DC offset, only the full-cycle DFT and Cosine filter show the good performance. For estimating the fundamental frequency component considering its small variation, however, the half-cycle DFT has shown the best performance.

Chapter 7. Conclusions

7.1. Summary

Measurement algorithms are the essential element of modern IEDs. Their function is to estimate the fundamental frequency component of the input current and voltage signals. The accuracy and speed of the estimation of the fundamental frequency component are important for the IEDs to successfully perform their protection functions.

Various versions of the DFT are the most widely used measurement algorithms. These algorithms show high performance in normal conditions. However, in fault conditions, their performance is degraded by the presence of a variety of nuisance signals. The nuisance signals are generated as a consequence of various uncertain factors. These nuisance signals mix with the fundamental frequency component to produce input signals with distortion.

Many methods have been proposed to measure the performance of measurement algorithms during fault conditions in a network. However, they are based on the local sensitivity analysis. In this method, the test scenarios are provided by varying only a single factor, commonly around its nominal value, while other factors are fixed at their

corresponding nominal values. These fault test scenarios are applied to the input of measurement algorithms and then the corresponding errors are calculated on their output. The produced fault test scenarios using this method, however, do not cover all realistic scenarios. Furthermore, the produced results also do not provide the overall (global) performance of the measurement algorithms.

A factor value is unpredictable but it is within a known range. Thus, measurement algorithms of IEDs should be evaluated for their performance over the complete known ranges of all factors. This thesis, therefore, proposes a new methodology to evaluate the performance of measurement algorithms implemented in the IEDs during the transient response. The methodology uses a systematic global uncertainty and sensitivity analysis to evaluate the performance of measurement algorithms. The measurement algorithm performance is calculated by analyzing in a global way the uncertainty output of measurement algorithms due to the uncertainty of factors involved. Beside, this method can also calculate the contribution of these factors to the output uncertainties.

The proposed methodology has been demonstrated on the Cosine filter algorithm in the simulation and the unknown measurement algorithm of a commercial IED in practical testing. This demonstration uses fault test scenarios: currents and voltages signals that are distorted by a variety of nuisance signals. The distortion (nuisance) signals are parameterized by selected factors.

In a steady state, the performance criteria are proposed to measure the performance of the measurement algorithm. They measure the capability of measurement algorithms to estimate the fundamental frequency component considering the practical off-nominal fundamental frequency; and also to attenuate the amplitude of the DC, third and fifth harmonic components. The steady state performance indices have been calculated numerically.

This thesis has drawn the following conclusions:

1. A new methodology that systematically evaluates the performance of measurement algorithms is proposed. It is based on the global uncertainty and sensitivity analysis. The proposed methodology provides two important results. The first is the result of the

uncertainty analysis that measures the uncertainty output of measurement algorithms (i.e. performance) due to its input uncertainty of nuisance factors. The second is the result of the sensitivity analysis that measures the contribution of input factors to the uncertainty output of measurement algorithms.

2.   The proposed methodology that can be implemented in two platforms has been presented. The first platform is based on computer simulation. In this platform, the proposed methodology can evaluate the performance of any measurement algorithms providing their mathematical algorithms are known. The second platform is proposed for practical testing. In the second platform, although measurement algorithms may be unknown (i.e. black or grey box), their performance can still be evaluated providing the input and output nodes of the evaluated IEDs are accessable.

3.   A two-stage global sensitivity analysis has been implemented consisting of the Morris and EFAST methods. The use of the two-stage sensitivity analysis method makes possible the implementation of the proposed methodology in simulation as well as in practical testing. Thus, the proposed methodology, particularly in practical testing, can be used to evaluate the performance of measurement algorithms of several available commercial IEDs. Moreover, the proposed method can be extended to compare the performances of protection algorithms of the IEDs.

4.   The performances of the Cosine filter in the simulation, as well as the unknown measurement algorithm of a commercial IED in the practical testing have been successfully evaluated. In the simulation, a generic model of the IED that includes the Cosine filter is used. In the practical testing, a commercial IED has been evaluated, in which its measurement algorithm is unknown. The aim of the implementation in two different platforms, therefore, is to demonstrate their implementation rather than to compare their results. However, during the uncertainty analysis, the obtained results show a close similarity, between the simulation and practical testing. Interestingly, identical results are also obtained for the identifying factors that contribute the most to transient response performance indices.

7.2. Future Work

The Quasi-Monte Carlo (QMC) with the Sobol sampling sequence is the most comprehensive method for global uncertainty and sensitivity analysis. This method measures the first-order and all orders of interaction effects. However, this method, like the EFAST method, is a sample-based method. A sample-based method often requires an extensive number of evaluations. Indeed, the QMC with the Sobol sampling sequence method requires a more extensive number of evaluations than the EFAST method since it measures all orders of interactions. In case the results of the higher-order interaction effects are required, we suggest using a two-stage global sensitivity analysis that combines the Morris and the QMC with the Sobol sequence sampling method.

This thesis presents the methodology to evaluate the performance of measurement algorithms implemented in IEDs using a global uncertainty and sensitivity analysis. Indeed, the presented methodology can be extended to evaluate the performance of any protection algorithms as well as fault locator algorithms. It is recommended that proposed methodology be used to draw a comparison between the performances of several commercial IEDs.

Appendix A. Sampling Strategy of Morris

Suppose we have three parameters that are scaled between (0-1). If we select four level grids ($L_G = 4$), then each parameter may contain values of $(0, 1/3,\ 2/3\ , 1)$. The predetermined perturbation, Δ is 2/3, where $\Delta = L_G/[2(L_G - 1)]$. The matrix of samples (M), to be generated is:

$$M = \begin{bmatrix} m_{11} & m_{12} & m_{13} \\ m_{21} & m_{22} & m_{23} \\ m_{31} & m_{32} & m_{33} \\ m_{41} & m_{42} & m_{43} \end{bmatrix}. \tag{A1}$$

The initial seed, which is random, of the three parameters can be a vector:

$$[m_{11} \quad m_{12} \quad m_{13}] = [1 \quad 2/3 \quad 0]. \tag{A2}$$

To obtain a second row of matrix *M*, the Morris method changes one parameter randomly in (A2) while the other parameters are kept constant. The change parameter value can be an increase or decrease by the pre-determined perturbation in a way that a new vector is still within their scale. The subsequent rows are obtained using a similar process by changing the next random parameter. For illustration, the change of third, first and second parameters and their corresponding second, third and forth rows are illustrated next:

$$M = \begin{bmatrix} 1 & 2/3 & 0 \\ 1 & 2/3 & 2/3 \\ 1/3 & 2/3 & 2/3 \\ 1/3 & 0 & 2/3 \end{bmatrix}. \tag{A3}$$

Then, the Morris method quantifies the elementary effect using the matrix *M*. We further assume that the simulation of a model using matrix sample *M* produces the corresponding output (*Y*) as:

$$Y = \begin{bmatrix} y_1 \\ y_2 \\ y_3 \\ y_4 \end{bmatrix}. \tag{A4}$$

The elementary effect of the third parameter (E_3) is calculated by using the output simulation of y_1 and y_2 that related to the changing of the third parameter.

$$E_3 = (y_2 - y_1)/\Delta. \tag{A5}$$

Similarly, the first and the second elementary effects are follows:

$$E_1 = (y_2 - y_3)/\Delta, \tag{A6}$$

$$E_2 = (y_3 - y_4)/\Delta. \tag{A7}$$

Appendix B. Parameters of CT and CVT

The fault test scenarios: current and voltage for the performance evaluation of measurement algorithms, is simulated using the model of CT and CVT respectively connected to a model of transmission line network. The parameters used to model CT and CVT are illustrated in this Appendix. Figure B.1 shows the V-I characteristics of the CT, whereas Tables B.1 and B.2 show the parameters used in the CT and CVT models.
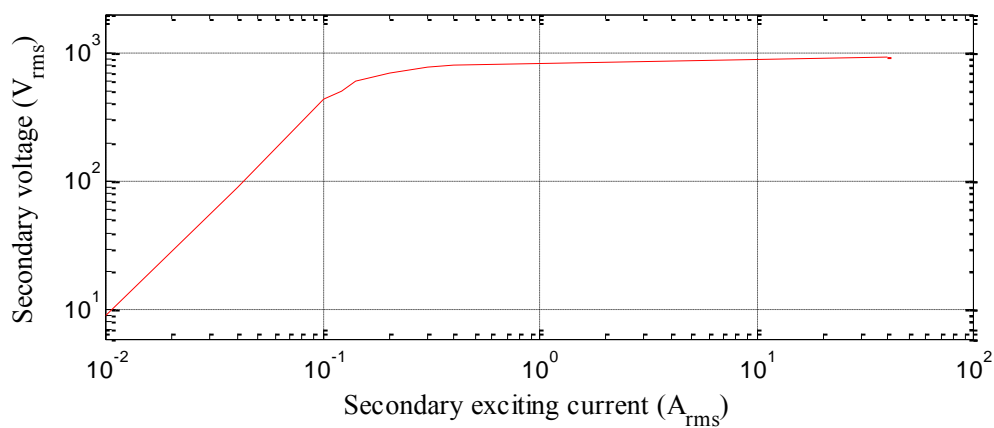
Figure B.1 The V-I characteristic of CT model

Table B.1 Parameters of CT model

Parameter	Value
R_P	0.576Ω
L_P	$0H$
R_S	0Ω
L_S	$1E-7mH$
$N1:N2$	$1:240$

Table B.2 Parameters of CVT model

Parameter	Value
R	$3.3k\Omega$
L	$76.1H$
C	$0.09uF$
R_f	$77.4k\Omega$
L_f	$315.3H$
C_f	$0.03uF$
Burden	$104k\Omega$

Appendix C. Model of IED

We model two main elements of IED using MATLAB program. The first is the anti-aliasing LPF and the second is the Cosine filter algorithm. The model of the LPF used is the second-order Butterworth LPF with cut-off frequency of 300Hz. The selected cut-off frequency allows the third and fifth harmonic components (150Hz and 250Hz) to be part of considered nuisance signals in this study. Their influence on output of measurement algorithm is investigated. The MATLAB script for this filter and its frequency response is as follows:

```
fs=4000;                            %Sampling frequency
fc=300;                             %Cut-off frequency
[Num,Den]=butter(2,2*fc/fs);

%% ANTI-ALIASING LPF
i2f=filter(Num,Den,i2);             %i2-input signal to LPF
                                    %i2f-output filtered signal
```
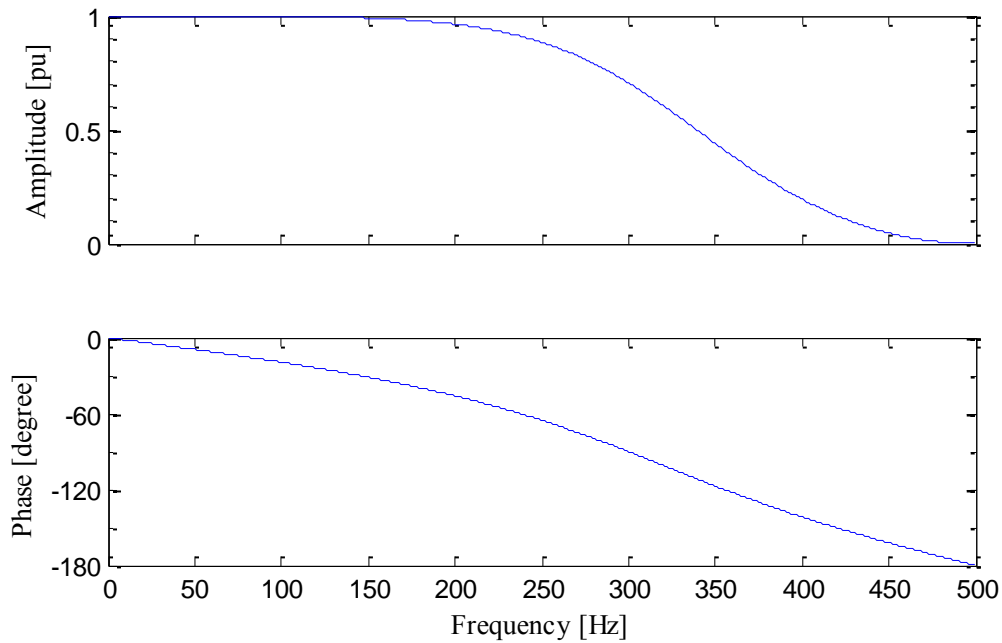
Figure C.1 Frequency response of 2nd order Butterworth LPF with cut-off frequency $(f_c = 300Hz)$

The output signals of the anti-aliasing LPF, which filter the high frequency components, are next applied to the input of Cosine filter algorithm. The MATLAB scripts of the Cosine filter are:

```
N=fs/f;                    %Number of sample/cycle
k=1:N;
c1=cos(2*pi*k/N);          %Cosine filter data window coefficients
x1=filter(c1,1,x);         %Real part of input signal(x)
h=[zeros(1,N/4) 1];        %Set quarter cycle delay
x2=filter(h,1,x1);         %Imaginary part of input signal(x)

Y=2/N*(x1+j*x2);           %Phasor of Cosine filter
```

Appendix D. Sample File

An example of a sample file (*.*sam*) created by SIMLAB is shown. The second and third row indicates the number of total executions, and the number of studied factors, respectively. The fifth and higher rows are the matrix of samples generated by SIMLAB. The matrix consists of five columns, where each column represents values of nuisance factor that are sampled based on method of sensitivity analysis used. Each row of matrix samples represents a set of scenarios. In this example, a number of 60 sets of scenarios, are generated.

```
0

60

5

0

16.875      48.5  6.256875   0.634375   68.065625

16.875      48.5  6.256875   0.634375   18.570625

61.875      48.5  6.256875   0.634375   18.570625
```

61.875	52.5	6.256875	0.634375	18.570625
61.875	52.5	6.256875	5.629375	18.570625
61.875	52.5	16.251875	5.629375	18.570625
84.375	51.5	6.256875	9.375625	80.439375
84.375	51.5	6.256875	9.375625	30.944375
39.375	51.5	6.256875	9.375625	30.944375
39.375	51.5	16.251875	9.375625	30.944375
39.375	47.5	16.251875	9.375625	30.944375
39.375	47.5	16.251875	4.380625	30.944375
73.125	53.5	18.750625	9.375625	92.813125
73.125	53.5	8.755625	9.375625	92.813125
73.125	53.5	8.755625	9.375625	43.318125
73.125	53.5	8.755625	4.380625	43.318125
28.125	53.5	8.755625	4.380625	43.318125
28.125	49.5	8.755625	4.380625	43.318125
28.125	52.5	13.753125	4.380625	80.439375
28.125	52.5	13.753125	9.375625	80.439375
28.125	52.5	13.753125	9.375625	30.944375
28.125	48.5	13.753125	9.375625	30.944375
73.125	48.5	13.753125	9.375625	30.944375
73.125	48.5	3.758125	9.375625	30.944375
39.375	50.5	8.755625	1.883125	18.570625
39.375	46.5	8.755625	1.883125	18.570625
39.375	46.5	8.755625	1.883125	68.065625
…	…	…	…	…
…	…	…	…	…
…	…	…	…	…
…	…	…	…	…
…	…	…	…	…
73.125	48.5	3.758125	5.629375	30.944375

Appendix E. ATP Template for Creating Fault Scenarios

The following script shows an example of the template created in the ATP/EMTP program for producing fault current test scenarios systematically. A variety of fault test scenarios can be simulated by changing factors and parameters that describe nuisance signals on the template of transmission line model. The changing requires a new factor value set from sample points generated by the SIMLAB program, which is described in Appendix D. In this example, the identified nuisance factors are labelled by the square box.

```
BEGIN NEW DATA CASE
C -------------------------------------------------------
C Generated by ATPDRAW  December, Thursday 23, 2010
C A Bonneville Power Administration program
C by H. K. Høidalen at SEfAS/NTNU - NORWAY 1994-2009
C -------------------------------------------------------
C  dT  >< Tmax >< Xopt >< Copt >
  .00025    .32
    500    1    1    1    1    0    0    1    0
C    1      2      3      4      5      6      7      8
C 345678901234567890123456789012345678901234567890123456789012345678901234567890
/BRANCH
```

```
C < n1 >< n2 ><ref1><ref2>< R >< L >< C >
C < n1 >< n2 ><ref1><ref2>< R >< A >< B ><Leng><><>0
 XX0001XX0009          15.3                    0
 XX0002XX0003         .3033 3.03                    0                R and L
 TRANSFORMER          TX0001  1.E5              0
     9999
 1NODE02XX0009         .576    240.
 2XX0005             1.E-7  1.
96NODE02IX0001        8888. 8888.                   0
      0.0        0.0
   0.014142    0.033762
   0.053673     0.33762
    0.1317     1.6056
    0.17505    1.8757
    0.18913    2.2508
    0.34131    2.6259
    0.56107     2.926
     0.976     3.0011
     94.4      3.4775
      9999
/SWITCH
C < n 1>< n 2>< Tclose ><Top/Tde ><  Ie  ><Vf/CLOP >< type  >
 XX0003NODE01                    MEASURING          1
 XX0005XX0002          1.E3                 Fundamental frequency
 XX0001NODE02
/SOURCE
C < n 1><>< Ampl. >< Freq. ><Phase/T0>< A1  >< T1  >< TSTART >< TSTOP >
14NODE01 0   1.5E4    50.    -20.              -1.   1.E3
11IX0001    1.2E4                     0.0   5.E-4          Inception angle
18XX0009    1.0
14NODE01 0   150.    150.   -20.          -1.   1.E3
14NODE01 0   250.    250.   -20.          -1.   1.E3
/OUTPUT
BLANK BRANCH                   Remanent flux
BLANK SWITCH
BLANK SOURCE                Amplitude of third harmonic
BLANK OUTPUT
BLANK PLOT                 Amplitude of fifth harmonic
BEGIN NEW DATA CASE
BLANK
```

Appendix F. Comparison of output transient response between AcSELerator and developed script

AcSELerator QuickSet program has the limitation that it is unable to automatically read the results file produced by SEL-421. Furthermore, the produced transient plot can be difficult to use for the calculation of the transient response performance indices since no script can be used in the program. Thus, we developed a script in MATLAB to automatically plot the transient response of the measurement algorithms that produced identical result as in the AcSELerator QuickSet. Moreover, we take advantages of the signal processing library function in the MATLAB program to easily calculate the performance indices. Figures F.1 and F.3 show examples of the output transient response of the unknown measurement algorithms to the input test current and voltage signal, respectively. The plots produced by our developed script using the MATLAB program are identical, and are shown by Figures F.2 and F.4, respectively. The mathematical script is based on the SEL-421 Application Handbook.

Figure F.1 The output transient response of the unknown measurement algorithm to current scenario plotted using AcSELerator QuickSet

Figure F.2 The output transient response of the unknown measurement algorithm to current scenario plotted using developed MATLAB script
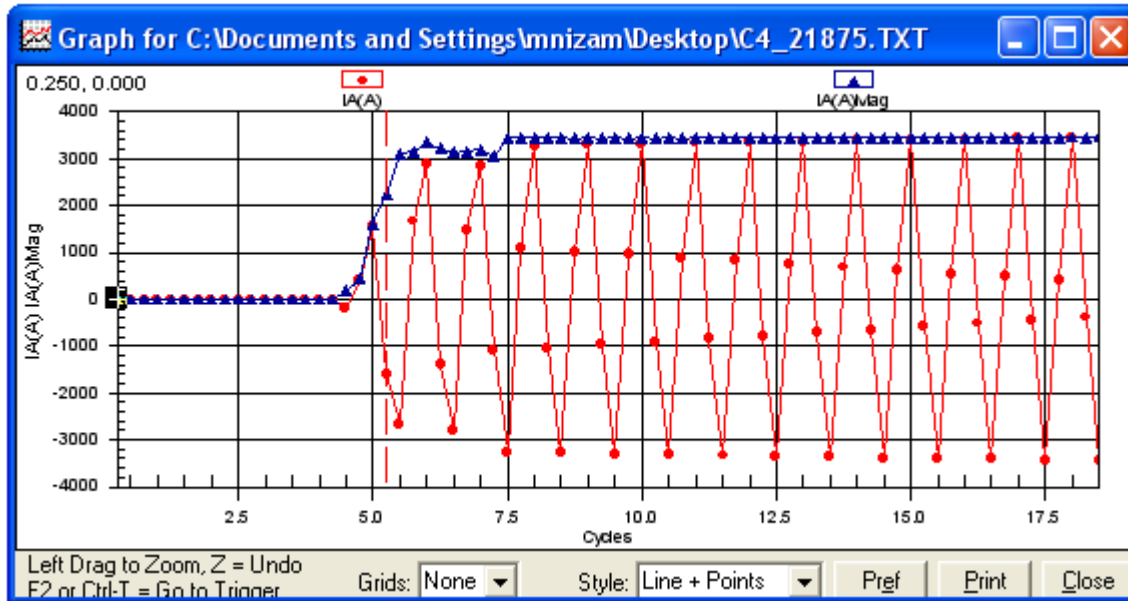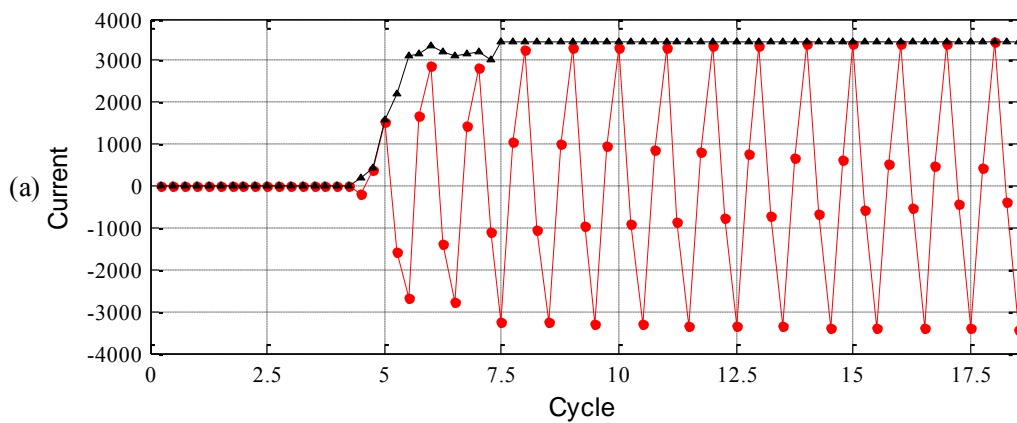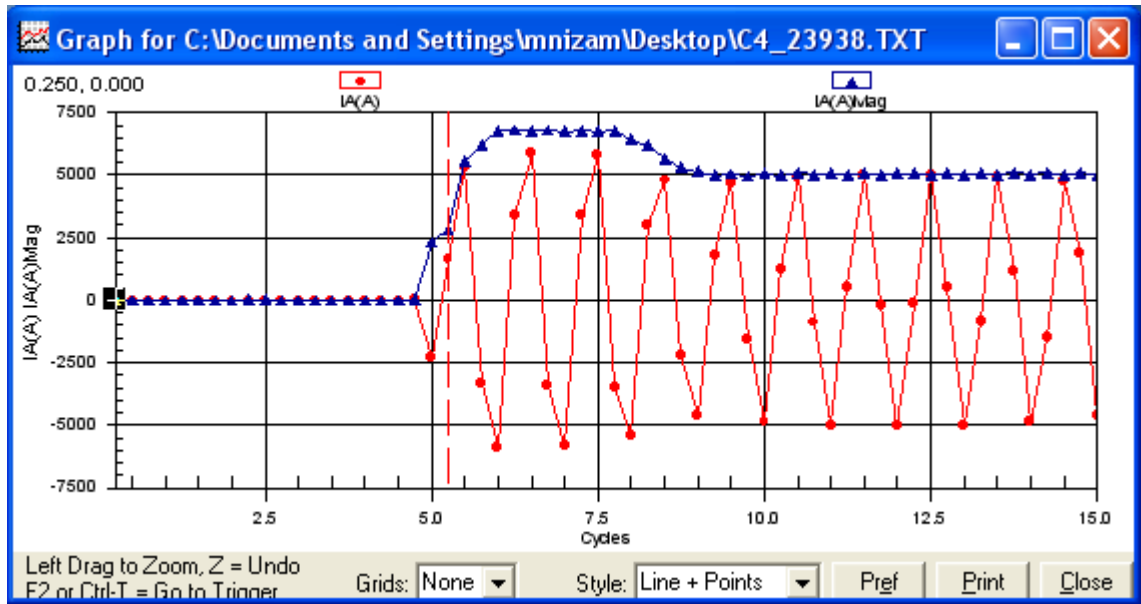
Figure F.3 The output transient response of the unknown measurement algorithm to voltage scenario plotted using AcSELerator QuickSet
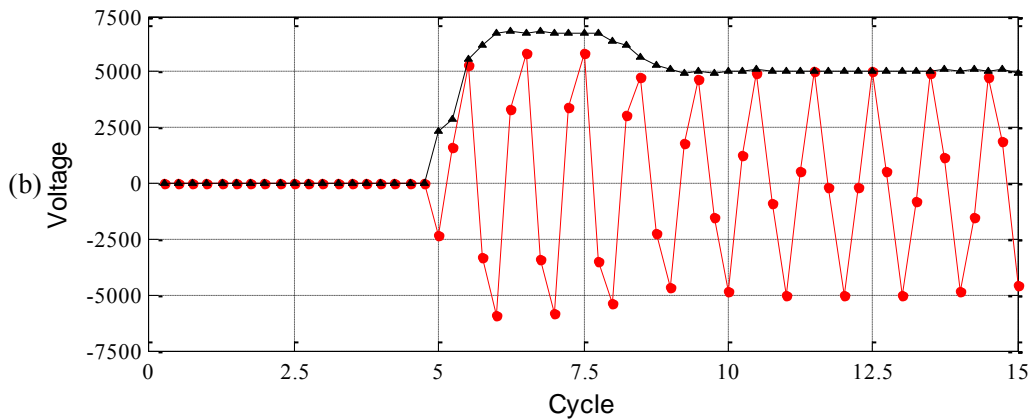
Figure F.4 The output transient response of the unknown measurement algorithm to voltage scenario plotted using developed MATLAB script

Appendix G. Coefficients of Measurement Algorithms

This Appendix shows the coefficients of three DFT measurement algorithms: the full-cycle DFT, half-cycle DFT and Cosine filter. These coefficients are calculated based on the number of samples per cycle ($N = 20$). For each measurement algorithm, two types of coefficients are calculated. The first is the real coefficient and the second is the imaginary coefficient.

Table G.1 Real coefficients (*k=1, 2 ...20*) of full-cycle DFT

k	$cos\left(\frac{2\pi k}{20}\right)$				
1 to 5	0.9511	0.8090	0.5878	0.3090	0.0000
6 to 10	-0.3090	-0.5878	-0.8090	-0.9511	-1.0000
11 to 15	-0.9511	-0.8090	-0.5878	-0.3090	0.0000
16 to 20	0.3090	0.5878	0.8090	0.9511	1.0000

Table G.2 Imaginary coefficients (*k=1, 2 …20*) of full-cycle DFT

k	$sin\left(\dfrac{2\pi k}{20}\right)$				
1 to 5	0.3090	0.5878	0.8090	0.9511	1.0000
6 to 10	0.9511	0.8090	0.5878	0.3090	0.0000
11 to 15	-0.3090	-0.5878	-0.8090	-0.9511	-1.0000
16 to 20	-0.9511	-0.8090	-0.5878	-0.3090	0.0000

Table G.3 Real coefficients (*k=1, 2 …10*) of half-cycle DFT

k	$cos\left(\dfrac{2\pi k}{20}\right)$				
1 to 5	0.9511	0.8090	0.5878	0.3090	0.0000
6 to 10	-0.3090	-0.5878	-0.8090	-0.9511	-1.0000

Table G.4 Imaginary coefficients (*k=1, 2 …10*) of half-cycle DFT

k	$sin\left(\dfrac{2\pi k}{20}\right)$				
1 to 5	0.3090	0.5878	0.8090	0.9511	1.0000
6 to 10	0.9511	0.8090	0.5878	0.3090	0.0000

Table G.5 Real and imaginary coefficients (*k=1, 2 …20*) of Cosine filter

k	$cos\left(\dfrac{2\pi k}{20}\right)$				
1 to 5	0.9511	0.8090	0.5878	0.3090	0.0000
6 to 10	-0.3090	-0.5878	-0.8090	-0.9511	-1.0000
11 to 15	-0.9511	-0.8090	-0.5878	-0.3090	0.0000
16 to 20	0.3090	0.5878	0.8090	0.9511	1.0000

Appendix H. MATLAB Scripts for Plotting Amplitude Response

This Appendix shows the MATLAB code to obtain frequency response of the full-cycle DFT, half-cycle DFT and Cosine filter algorithm.

```
clear all; clc;
N=20;                 %Number of samples/cycle

%FULL-CYCLE DFT and COSINE FILTER --------------------------------
k  = 1:N;
m=exp(-1i*2*pi*k/N);
r=real(m)*(2/N);
i=imag(m)*(2/N);
[h,w]=freqz(r,1,0:0.1:300,50*N);
[i,w]=freqz(i,1,0:0.1:300,50*N);
h1=abs(h);
i1=abs(i);

%HALF-CYCLE DFT --------------------------------------------------
k  = 1:N/2;
m=exp(-1i*2*pi*k/N);
r=real(m)*(4/N);
i=imag(m)*(4/N);
[h,w]=freqz(r,1,0:0.1:300,50*N);
[i,w]=freqz(i,1,0:0.1:300,50*N);
h2=abs(h);
```

```
i2=abs(i);

f1=figure(1);
subplot (311);plot(w,h1,w,i1,'--r'); grid on;
xlim([0 300]); ylim([0 1.3]);
set(gca,'xticklabel',[],'fontname','times'); legend('real','imaginary');
text(-45,1.3/2,'(a)','fontname','times');

subplot (312);plot(w,h2,w,i2,'--r'); grid on;
xlim([0 300]); ylim([0 1.34]);
ylabel('Amplitude response [pu]','fontname','times');
set(gca,'xticklabel',[],'fontname','times'); legend('real','imaginary');
text(-45,1.34/2,'(b)','fontname','times');

subplot (313);plot(w,h1); grid on; ylim([0 1.3]);
xlim([0 300]); xlabel('Frequency [Hz]','fontname','times');
set(gca,'fontname','times'); legend('real & imaginary');
text(-45,1.3/2,'(c)','fontname','times');
set(f1,'position',[50 50 560 170*3]);
```

Reference List

[1] E. Schweitzer III and D. Hou, "Filtering for protective relays," *IEEE on WESCANEX 93 Communications, Computers and Power in the Modern Environment,* pp. 15-23, 2002.

[2] C. M. Smith and N. K. C. Nair, "Evaluation of Discrete Wavelet Transform implementation for protective relaying," *IEEE Region 10 Conference on TENCON 2009,* pp. 1-5, 2009.

[3] H. Bentarzi, "Improving monitoring, control and protection of power grid using wide area synchro-phasor measurements," *Proceedings of the 12th WSEAS International Conference on AUTOMATIC CONTROL, MODELLING & SIMULATION,* pp. 93-98, 2010.

[4] H. Pascual and J. Rapallini, "Behaviour of Fourier, cosine and sine filtering algorithms for distance protection, under severe saturation of the current magnetic transformer," *Proceedings of IEEE Porto Power Tech Conference, Porto, Portugal,* vol. 4, p. 6, 2002.

[5] G. Benmouyal and S. Zocholl, "The impact of high fault current and CT rating limits on overcurrent protection," 2002.

[6] D. Hou, A. Guzman and J. Roberts, "Innovative solutions improve transmission line protection," *24th Annual Western Protective Relay Conference, Spokane, Washington,* pp. 21–23, 1997.

[7] J. R. Taylor, *An introduction to error analysis: The study of uncertainties in physical measurements*, Second Edition: University Science Books, 1982.

[8] A. Saltelli, S. Tarantola, F. Campolongo and M. Ratto, *Sensitivity analysis in practice: A guide to assessing scientific models*: John Wiley & Sons, Ltd, 2004.

[9]   L. Wang, "Frequency responses of phasor-based microprocessor relaying algorithms," *IEEE Transactions on Power Delivery,,* vol. 14, pp. 98-109, 1999.

[10]   CanAm EMTP User Group, *Alternative Transient Program (ATP) Rule Book*, Portland,.

[11]   MATLAB, The MathWorks Inc., http://www.mathworks.com.

[12]   M. Morris, "Factorial sampling plans for preliminary computational experiments," *Technometrics,* vol. 33, pp. 161-174, 1991.

[13]   A. Saltelli, S. Tarantola and K. Chan, "A quantitative model-independent method for global sensitivity analysis of model output," *Technometrics,* vol. 41, pp. 39-56, 1999.

[14]   A. Phadke, "Synchronized phasor measurements in power systems," *IEEE Computer Applications in Power,* vol. 6, pp. 10-15, 1993.

[15]   A. Phadke and J. Thorp, *Synchronized phasor measurements and their applications*: Springer, 2008.

[16]   V. Centeno, M. Donolo and J. Depablos, "Software synchronization of phasor measurement unit," *Francia,* 2004.

[17]   IEEE Power System Relaying Committee, "Understanding microprocessor-based technology applied to relaying," 2004.

[18]   G. Benmouyal, "Removal of DC-offset in current waveforms using digital mimic filtering," *IEEE Transactions on Power Delivery,* vol. 10, pp. 621-630, 1995.

[19]   A. Phadke and J. Thorp, *Computer relaying for power systems*. New York: John Wiley & Sons, 1988.

[20]   P. S. R. Diniz, E. A. B. Silva and S. L. Netto, *Digital signal processing*: Cambridge University Press, 2010.

[21]   A. Osman and O. Malik, "Transmission line distance protection based on wavelet transform," *IEEE Transactions on Power Delivery,* vol. 19, pp. 515-523, 2004.

[22]   A. T. Johns and S. K. Salman, *Digital protection for power systems*: Peter Peregrinus Ltd, 1997.

[23]   B. Mann and I. Morrison, "Digital calculation of impedance for transmission line protection," *IEEE Transactions on Power Apparatus and Systems,* pp. 270-279, 1971.

[24]   B. Mann and I. Morrison, "Relaying a three phase transmission line with a digital computer," *IEEE Transaction on Power Apparatus System,* vol. 90, 1971.

[25]   G. Gilcrest, G. Rockefeller and E. Udren, "High-Speed Distance Relaying Using a Digital Computer I-System Description," *IEEE Transactions on Power Apparatus and Systems,* pp. 1235-1243, 1971.

[26]   G. Rockefeller and E. Udren, "High-Speed Distance Relaying Using a Digital Computer II-Test Results," *IEEE Transactions on Power Apparatus and Systems,* pp. 1244-1258, 1972.

[27]   J. Makino and Y. Miki, "Study of operating principles and digital filters for protective relays with digital computers," *IEEE PES Winter Power Meeting,* pp. 1-8, 1975.

[28]   J. Gilbert and R. Shovlin, "High speed transmission line fault impedance calculation using a dedicated minicomputer," *IEEE Transactions on Power Apparatus and Systems,* vol. 94, pp. 872-883, 1975.

[29]   P. McLaren and M. Redfern, "Fourier-series techniques applied to distance protection," *IEEE Proceedings,* vol. 122, pp. 1301–1305, 1975.

[30] A. Phadke, M. Ibrahim and T. Hlibka, "Fundamental basis for distance relaying with symmetrical components," *IEEE Transactions on Power Apparatus and Systems,* vol. 96, pp. 635-646, 2006.

[31] M. Kezunovic, S. Kreso, J. Cain and B. Perunicic, "Digital protective relaying algorithm sensitivity study and evaluation," *IEEE Transactions on Power Delivery,* vol. 3, pp. 912-922, 1988.

[32] F. Altuve, V. Diaz and M. Vazquez, "Fourier and Walsh digital filtering algorithms for distance protection," *IEEE on Power Industry Computer Application Conference,* pp. 423-428, 1995.

[33] Y. Chi-Shan, H. Yi-Sheng and J. Joe-Air, "A Full- and Half-Cycle DFT-based technique for fault current filtering," *2010 IEEE International Conference on Industrial Technology (ICIT),* pp. 859-864, 14-17 March 2010 2010.

[34] M. Karimi-Ghartemani, B. T. Ooi and A. Bakhshai, "Investigation of DFT-based phasor measurement algorithm," *IEEE Power Engineering Society General Meeting 2010,* pp. 1-6, 2010.

[35] *IEEE Standard Format for Synchrophasor for Power Systems,* IEEE Standard C37.118-2005, IEEE Power System Relaying Committee of the Power Engineering Society, 2005

[36] S. E. Zocholl and G. Benmouyal, "How microprocessor relays respond to harmonics, saturation, and other wave distortions," *Schweitzer Engineering Laboratories, Inc. Summer,* 2003.

[37] J. M. Kennedy, G. E. Alexander and J. S. Thorp, "Variable digital filter response time in a digital distance relay," 1993.

[38] B. Kasztenny, D. Sharples, V. Asaro and M. Pozzuoli, "Distance relays and capacitive voltage transformers-balancing speed and transient overreach," *Annual Relay Conference for Protective Relay Engineers, Canada,* 2000.

[39] H. W. Coleman and W. G. Steele, *Experimentation, validation, and uncertainty analysis for engineers*: Wiley, 2009.

[40] A. Yegnan, D. Williamson and A. Graettinger, "Uncertainty analysis in air dispersion modeling," *Environmental Modelling & Software,* vol. 17, pp. 639-649, 2002.

[41] F. Campolongo, J. Cariboni and A. Saltelli, "An effective screening design for sensitivity analysis of large models," *Environmental Modelling & Software,* vol. 22, pp. 1509-1518, 2007.

[42] A. Saltelli, M. Ratto, S. Tarantola and F. Campolongo, "Sensitivity analysis for chemical models," *Chemical Reviews,* vol. 105, pp. 2811-2828, 2005.

[43] R. Gelinas and J. Vajk, "Systematic sensitivity analysis of air quality simulation models," *Final Report to US Environmental Protection Agency under Contract,* p. 2942.

[44] R. Cukier*, et al.*, "Study of the sensitivity of coupled reaction systems to uncertainties in rate coefficients. I Theory," *The Journal of Chemical Physics,* vol. 59, p. 3873, 1973.

[45] J. H. Schaibly and K. E. Shuler, "Study of the sensitivity of coupled reaction systems to uncertainties in rate coefficients. II applications," *The Journal of Chemical Physics,* vol. 59, p. 3879, 1973.

[46] M. Koda, G. J. Mcrae and J. H. Seinfeld, "Automatic sensitivity analysis of kinetic mechanisms," *International Journal of Chemical Kinetics,* vol. 11, pp. 427-444, 1979.

[47] G. J. McRae, J. W. Tilden and J. H. Seinfeld, "Global sensitivity analysis--a computational implementation of the Fourier Amplitude Sensitivity Test (FAST)," *Computers & Chemical Engineering,* vol. 6, pp. 15-25, 1982.

[48] J. Dresch, X. Liu, D. Arnosti and A. Ay, "Thermodynamic modeling of transcription: sensitivity analysis differentiates biological mechanism from mathematical model-induced effects," *BMC systems biology,* vol. 4, p. 142, 2010.

[49] S. Marino, I. B. Hogue, C. J. Ray and D. E. Kirschner, "A methodology for performing global uncertainty and sensitivity analysis in systems biology," *Journal of Theoretical Biology,* vol. 254, pp. 178-196, 2008.

[50] R. Cukier, H. Levine and K. Shuler, "Nonlinear sensitivity analysis of multiparameter model systems," *Journal of computational physics,* vol. 26, pp. 1-42, 1978.

[51] L. Torelli and S. Moorthy, "Transient overvoltages and distance protections: Problems and solutions," *Managing the Change, 10th IET International Conference on Developments in Power System Protection (DPSP 2010),* pp. 1-5, 2010.

[52] A. Greenwood, *Electrical transients in power systems*: New York, NY (USA); John Wiley and Sons Inc., 1991.

[53] G. Ziegler, *Numerical distance protection: principles and applications*: Wiley-VCH, 2008.

[54] D. Hou and J. Roberts, "Capacitive voltage transformer: transient overreach concerns and solutions for distance relaying," 2002, pp. 119-125.

[55] J. Arrillaga, *Power system harmonic analysis*: John Wiley & Sons Inc, 1997.

[56] Y. Kang, U. Lim, S. Kang and P. Crossley, "Compensation of the distortion in the secondary current caused by saturation and remanence in a CT," *IEEE Transactions on Power Delivery,* vol. 19, pp. 1642-1649, 2004.

[57] G. Pradeep Kumar, S. S. Tarlochan and F. Gregory James, "Current Transformer Dimensioning for Numerical Protection Relays," *IEEE Transactions on Power Delivery,* vol. 22, pp. 108-115, 2007.

[58] A. Bakar, C. Lim and S. Mekhilef, "Investigation of transient performance of capacitor voltage transformer," pp. 509-515, 2007.

[59] I. Zamora*, et al.*, "Influence of power quality on the performance of digital protection relays," *IEEE Power Tech, Russia,* pp. 1-7, 2005.

[60] M. S. Thomas, A. Prakash and Nizamuddin, "Modeling and Testing of Protection Relay IED," *Joint International Conference on Power System Technology and IEEE Power India Conference, 2008. POWERCON 2008. ,* pp. 1-5, 12-15 Oct. 2008.

[61] L. Kojovic, "CT Modeling Techniques for Relay Protection System Transient Studies," *International Conference on Power Systems Transients-IPST 2003,* 2003.

[62] L. Kojovic, "Comparison of different current transformer modeling techniques for protection system studies," *IEEE/PES Summer Meeting, Chicago, Illinois,* vol. 3, pp. 1084-1089, 2002.

[63] R. Folkers, "Determine current transformer suitability using EMTP models," *Proceedings of the 26th Annual Western Protective Relay Conference, Spokane, WA,* 1999.

[64] D. Angell and D. Hou, "Input Source Error Concerns for Protective Relays," 2006.

[65] D. Tziouvaras, J. Roberts, G. Benmouyal and D. Hou, "The effects of conventional instrument transformer transients on numerical relay elements," *28th. Annual Western Protective Relay Conference, Pullman, WA, USA,* 2001.

[66] M. Hughes, "Distance relay performance as affected by capacitor voltage transformers," *IEEE Proceedings,* pp. 1557-1566, 1974.

[67] E. Abedi and S. Sadeghi, "Study of capacitive voltage transformer transient effects on the performance of distance relays," *International Electric Machines and Drives Conference, 2009. IEMDC '09,* pp. 864-869, 3-6 May 2009 2009.

[68] M. N. Ibrahim and R. Zivanovic, "Impact of CT saturation on phasor measurement algorithms: Uncertainty and sensitivity study," 2010, pp. 728-733.

[69] C. S. Yu, "A discrete Fourier transform-based adaptive mimic phasor estimator for distance relaying applications," *IEEE Transactions on Power Delivery,* vol. 21, pp. 1836-1846, 2006.

[70] M. Kezunovic and B. Kasztenny, "Design optimization and performance evaluation of the relaying algorithms, relays and protective systems using advanced testing tools," *IEEE Transactions on Power Delivery,* vol. 15, pp. 1129-1135, 2000.

[71] M. Musaruddin, M. Zaporoshenko and R. Zivanovic, "Remote protective relay testing," *Proceedings of Australasian Power Engineering Conference (AUPEC 2008),* pp. 1-4, 2009.

[72] Schweitzer Engineering Laboratories, "SEL-RTS Relay Test System, Instruction Manual," USA, February 1997. Available: http://www.selinc.com.

[73] Schweitzer Engineering Laboratories website. Available: http://www.selinc.com.

[74] IEEE Standard C.37.111-1999, March 1999

[75] Schweitzer Engineering Laboratories, Inc., "SEL-RTS Relay Test System," 1997.

[76] C. Henville, B. Hydro and J. Mooney, "Low level testing for protective relays," *Canadian Conference on Electrical and Computer Engineering,* vol. 2, pp. 724-728 vol. 2, 1996.